USGS
OFR 82-106
Copy 2.

MENGIS OFR 82-106 c.2

UNITED STATES
DEPARTMENT OF THE INTERIOR
GEOLOGICAL SURVEY

MODELING OF A TRANSIENT STREAMBED IN THE RIO GRANDE, COCHITI DAM TO NEAR ALBUQUERQUE, NEW MEXICO

By Robert C. Mengis

Open-File Report 82-106

Denver, Colorado

1981

UNITED STATES DEPARTMENT OF THE INTERIOR

JAMES G. WATT, Secretary

GEOLOGICAL SURVEY

Dallas L. Peck, Director

For additional information write to:

U.S. Geological Survey
Water Resources Division
Mail Stop 413, Box 25046
Denver Federal Center
Denver, Colorado 80225

For purchase write to:

Open File Services Section
U.S. Geological Survey
Box 25425
Denver Federal Center
Denver, Colorado 80225
(303) 234-5888; FTS 234-5888

CONTENTS

CONTENTS--Continued

ILLUSTRATIONS

TABLES

CONVERSION TABLE

Metric units in this report may be converted to inch-pound units by using the following conversion factors:

Multiply metric units	By	To obtain inch-pound units
millimeter (mm)	0.0394	inch (in)
millimeter (mm)	0.00328	foot (ft)
meter (m)	3.28	foot (ft)
kilometer (km)	0.622	mile (mi)
meter^2 (m^2)	10.76	foot^2 (ft^2)
meter^3 per second (m^3/s)	35.31	foot^3 per second (ft^3/s)
megagram (Mg)	1.102	ton, short (2,000 lb)
gigagram (Gg)	1102.3	ton, short (2,000 lb)

DEFINITION OF SYMBOLS

Symbol		Unit of measure
a	Thickness of bedload layer	m
A	Cross-sectional area of water	m^2
A_1	Thickness of bedload layer relative to depth	-
C	Chezy discharge coefficient	-
C_1	Upstream discharge coefficient	-
C_2	Downstream discharge coefficient	-
C'	Average volumetric concentration of suspended bed material, (the ratio of volume of sediment to volume of water)	-
C'_t	Concentration of the total bed material load	mg/L
c'_a	Concentration by weight at the bed	kg/m^3
c'_b	Volumetric concentration at the bed	-
c'	Depth variate concentration distribution	kg/m^3
d	Representative diameter of bed material	mm
d_{50}	Mean diameter of the total grain distribution	mm
D	Hydraulic or average depth	m
E	Energy gradient	-
g	Gravitational constant	m/s^2
H	Water surface elevation or stage	m
I_1, I_2	Dimensionless integrals involved in the computation of suspended load	-
K	Conversion factor	-
k_s	Grain surface roughness	mm

	Symbol	Unit of measure
N	Parameter controlling the thickness of active layer	-
p	Probability of particle movement	-
Q	Water discharge	m^3/s
Q_s	Sediment discharge	m^3/s or m^3/d
q_s'	Suspended sediment discharge per unit width	m^2/s or m^3/d
q_b	Bedload discharge per unit width	m^2/s
s	Relative density of sediment (2.65)	-
S	Water-surface slope	-
S_f	Energy-grade line slope	-
t	Time	s or d
T	Top width of channel	m
T_1	Active layer thickness	m
T_2	Inactive layer thickness	m
TH	Energy head at a section	m
u	Depth variate velocity distribution	m/s
V	Average velocity in the x-direction	m/s
V_1	Upstream average velocity	m/s
V_2	Downstream average velocity	m/s
V*	Shear velocity	m/s
V*'	Effective shear velocity	m/s
V_{cr}	Velocity of incipient motion	m/s
W	Active width of sediment transport	m
x	Downstream distance	m

Symbol		Unit of measure
Y	Flow depth	m
z	Rouse number	-
Z	Bed elevation (above National Geodetic Vertical Datum of 1929)	m
β	Tangent of the dynamic friction angle (0.51)	-
η	One minus the porosity of natural material	-
ν	Kinematic viscosity of water	m^2/s
λ_b	Linear concentration at the bed	-
Θ	Nondimensional shear stress	-
Θ'	Effective nondimensional shear stress	-
Θ_c	Nondimensional shear stress of incipient motion (0.05)	-
ω	Fall velocity of particle	m/s
ω_e	Effective fall velocity	m/s
Φ_b	Bedload intensity	-
Φ_s	Suspended load intensity	-
ϕ	Size fraction	-

Integer Conventions

i	Cross-sectional index (increasing downstream)
m	Size-class index
j	Time-step index
NSZ	Total number of size classes
NXT	Total number of cross sections

MODELING OF A TRANSIENT STREAMBED IN THE RIO GRANDE, COCHITI DAM TO NEAR ALBUQUERQUE, NEW MEXICO

By

Robert C. Mengis

ABSTRACT

A one-dimensional surface water-sediment transport model based on finite differences, involving no initial load conditions and considering multisize transport and bed armoring, was developed for simulating long-term transient-streambed conditions in streams for which only few hydraulic and sediment data are available. Steady, nonuniform, subcritical flow was assumed, and there was no time-step restriction on the finite difference scheme for convergence and stability. Hydraulic, sediment, and bed-elevation data collected downstream from the Cochiti Dam site on the Rio Grande in New Mexico, from May 1970 to November 1975, were used in a pre-dam 16-day calibration simulation, and to evaluate predictions obtained during post-dam 204-day, 700-day, and 24-month simulations. Engelund and Fredsøe's transport equation used with Deigaard's normalization method did not accurately predict bed-material transport by size class in the study reach; whereas, Yang's equation did except for large size classes. The active-layer thickness varies directly, but less than linearly, with the time-step size. Coupling of Chezy discharge coefficients at a section is a simple and accurate method for reproduction of a given water-surface profile. The 900 percent exaggeration of degradation at cross section 2 by the model is thought to be due to improper characterization of bed-size distribution there, as well as at some

other cross sections in the upstream reach. The model tends to exaggerate the actual degradation in a ratio of 2 to 1 on a net reach-change basis. The fact that the estimated net actual bed material outflow is 100 percent greater than the outflow computed from the bed changes in the reach, is an indication that perhaps actual bed material is much coarser than the representation of bed material used in the simulations.

INTRODUCTION

If an alluvial stream bed is expected for some reason to change from one equilibrium profile to another during a period of time, it is useful to be able to predict where the major changes will take place and how long it takes for such changes to occur.

This paper describes such a predictive tool based on finite differences that models the transient period of the bed; that is, the period during which the bed profile is moving to the new equilibrium profile, unlike certain analytic models (de Vries, 1977) that predict only the final equilibrium profile. The model is an in-between tool, in that it does not require as much data collection for calibration purposes and initial conditions as others (Bennett and Nordin, 1977), but requires more than is needed for analytical methods. Some other features are: (1) There is no time-step size restriction in the finite difference scheme for convergence and stability; (2) the model takes the presence of a nonuniform sediment size distribution into account, that is, armoring; and (3) no initial sediment-load conditions are required.

Like most sediment-routing models, the governing equations consist of: (1) A flow equation or equations with a friction-slope formulation;

(2) a sediment-transport function; and (3) a sediment-continuity equation. The development of these equations and the assumptions involved in the development are discussed in the first part of this paper. The solution technique is a sequential stage, uncoupled mode (Chen, 1973) with known constant discharge input. There is extensive discussion on boundary and initial conditions, calibration, and application of the model to an actual study reach. An attempt was made to model actual bed transient, using either Yang's transport function (Yang, 1973), or Engelund's formulation (Engelund and Fredsøe, 1976).

EQUATIONS AND BACKGROUND ASSUMPTIONS

The St. Venant equations (Strelkoff, 1969) of one-dimensional, gradually varied, unsteady flow in an open channel are the continuity or conservation of mass equation,

$$\frac{\partial A}{\partial t} + \frac{\partial Q}{\partial x} = 0; \qquad (1)$$

and the momentum or conservation of energy equation,

$$\frac{\partial V}{\partial t} + \frac{\partial (V^2/2g + H)}{\partial x} + S_f = 0; \qquad (2)$$

where, in the latter, S_f is the friction-slope formulation and is defined as:

$$S_f = \frac{V^2}{C^2 D} . \qquad (3)$$

In the above equations:

x = downstream distance,

t = time,

H = H(x,t), is the water surface elevation or stage,

$D = D(x,t)$, is the hydraulic depth at a cross section,

$A = A(x,H(x,t))$, is the cross-sectional area of water,

$D = A/T$, where $T = T(x,H(x,t))$ is the top width of channel,

$V = V(x,t)$ is the average velocity of flow in the x-direction,

$Q = Q(x,t)$ is the water discharge in volume per unit time,

(note that $Q = VA$),

C = the Chezy dischange coefficient, and

g = the gravitational constant.

A derivation of these equations is given by Strelkoff (1969); definition sketches for dependent variables are shown in figure 1. Gradually varied flow means that $\frac{\partial A}{\partial x}$ is relatively small. Gradually varied flow can be either subcritical $\frac{V}{\sqrt{gD}} < 1$, or supercritical $\frac{V}{\sqrt{gD}} > 1$.

This coupled system of partial differential equations has been solved by many methods (Chen, 1973), but the method proving the most practical and adequately accurate is a linear implicit finite difference approach. In theory, an implicit method is stable for any selection of time-step size, Δt, given the physical constraints, Δx; however, this is not the case in practice, and Bennett and Nordin (1977) indicate that if the Courant restriction is exceeded by an order of 10, the scheme becomes unstable.
The Courant restriction is:

$$\Delta t \leq \frac{\Delta x}{V + \sqrt{gD}} \quad . \tag{4}$$

In practice, it is not economical to use an implicit finite difference solution scheme for the above equations, except for a short-term, highly unsteady flow. For long-term gradually varied subcritical flow, it was

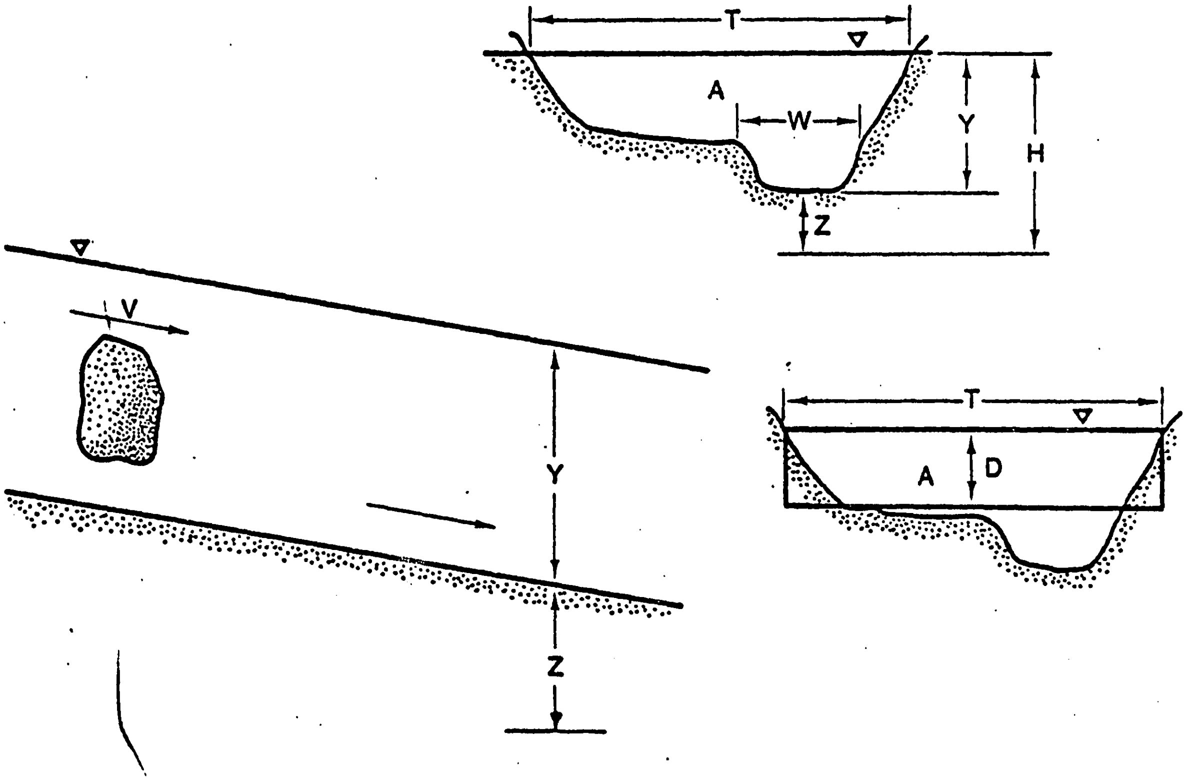

Figure 1.--Definition sketch of dependent variables; (see Definition of symbols on page viii).

found that movement at the stream bed had little effect on the water movement; in other words, bed transients propagate at a much slower rate than water surface transients (de Vries, 1977, p. 1-11). This leads to a steady nonuniform flow assumption: $\frac{\partial Q}{\partial x} = 0$, which implies $\frac{\partial A}{\partial t} = 0$, or A=A(x,H(x)) for equation 1. Discharge, Q, is not considered to vary during the time step; this is a common practice, if the discharge is averaged during a period equal to the time-step size. This known constant discharge assumption, $\frac{\partial Q}{\partial t} = 0$, leads to $\frac{\partial V}{\partial t} = 0$, or V=V(x) by $\frac{\partial A}{\partial t} = 0$; combined with continuity at a point or cross section, Q=VA.

Hence, given a fixed Q input to a stream reach, and given a fixed cross section or x, the area of flow is determined solely by the characteristic area vs. stage relationship: A=A(H); and the average velocity is subsequently determined by V=Q/A. Thus, equations 1 and 2 reduce to the backwater equation:

$$\frac{d(V^2/2g + H)}{dx} + S_f = 0. \qquad (5)$$

Equation 5 can determine an actual water-surface profile quite accurately by treating Chezy C at each cross section as a parameter; this is contingent, of course, on having an accurate A(H) relationship at each cross section. Chezy C is defined as:

$$C = \frac{V}{\sqrt{DS}}, \qquad (6)$$

where S is water-surface slope. However, values computed by equation 6 did not agree with the values determined as parameters of calibration. Because Chezy C is unpredictable in varied flow, Bennett and Nordin (1977) chose to fix a constant C for the entire study reach; that is: C for all cross sections for the whole of simulation time was based on a minimization of error with measured data. Krishnappan and Snider (1977, p. 23) chose to update C with an algorithm given by Kishi and Kuroki. If simulated flows vary greatly, it may be necessary to update Chezy C.

The equations completing the system are the sediment-continuity equation:

$$\eta W \frac{\partial Z}{\partial t} + A \frac{\partial C'}{\partial t} + \frac{\partial Q_s}{\partial x} = 0 \; ; \qquad (7)$$

and the sediment-transport function:

$$Q_s = f(V,d,P) . \qquad (8)$$

In the above,

$Z = Z(x,t)$ is the bed elevation above National Geodetic Vertical Datum of 1929,

$C' = C'(x,V(x,t))$ is the average volumetric concentration of suspended bed material,

Q_s = the total volumetric sediment discharge,

$W = W(x)$ is the active width of sediment transport at a cross section,

η = one minus the porosity of natural material,

d = the representative diameter of bed material, and

P = a family of parameters.

The family of parameters is indicative of a particular function; it includes: water-surface slope, water temperature, hydraulic depth, and so forth, depending on the function. The active width of channel (fig. 1) is defined (Bennett and Nordin, 1977) as that part of channel width where active transport takes place.

Equation 7 can be derived in the same manner as equation 1, but area and discharge of sediment are considered instead of water (Krishnappan and Snider, 1977). In equation 7, the change in average suspended concentration with time can be considered to be zero: $\frac{\partial C'}{\partial t} = 0$, because $C' = C'(x,V(x,t))$; and $\frac{\partial V}{\partial t} = 0$ from the known constant discharge input assumption. Also, because none of the parameters in the sediment transport function change during the time step;

$$\frac{\partial Q_s}{\partial t} = 0 \text{ or } Q_s = Q_s(x);$$

then:

$$\eta W \frac{\partial Z}{\partial t} + \frac{dQ_s}{dx} = 0. \qquad (9)$$

Since equation 7 is replaced with equation 9, the resulting system of equations is,

$$\frac{d(V^2/2g + H)}{dx} + S_f = 0; \qquad (5)$$

$$\eta W \frac{\partial Z}{\partial t} + \frac{dQ_s}{dx} = 0; \qquad (9)$$

$$Q_s = f(V,d,P). \qquad (8)$$

Ponce and others (1979a) have solved the resulting system with a linear-implicit finite-difference method with coupled equations 5 and 9, and Z and Y (depth), the dependent variables. Ponce and others (1979b) also did an elaborate convergence and stability analysis in a subsequent paper. However, the transport function, equation 8, was assumed to have a special form, and there was no allowance for armoring.

Bennett and Nordin (1977) accounted for armoring in their model; it is characterized by a sophisticated sediment-continuity equation that considers the total load as composed of bed and suspended loads and a flux between the two. The suspended load is determined analytically, and the transport function is a bedload equation. But this model requires considerable data for the calibration of the bedload equation, as well as both suspended and bedload initial and boundary conditions. Such complete field data are rarely available.

Komura and Simons (1967) considered degradation downstream from a dam with an armoring factor on the shear velocity; however, there was no provision for multisize transport in their model.

Deigaard (1978) used Engelund and Fredsøe's (1976) total load formulation, with the sum of the loads per size class normalized back to the predicted load, through using a single representative size. Armoring was simulated, but special assumptions about profile shape and upstream discharges were made; no backwater equation was incorporated. A discussion of armoring follows.

Armoring

Armoring occurs if grains of many sizes are present in a river bed; the result is that the finer sizes are transported, and the coarser sizes remain to protect the bed from further scour. It is a limiting process; less scour is expected than if the bed material was all one size.

Hence, to consider multisize transport, a bed grain-size distribution must be divided into size fractions (fig. 2), and there must be some kind of accounting procedure for the change in those size fractions as the bed is scoured or deposition occurs.

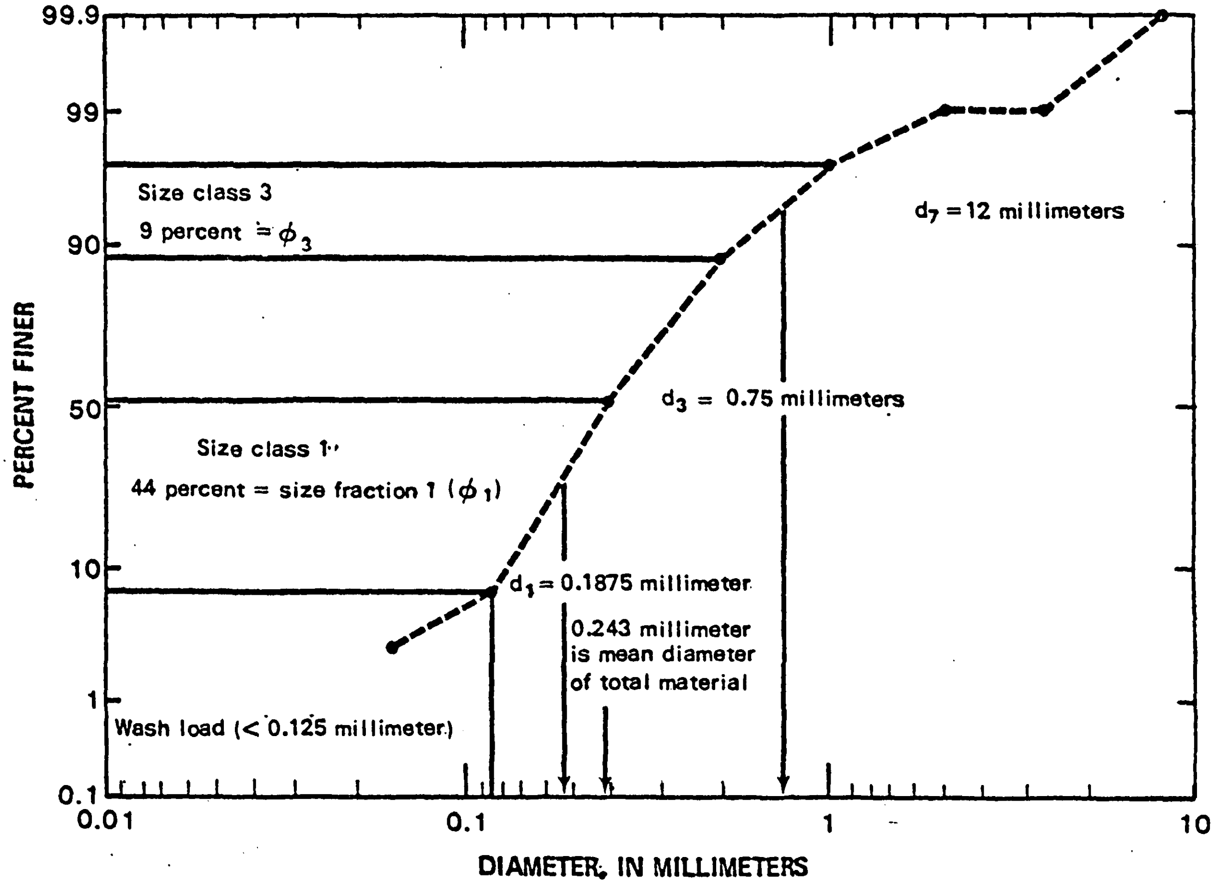

Figure 2.--Sample discretization of bed grain-size distribution.

Assumptions and objectives for the solution of the system of equations 5, 9, and 8 follow:

Assumptions and Objectives

1. Gradual varied subcritical flow is assumed.
2. No initial load conditions are necessary, because every dependent variable (except Z) is averaged during the time step. ΔZ per time step must be small, and the size fractions will change during the time step, depending on scour or deposition.
3. $\frac{\partial Q}{\partial t} = 0$ and $\frac{\partial Q}{\partial x} = 0$ imply $\frac{\partial Q_s}{\partial t}, \frac{\partial V}{\partial t}, \frac{\partial A}{\partial t}, \frac{\partial D}{\partial t}, \frac{\partial H}{\partial t}, \frac{\partial C'}{\partial t} = 0$.
4. Equation 8 will be written for each size fraction, and armoring will be considered.
5. Initial values of Chezy C may have to be updated, if there is great variance in water discharge during the period of simulation.

SOLUTION METHOD

The solution technique amounts to solving equation 5, the flow equation for the stage (H) and velocity (V) at each cross section; then using equation 8, the sediment transport equation, to predict the sediment discharge at each cross section (Q_s); thereby deriving the sediment load gradient, $\frac{dQ_s}{dx}$; and finally, solving explicitly for the change in the bed level, ΔZ, in equation 9, the sediment-continuity equation. It is a nonsimultaneous sequential stage solution, but satisfies all the assumptions and goals postulated in the previous section; the flow variables are not considered to change during the time step, and thus can be used as constant parameters in the determination of a transport correction to the initial bed level in the same time step. de Vries (1977) and Chen (1973) both mention this uncoupled-mode solution, and Bennett and Nordin (1977) use the same technique in the solution of the unsteady flow equations combined with the transport equations, by averaging all hydraulic variables during the time step before using them as parameters in the solution of the transport equations.

The flow-equation solution will be discussed first in this report followed by the specific solution of the transport equations; simulation of armoring concludes the discussion.

Flow-Equation Solution

Equation 5 is solved by substituting a finite-difference scheme for the nonlinear differential equation, and then solving the resulting algebraic equation by Newton's Method. The equation is nonlinear because:

$$\frac{d[V^2(x)/2g + H(x)]}{dx} + S_f = \frac{d[Q^2/2gA^2(x,H(x)) + H(x)]}{dx} + S_f,$$

where H(x) is the iterated variable, and the A(x,H(x)) is a known relation at each cross section. Note that S_f also is nonlinear in the same manner; that is, V^2 is involved, but was not so written in the above equation.

So far in this development, the standard backwater equation has been discussed, but there is no provision for changing bed level in the standard version. It is possible that streambed elevation can change several meters during simulation in which instance it would not have the same area versus stage relation, A(H), at that cross section of change. It is, therefore, appropriate and necessary to make the substitution Y=H-Z for the iterated variable H. Depth (Y) becomes the iterated variable, because Z is a known value at a section. For example, if there is erosion of 2m, the mean bed elevation at the cross section is considered to have fallen two meters in simulation, and the same area versus depth relation, A(Y), will be preserved.

The finite-difference scheme is a two-point scheme, and a boundary condition is necessary to begin solution. The downstream stage is customarily obtained from a rating curve, and one works upstream with the scheme; the upstream depth (Y) is the iterated variable in the scheme pairing (fig. 3). A rating curve is a relation of the form H=f(Q); that is, given the input Q, the stage is given. Once H is known, area is deduced from A=A(H); subsequently, velocity is deduced from Q/A. The bed elevation must not change at the downstream boundary; otherwise, the rating curve has no validity.

Upstream water discharge, Q, is considered constant throughout the reach in the time step; Q in equals Q out. However, allowance is made for significant mid-reach tributary inflow; in which instance the total reach must be subdivided into subreaches, and the determined upstream value of one subreach becomes the downstream boundary condition for the immediate upstream subreach, and so forth.

The finite difference schemes substituted are:

$$\frac{d(Q^2/2gA^2 + Y + Z)}{dx} = \frac{TH_{i+1} - TH_i}{\Delta x_i}, \text{ where } TH_i = Q^2/2gA_i^2\,(Y_i) + Y_i + Z_i;$$

and $S_f = (S_{f_i} + S_{f_{i+1}})/2$; where $S_{f_i} = \dfrac{Q^2}{A_i^2(Y_i)C_i^2D_i}$, where i is the cross section number increasing in the downstream direction. The top width relation with depth, T(x,Y(x)) must be known at each section, in order that hydraulic depth can be computed, that is, D=A/T.

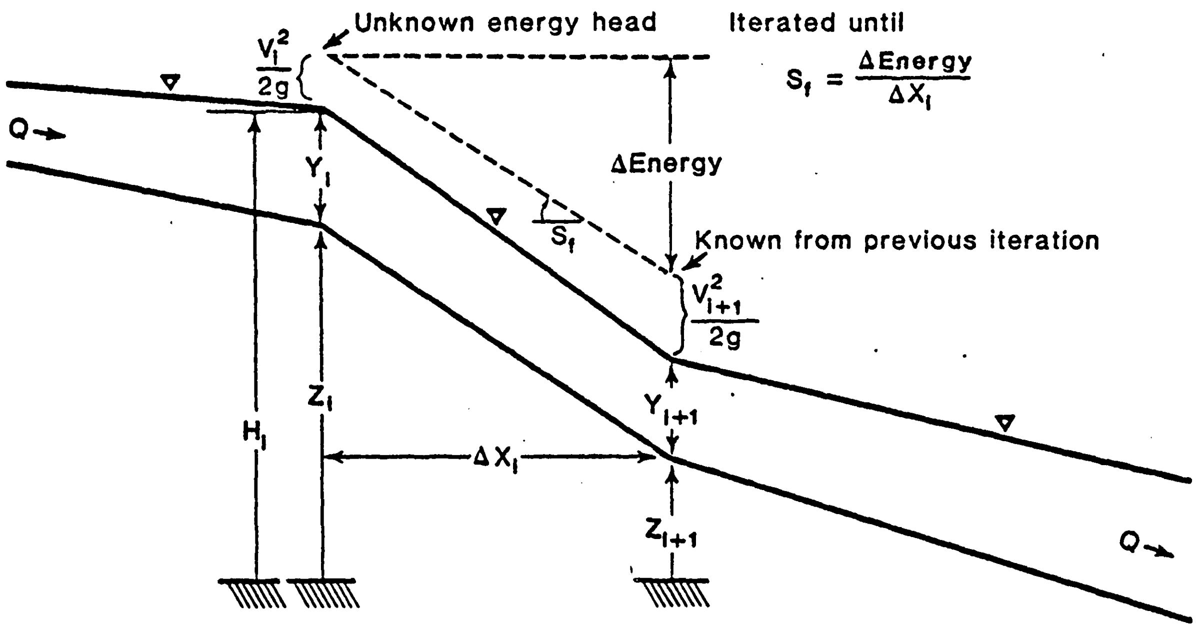

Figure 3.--Two-point flow iteration scheme.

Upon discretization then, equation 5 becomes,

$$F(Y_i) = TH_{i+1} - TH_i + \frac{\Delta x_i}{2}(S_{f_{i+1}} + S_{f_i}) = 0; \tag{10}$$

and $$\frac{dF}{dY_i} = -\frac{d(TH_i)}{dY_i} + \frac{d(S_{f_i})}{dY_i}\frac{(\Delta x_i)}{2};$$

or $$\frac{dF}{dY_i} = \left(\frac{dA_i}{dY_i}\right)\frac{Q^2}{gA_i^3} - 1 - \frac{\Delta x_i S_{f_i}}{2}\left(2\frac{\frac{dA_i}{dY_i}}{A_i} + \frac{\frac{dD_i}{dY_i}}{D_i}\right);$$

where $$\frac{dD_i}{dY_i} = \left(\frac{dA_i}{dY_i}\right)/T_i; \text{ and } \frac{dA_i}{dY_i} = \frac{A_i(Y_i + \Delta Y_i) - A_i(Y_i)}{\Delta Y_i}.$$

The depth will be determined from;

$$Y_{i_{k+1}} = Y_{i_k} - F(Y_{i_k})/\frac{dF(Y_{i_k})}{dY_i},$$

where k denotes the iteration number. The value of Y_{i_1} is picked arbitrarily. Discussion of the first guess (Y_{i_1}) and convergence is presented in the next section on calibration.

Once depth at each cross section is known, velocity is obtained at each; the next step is the transport part of the solution; however, before proceeding, it may be necessary to know the water-surface slope (S) for an update on Chezy C, or because it is required by the sediment-transport function as one of the parameters in P. In any instance

$$S_i = \frac{\frac{(H_{i-1} - H_i)}{\Delta x_{i-1}} + \frac{(H_i - H_{i+1})}{\Delta x_i}}{2} ; \qquad (11a)$$

or $$S_i = \frac{(H_i - H_{i+1})}{\Delta x_i} . \qquad (11b)$$

These equations are possible approximations of the water-surface slope. Equation 11a is more useful than equation 11b, because each cross section actually represents a discontinuity in the water-surface profile; however, use of equation 11a requires an upstream stage-boundary condition (equation 11b does not; see fig. 3); this can pose certain problems that will be discussed in the next section on calibrations and boundary conditions.

Transport-Equations' Solution

The first part of the solution involves finding the total sediment discharge at a cross section using equation 8, the sediment-transport function. Actually, since armoring is simulated, sediment transport per size class must be calculated. Then, change in bed elevation is computed with the sediment-continuity equation, equation 9; if degradation is indicated at a cross section, then the armoring of the bed must be considered. The sediment-transport function will be discussed first in the following subsection; then the sediment routing with the sediment-continuity equation; and, finally, the armoring simulation will be presented.

Sediment-Transport Function

Two transport functions predict the load at a section. A simulation using each equation will be described, and results compared in the next section. Yang's general equation (1973) based on unit stream power was developed on its agreement with actual data; hence, it is more empirically founded than Engelund and Fredsøe's equation (1976). Engelund and Fredsøe's equation is used with the normalizing scheme developed by Deigaard (1978).

Yang's equation

Yang's equation computes the total sediment concentration, C_t', including bedload, as a function of dimensionless effective unit stream power. The nondimensional unit stream power is the product of average velocity and water-surface slope divided by the fall velocity of the particle; that is, VS/ω, where ω is the fall velocity.

The effective dimensionless unit stream power is determined by subtracting off a critical stream power for incipient motion; that is, $VS/\omega - V_{cr}S/\omega$. The critical stream power of incipient motion is derived from the shear velocity Reynolds number:

$$\frac{V^*d}{\nu}, \tag{12}$$

where V^* is shear velocity; that is, $V^* = \sqrt{gDS}$; (13)

and ν is the kinematic viscosity of water in area per unit time.

The criterion for incipient motion (Yang, 1973, p. 1686-1688) follows:

If $0 < \frac{V^*d}{\nu} < 70$,

then
$$\frac{V_{cr}}{\omega} = \frac{2.5}{\log\left(\frac{V^*d}{\nu}\right) - 0.06} + 0.66; \tag{14}$$

and if $\frac{V^*d}{\nu} > 70$,

then
$$\frac{V_{cr}}{\omega} = 2.05. \tag{15}$$

Once the critical unit stream power is known, the total concentration, C_t' is computed as:

$$\log C_t' = 5.435 - 0.286 \log \frac{\omega d}{\nu} - 0.457 \log \frac{V*}{\omega} +$$

$$(1.799 - 0.409 \log \frac{\omega d}{\nu} - 0.314 \log \frac{V*}{\omega}) \quad \log (\frac{VS}{\omega} - \frac{V_{cr}S}{\omega}). \quad (16)$$

Equation 16 is Yang's general equation, which is based on a multiple regression with 463 sets of laboratory data (Yang, 1973).

In the application of equation 16, V and D are determined from the backwater routine; d is actually d_m, the mean diameter of the size class limits (size class m); ω and ν are temperature dependent, and their temperature variate relations are stored in the computer.

When the total concentration is known, then the total bed material discharge per size class is determined by:

$$Q_{s_m} = KQC_t'\phi_m , \quad (17)$$

where K is a conversion factor to get the desired units for Q_{s_m}; in the simulation, K was equal to about 0.0627 in the inch-pound system; and ϕ_m is the fraction of the size class in question.

The total load at a section is then the sum of the size class loads over all size classes; that is, $Q_{s_i} = \sum_{m=1}^{NSZ} Q_{s_{mi}}$, where NSZ is the total number of size classes; and i is the cross-section index.

Once each $Q_{s_{mi}}$ is known, the next step is the sediment continuity equation solution.

Engelund's formulation with normalization

Engelund computes a bedload, Q_b, based on a dimensionless shear stress, θ; at the same time relating the concentration at the bed, c'_a, to that same shear stress; thus enabling calculation of the suspended load. Then the total load is equal to the suspended load plus the bedload. The equations are presented in the next pages, followed by an explanation of the normalization technique used.

Engelund's bedload equation is:

$$\Phi_b = 5p(\sqrt{\theta'} - 0.7\sqrt{\theta_c}) \; ; \tag{18}$$

in which

$$\theta' = \frac{V*'^2}{(s-1)gd} \; ; \tag{19}$$

$$\Phi_b = \frac{q_b}{(s-1)gd^3} \; ; \tag{20}$$

$$p = 1\left(+\left[\frac{\pi \, \beta/6}{(\Theta-\Theta_c)}\right]^4\right)^{-1/4} \; ; \tag{21}$$

where

Θ_c = the critical nondimensional shear stress of incipient motion, and is taken as 0.05 in this simulation;

s = the relative density of sediment (taken to be 2.65);

q_b = the volumetric bedload per unit width of channel;

β = the tangent of the dynamic friction angle, and is taken as $\beta = \tan 27^o = 0.51$;

$V*'$ = the effective velocity with bed forms considered;

p = the probability of particle movement;

Θ' = the effective dimensionless shear stress with bed forms considered; and Φ_b = the dimensionless bedload intensity.

V*' is computed by a method of successive approximations from Einstein's equation (1950):

$$\frac{V}{V*'} = 6 + 2.5 \ln \left(\frac{V*'^2}{gSk_s}\right) \quad (22)$$

where k_s is the grain surface roughness, and is 2.5d in Engelund's formulation.

The linear concentration of sediment at the bed (λ_b) is computed using:

$$\lambda_b 2 = \frac{\theta' - \theta_c \ 0.267 \ p}{0.027s \ \theta'} ; \quad (23)$$

where the volumetric concentration at the bed (c_b') is determined as:

$$c_b' = \frac{0.65}{(1 + 1/\lambda_b)^3} . \quad (24)$$

The thickness of bedload layer (a) is assumed to be two times the grain diameter; that is, a = 2d. The Rouse number (Einstein, 1950) is determined by

$$z = \frac{\omega}{0.4V*'} . \quad (25)$$

The suspended load is calculated by

$$q_{s'} = \int_a^D u \ c' \ dY ; \quad (26)$$

where

$q_{s'}$ = the volumetric suspended load per unit width of channel;

u = the mean flow velocity at a distance Y from the bed; and

c' = the concentration, at a distance Y from the bed. The distributions assumed for u and c' are:

$$u = 5.75 V*' \ln\left(\frac{30Y}{k_s}\right) ; \tag{27}$$

and

$$c' = c'_a \left(\frac{D-Y}{Y} \; \frac{a}{D-a}\right)^z . \tag{28}$$

Einstein (1950) developed the following relations for the practical calculation of the suspended load (that is, evaluation of equation 26):

$$\Phi_s = 11.6\sqrt{\theta'} \, c'_b \left(\frac{a}{d}\right) \left(I_1 \ln\left(\frac{30D}{k_s}\right) + I_2\right) ; \tag{29}$$

in which Φ_s is the dimensionless suspended load intensity,

and $$I_1 = 0.216 \frac{A_1^{\,z-1}}{(1-A_1)^z} \int_{A_1}^{1} \left(\frac{1-Y}{Y}\right)^z dY ; \tag{30}$$

$$I_2 = 0.216 \frac{A_1^{\,z-1}}{(1-A_1)^z} \int_{A_1}^{1} \left(\frac{1-Y}{Y}\right)^z \ln Y \, dY ; \tag{31}$$

where $A_1 = \frac{a}{D}$.

The integrals of I_1 and I_2 are evaluated numerically by Simpson's Rule, and sufficient accuracy is obtained.

The total load is found by:

$$Q_s = W(\Phi_b + \Phi_s) \sqrt{(s-1)gd^3} . \tag{32}$$

In the normalization process (Deigaard, 1978), the mean diameter of the whole distribution is used to calculate a bed load, $q_b(d_{50})$, and a concentration at the bed. Then, for all size class fall velocities such that:

$$\frac{\omega_m}{V*'} < 1; \tag{33}$$

an effective fall velocity, ω_e; is computed:

$$\omega^e = \frac{\Sigma\omega_m \phi_m}{\Sigma\phi_m} \quad (\omega_m < V*') \; ; \tag{34}$$

ω_e is then substituted into equation 25, and a suspended load, $q_{s'}(d_{50}, \omega_e)$, is computed using equation 29. Using the mean diameter of the size class limits, each size class bedload is summarily computed, and each size class suspended load is computed, if the fall velocity of the mean diameter satisfies equation 33. Then each load is multiplied by its respective size fraction to give a bedload q_{b_m}, and a suspended load, $q_{s'_m}$. The loads are summed in each category: suspended and bedload.

Then, q'_{b_m}, the final bedload per size class is:

$$q'_{b_m} = q_{b_m} \frac{q_b \, (d_{50})}{\sum_{m=1}^{NSZ} q_{b_m}} \; ; \tag{35}$$

and, $q'_{s'_m}$, the final suspended load per size class is:

$$q'_{s'_m} = q_{s'_m} \frac{q_{s'} \, (d_{50}, \omega_e)}{\sum_{m=1}^{NSZ} q_{s'_m}} \; ; \tag{36}$$

where d_{50} is the mean diameter of the total grain distribution. The total load for all size classes is:

$$W(q_b(d_{50}) + q_{s'} \, (d_{50}, \omega_e)); \tag{37}$$

which is equal to:

$$W\left(\sum_{m=1}^{NSZ} (q'_{b_m} + q'_{s'_m})\right).$$

Sediment Continuity Equation

Equation 9 is discretized as follows:

$$\eta W \frac{\partial Z}{\partial t} = \frac{\eta(2W_i + W_{i+1} + W_{i-1})\Delta Z_{mi}}{4\Delta t} ; \tag{38}$$

and,

$$- \frac{dQ_s}{dx} = \frac{(Q_{s_{mi-1}} - Q_{s_{mi}})}{\frac{(\Delta x_i + \Delta x_{i-1})}{2}} ; \tag{39}$$

where m is the size-class index; and i is the cross-sectional index. The above discretization results in the bed level change being distributed as shown in figure 4. $Q_{s_{m1}}$ is the sediment discharge at the upstream boundary, and is obtained from a rating curve; that is, given the upstream water discharge, Q, the sediment load per size class is given. One works from upstream to downstream with the schemes given above, unlike the flow computation, where the downstream boundary condition is given. $Q_{s_{mi-1}}$ is already known, having been previously calculated or from the boundary condition; $Q_{s_{mi}}$ is predicted with the sediment transport function; and ΔZ_{mi} is solved for by equating equations 38 and 39:

$$\Delta Z_{mi} = \frac{8\Delta t(Q_{s_{mi-1}} - Q_{s_{mi}})}{\eta(2W_i + W_{i-1} + W_{i+1})\ (\Delta x_i + \Delta x_{i-1})} . \tag{40}$$

Note that Z_{mi} will be less than 0 if $Q_{s_{mi}} > Q_{s_{mi-1}}$, indicating erosion or scour; conversely, if aggradation is simulated, that ΔZ_{mi} will be positive (fig. 4).

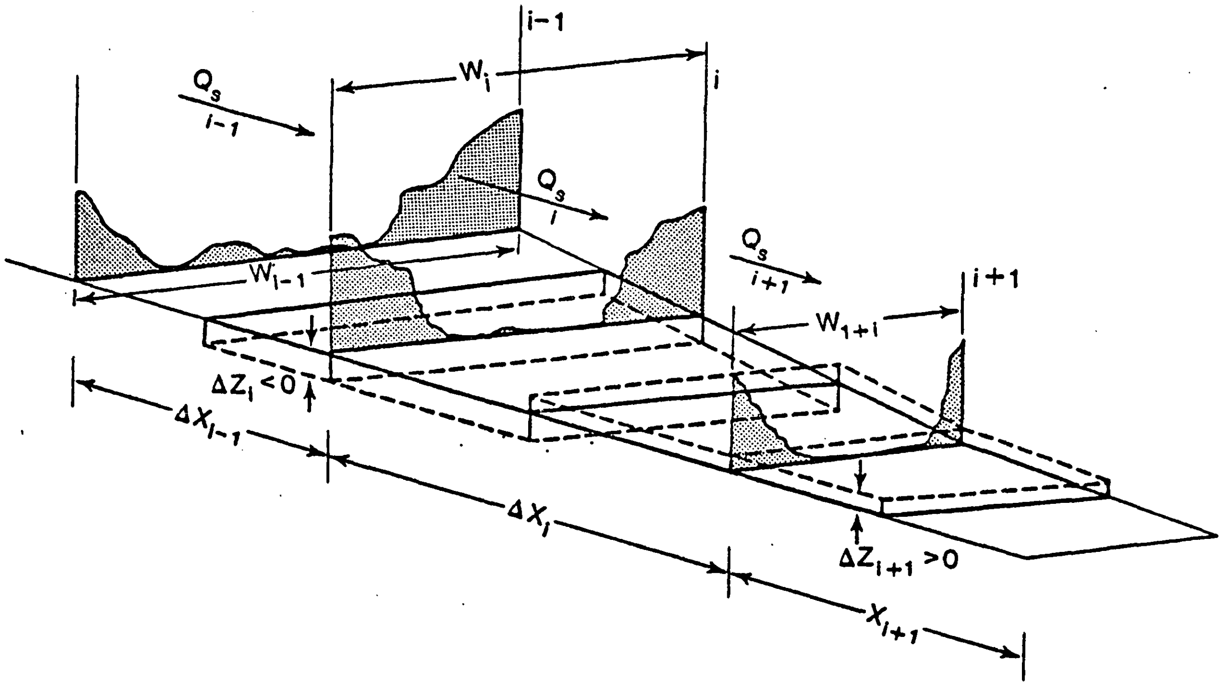

Figure 4.--Load distribution at a cross section.

Equation 39 is a two-point routing scheme; after the bed change in each size class is found at a particular section, that section is paired with the next downstream section, and loads are computed with the sediment transport function; then, the whole sediment routing process is repeated until one reaches the downstream boundary.

The total net change at the cross section i is found by summing the bed changes over all size classes; that is, if NSZ is the total number of size classes then, $\Delta Z_i = \sum_{m=1}^{NSZ} Z_{mi}$. ΔZ_i is the transport correction to the initial Z_i, and is added to that Z_i to obtain the final Z_i for the time step. Therefore, the final bed elevation for one time step is the initial bed elevation for the next time step. Excepting the size fractions, no other dependent variable changes over the time step but Z.

After the net bed elevation change is found at each cross section, a new Q is input, and the system rises to a new time level. The solution process begins anew with the flow solution (fig. 5). The provision for armoring, however, introduces a slight modification in the solution process, as discussed hereafter.

Simulation of Armoring

Armoring occurs when the predicted $Q_{s_{mi}}$ is too large, meaning that the ΔZ_{mi} determined from equation 40 is larger than the thickness of that particular size class available for scour (T_{1m}). ΔZ_{mi} is then fixed as that thickness, T_{1m}, and the smaller $Q_{s_{mi}}$ becomes the unknown variable, when equations 38 and 39 are equated (fig. 6). The above-mentioned thickness of the bed in a certain size class, T_{1m}, is determined by multiplying the size fraction of

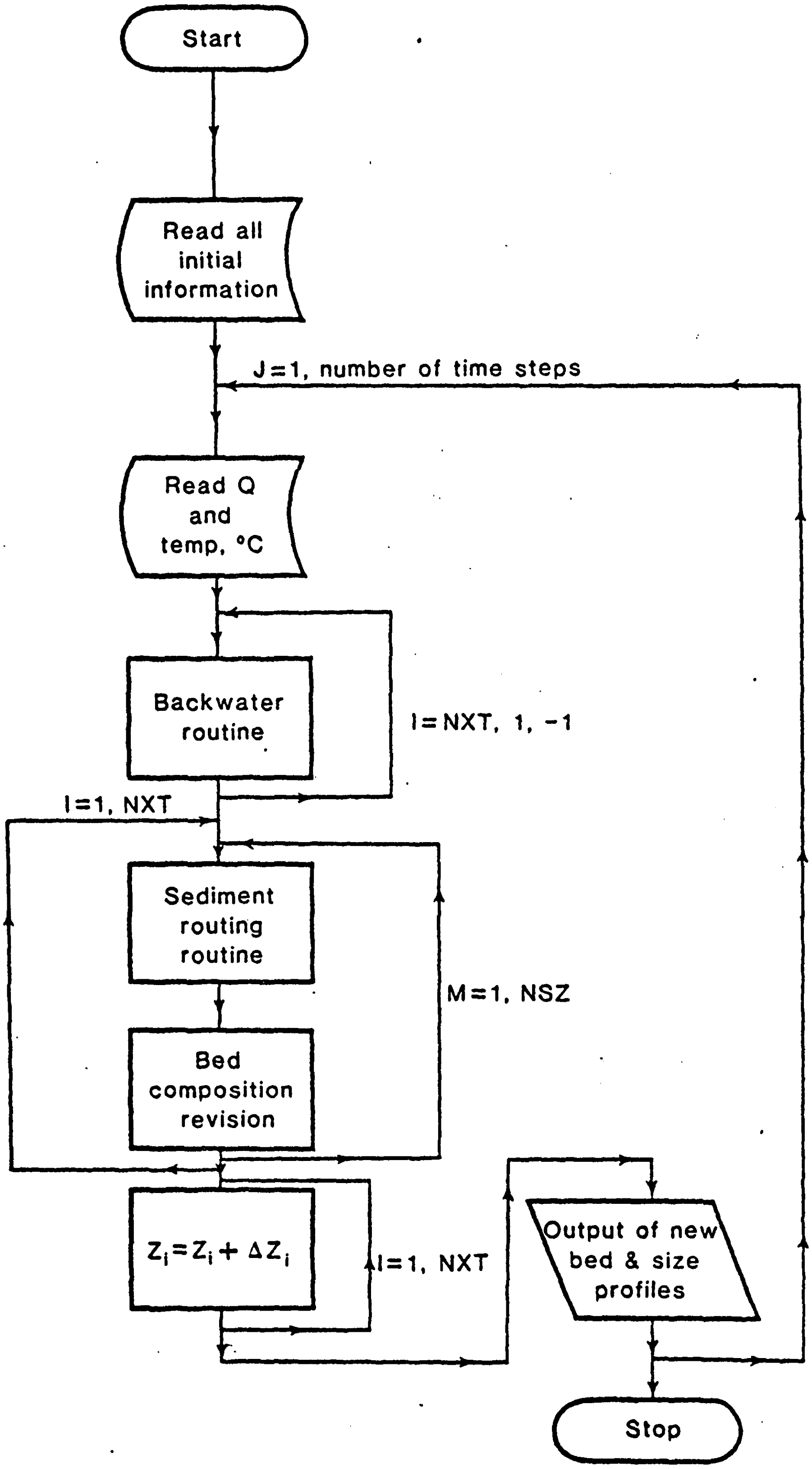

Figure 5.--Sequential stage-solution flow diagram.

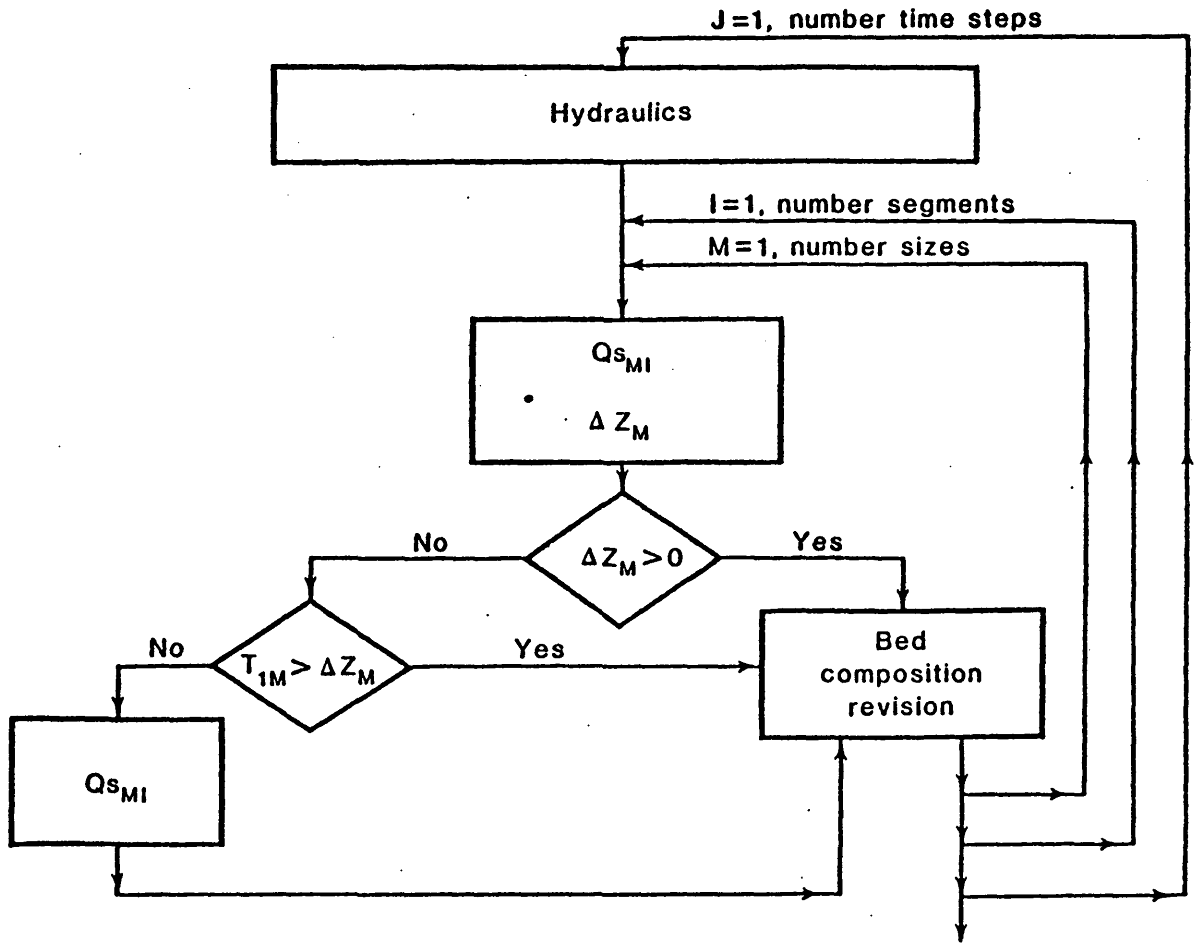

Figure 6.--Armoring logic diagram.

the bed material distribution times the total thickness of mixing layer or active layer (fig. 7). The size fraction of the bed material distribution is larger than the size fraction of the total distribution. This simulation of armoring and the bed composition accounting to be presented hereafter were conceived by Bennett and Nordin (1977); the situation described above is termed availability limited transport.

Bed-composition updating takes place regardless of scour or aggradation. The active-layer thickness is fixed throughout the simulation. Theoretically, the active layer represents the bed-material layer that can be sorted through by the action of the flowing water in a time step, Δt. Its thickness is controlled by parameter N (fig. 7). Parameter N is discussed in further detail in the calibration discussion. If deposition in a certain size class occurs, the active layer is moved up, and a thickness equal to that deposited is left underneath, and is called the inactive deposition layer (fig. 7). The compositions of both active and inactive layers are updated accordingly; the bed becomes more plentiful in the size class of aggradation.

Erosion in a particular size class is simulated by removing the required thickness from the active layer. The active layer moves down; then an equal thickness of inactive deposition or original material, as the case may be, is mixed in to keep the active-layer thickness constant. Then both active and inactive layer compositions are updated; the bed becomes less rich in the size class of scour. This process is repeated for all size classes and at each cross section. For the same hydraulic conditions, it is possible to have aggradation in one size class and degradation in another.

The next section deals with the data used in testing this model, and calibration of the parameters involved.

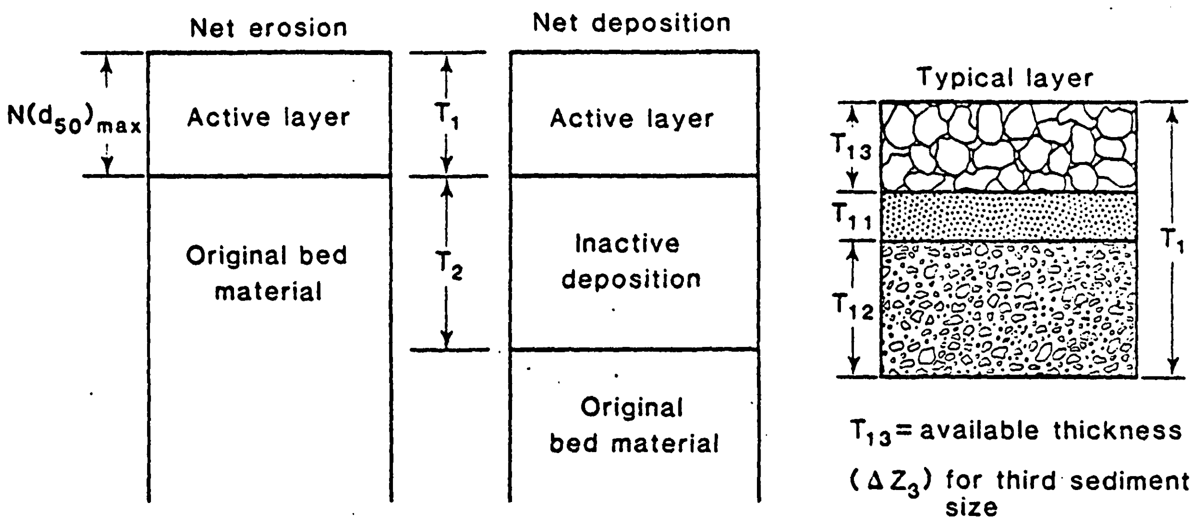

Figure 7.--Bed-composition accounting procedures.

BOUNDARY AND INITIAL CONDITIONS

Because no change in the bed level can be predicted at the upstream boundary cross section (fig. 4), it is used as an input section, and the actual transient reach consists of one less than the total number (NXT) of cross sections. Because the upstream stage is needed in calculation of the water surface slope (S) a stage-discharge relation must be provided. For this relation to be valid, as in the downstream-stage boundary condition, bed elevation must not change. If time history of the bed-level change is available, and a depth-area relation also, then the upstream or downstream cross section can be included in the transient reach.

In addition to the stage-discharge relation, the known-constant water discharge, the constant-total bed-material discharge per size class, and the average temperature of water in degrees Celsius are input per time step at the upstream section.

When just water, as opposed to sediment-laden water, is coming into the study reach, the total bed material discharge input is zero.

The initial bed levels, Chezy Cs, and size fractions in each size class must be given at each section (size class limits having been decided previously). The active width of transport must be supplied for each section; and area-depth and top-width-depth relations at each section must be provided.

The Rio Grande study reach is presented next as an actual example, followed by the calibration and application of the model to simulate the actual situation.

STUDY REACH AND THE DATA

Data were collected in the reach downstream from Cochiti Dam on the Rio Grande, because the bed was expected to change from a pre-dam profile to an eventual post-dam profile. Degradation is conjectured, because, in theory, the dam will trap most of the sediment, and the water discharged from the dam will have rejuvenated sediment-transport capabilities and should scour the bed more than previously.

The study reach is located approximately 64 km north of Albuquerque, New Mexico, and 35 km southwest of Santa Fe (fig. 8). The reach has 37 cross sections distributed throughout its 95-km length (fig. 9). Streamflow stations along the reach are downstream from Cochiti Dam, cross section 2; San Felipe, cross section 17; the Jemez River confluence, cross section 25; and Albuquerque, cross section 36. Isleta Diversion Dam is the downstream control point.

Elevations of bed and water surface are tabulated in table 1 for each of the 37 sections. Sediment in the reach is not supposed to be uniform grain size; although, downstream of the confluence of Jemez River, the reach is mostly sand. Average bed grain-size distributions for pre-dam and post-dam time intervals are presented in table 2.

Typical average bed-size distributions for cross sections 5, 20, and 34 are given in figure 10 for pre-dam conditions and in figure 11 for post-dam conditions. In addition to the typical grain-size distribution, hydraulic relationships between water-surface elevation and top-width, area, and discharge for cross section 2 are presented in figure 12.

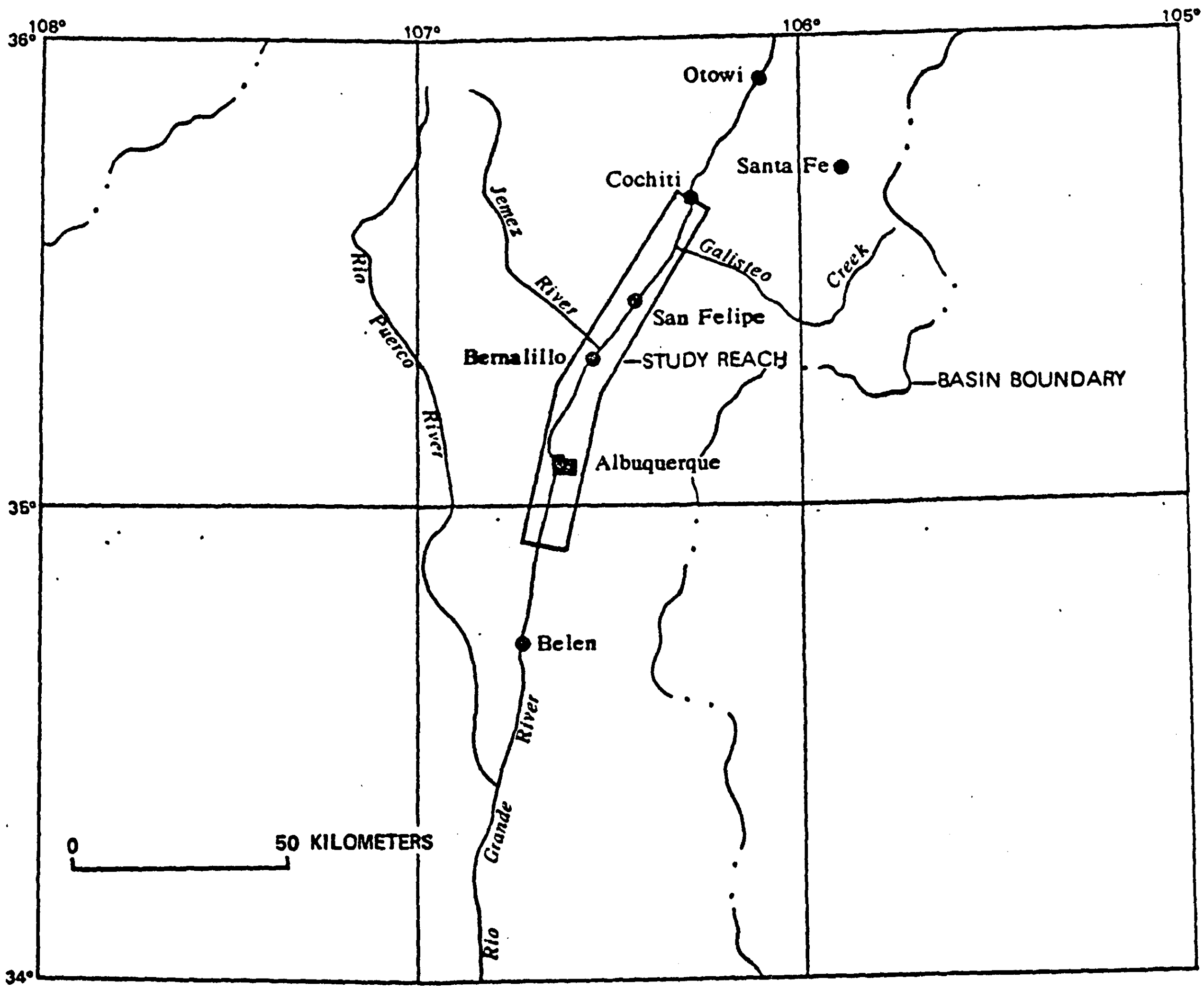

Figure 8.— Location of study reach.

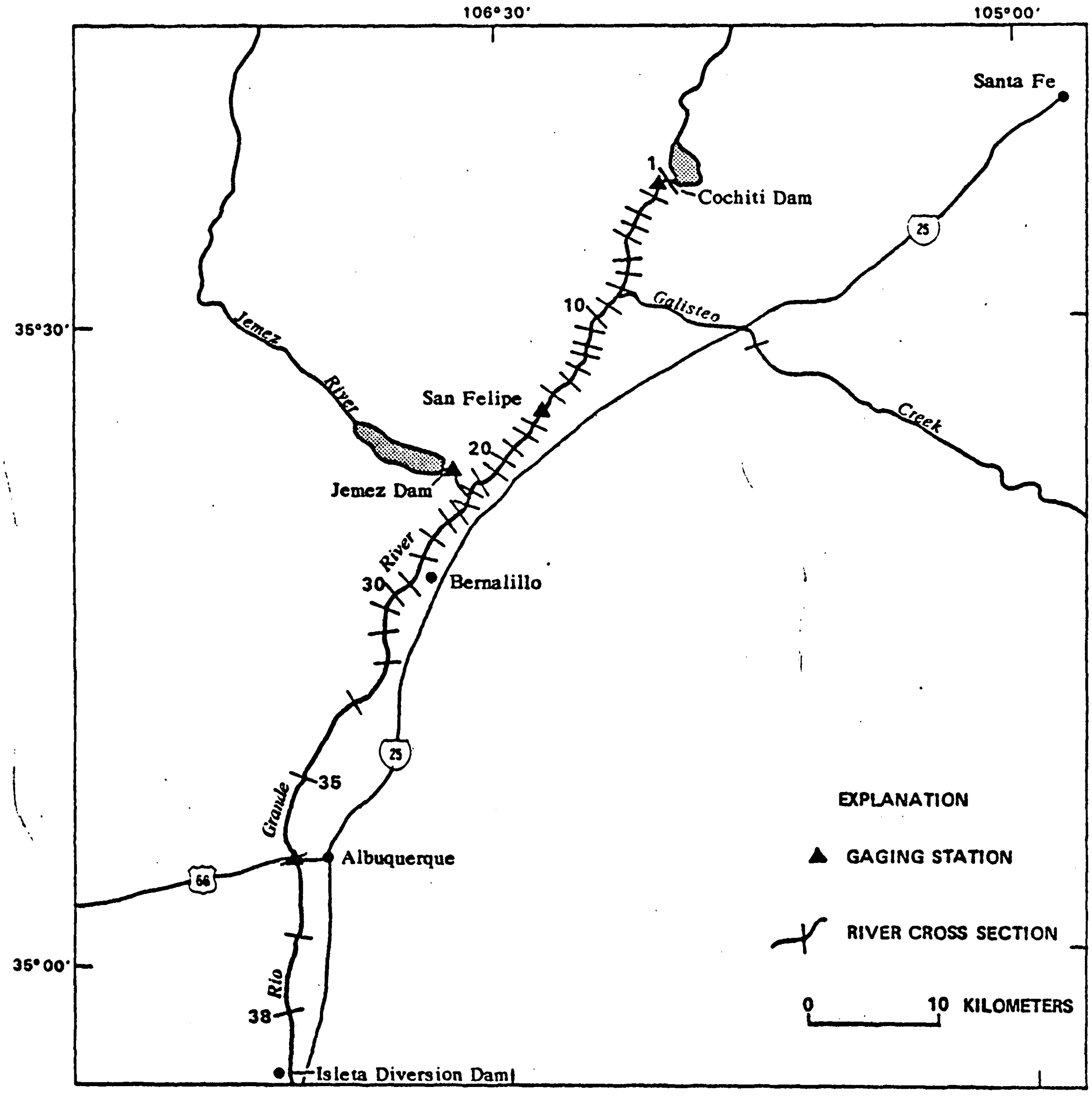

Figure 9.—— Location of cross sections.

Table 1.—*Pre-dam and post-dam bed and water-surface elevations at each cross section*

Cross-section number	Location downstream from dam (km)	Mean bed elevation (m)		Mean water surface elevation (m)	
		Pre-dam 5/11-26/73	Post-dam 5/22-31/73	Pre-dam 5/11-26/73	Post-dam 5/22-31/74
2	3.4	1,590.06	1,589.74	1,591.22	1,589.75
3	5.3	1,587.10	1,587.06	1,587.91	1,586.97
4	6.8	1,585.07	1,584.60	1,585.26	1,584.47
5	8.2	1,582.71	1,582.66	1,583.50	1,582.73
6	9.7	1,580.39	1,580.27	1,580.81	1,579.36
7	10.5	1,579.04	1,579.14	1,579.68	1,578.11
8	12.2	1,576.26	1,576.23	1,576.89	1,576.03
9	13.4	1,574.69	1,574.70	1,575.42	1,574.75
10	15.0	1,572.98	1,572.73	1,573.66	1,572.66
11	16.4	1,570.23	1,570.05	1,571.84	1,570.72
12	17.4	1,569.87	1,569.88	1,570.79	1,569.63
13	19.3	1,566.82	1,567.00	1,567.74	1,566.84
14	20.9	1,565.18	1,565.21	1,566.01	1,565.11
15	22.5	1,563.15	1,563.30	1,564.39	1,563.51
16	24.0	1,561.28	1,561.22	1,562.87	1,561.79
17	25.4	———	1,560.51	———	1,560.61
18	27.4	1,556.96	1,557.06	1,558.07	1,557.33
19	28.5	1,556.03	1,555.79	1,556.85	1,555.79
20	30.1	1,553.54	1,553.92	1,554.85	1,554.37
21	31.5	1,552.17	1,552.44	1,553.32	1,552.92
22	32.2	1,550.98	1,550.89	1,551.84	1,551.40
23	34.4	1,550.00	1,549.89	1,550.64	1,550.05
24	36.2	1,547.98	1,547.91	1,548.30	1,547.96
25	37.7	———	1,546.67	———	1,546.54
26	38.3	1,544.62	1,545.14	1,545.87	1,545.50
27	39.3	1,544.24	1,544.93	1,544.86	1,544.57
28	41.2	1,542.02	1,542.08	1,542.66	1,542.30
29	43.0	1,540.38	1,540.27	1,540.86	1,540.45
30	45.9	1,537.50	1,537.44	1,537.81	1,537.58
31	47.3	1,536.05	1,536.29	1,536.77	1,536.51
32	48.9	1,533.93	1,534.18	1,534.86	1,534.45
33	51.3	1,532.49	1,532.25	1,532.86	1,532.34
34	59.1	1,523.88	1,524.04	1,524.62	1,524.20
35	65.7	1,517.41	1,517.40	1,517.72	1,517.48
36	73.9	1,509.07	1,509.08	1,509.56	1,509.24
37	81.4	1,501.27	1,501.67	1,502.20	1,501.88
38	89.3	1,495.03	1,495.11	1,495.47	1,495.00

Table 2.—Average pre-dam and post-dam bed-size distributions at each cross section

Cross-section number		Percent finer than: 0.125 mm	0.25 mm	0.5 mm	1.0 mm	2.0 mm	4.0 mm	8.0 mm	16.0 mm	32.0 mm
2	Pre-dam	8.7	33.7	67.9	85.0	89.7	94.3	96.0	97.3	100.0
	Post-dam	——	1.0	37.0	68.0	86.0	96.0	99.0	100.0	——
3	Pre-dam	9.6	38.6	73.4	86.4	88.3	90.8	92.2	93.2	100.0
	Post-dam	8.3	10.5	23.5	39.0	75.8	38.5	95.0	97.8	100.0
4	Pre-dam	17.6	46.5	69.6	79.0	82.4	84.9	87.1	89.8	100.0
	Post-dam	1.0	16.0	58.0	71.0	86.5	95.0	99.0	100.0	——
5	Pre-dam	11.8	50.3	78.0	88.8	91.8	93.7	96.0	99.0	100.0
	Post-dam	1.0	13.0	38.0	62.0	71.0	82.4	90.4	95.8	100.0
6	Pre-dam	14.3	47.2	74.7	85.7	91.3	97.5	99.5	100.0	——
	Post-dam	4.0	16.0	45.0	69.0	80.0	88.0	96.0	100.0	——
7	Pre-dam	9.0	59.9	85.2	90.9	92.0	93.3	95.9	98.2	——
	Post-dam	——	1.0	31.0	68.0	91.0	99.0	100.0	——	——
8	Pre-dam	6.0	31.0	74.3	94.5	97.3	99.3	100.0	——	——
	Post-dam	1.0	2.5	17.0	36.3	57.8	74.0	85.3	92.5	100.0
9	Pre-dam	13.0	36.8	61.3	74.4	76.9	83.4	89.3	95.5	100.0
	Post-dam	9.7	19.9	36.3	54.4	65.9	71.9	77.3	85.1	92.9
10	Pre-dam	23.1	52.8	80.1	90.8	94.3	96.2	97.7	99.2	100.0
	Post-dam	3.4	9.9	39.1	61.8	74.6	84.9	92.2	98.3	100.0
11	Pre-dam	5.4	33.6	78.0	92.2	95.8	97.6	99.4	100.0	——
	Post-dam	1.0	6.4	51.4	74.6	87.6	94.0	97.6	99.4	100.0
12	Pre-dam	5.7	34.4	70.1	81.6	84.4	92.1	94.1	96.9	100.0
	Post-dam	1.8	5.0	33.0	62.3	77.8	84.3	88.5	92.8	94.5
13	Pre-dam	4.2	25.7	63.8	81.0	84.2	90.6	95.0	97.6	100.0
	Post-dam	1.0	2.8	28.2	57.3	74.2	83.2	88.6	93.0	96.6
14	Pre-dam	11.9	48.3	79.4	90.0	91.5	93.0	94.8	95.7	100.0
	Post-dam	2.3	10.2	48.0	78.0	91.7	97.2	99.5	100.0	——
15	Pre-dam	9.2	45.2	80.7	93.0	96.7	97.5	98.0	98.5	100.0
	Post-dam	3.3	10.5	62.8	90.8	97.0	98.8	99.3	100.0	——
16	Pre-dam	4.4	40.4	81.2	94.6	98.4	99.2	99.6	99.8	100.0
	Post-dam	1.0	5.0	41.5	76.2	90.7	96.3	99.2	100.0	——
17	Pre-dam	10.9	46.3	69.9	75.7	77.4	79.4	82.1	84.6	100.0
	Post-dam	9.0	12.7	62.0	85.7	95.0	98.7	99.7	100.0	——
18	Pre-dam	8.5	52.0	87.0	96.5	98.5	98.5	99.5	100.0	——
	Post-dam	4.8	23.0	74.0	92.8	98.0	99.6	100.0	——	——
19	Pre-dam	4.6	44.7	79.0	91.3	95.0	96.0	96.8	98.5	100.0
	Post-dam	1.3	6.8	58.7	79.3	90.3	95.2	97.5	99.3	100.0
20	Pre-dam	6.2	42.0	84.8	95.2	96.8	98.0	99.5	99.8	100.0
	Post-dam	1.0	9.3	59.6	84.1	93.6	97.4	99.4	100.0	——
21	Pre-dam	8.8	45.8	87.3	97.3	99.1	99.6	99.9	100.0	——
	Post-dam	1.1	11.1	64.4	84.1	91.5	95.3	97.5	98.6	100.0
22	Pre-dam	12.3	42.0	79.0	93.0	96.3	98.3	98.3	99.8	100.0
	Post-dam	2.2	14.2	71.5	89.8	94.8	97.5	99.0	99.7	100.0
23	Pre-dam	6.0	51.5	88.7	96.9	97.5	99.0	99.8	100.0	——
	Post-dam	5.0	21.7	72.1	85.7	94.0	96.7	99.0	100.0	——
24	Pre-dam	24.1	60.5	89.1	96.5	97.5	98.4	98.9	100.0	——
	Post-dam	3.8	30.1	79.1	90.4	94.6	96.3	97.1	97.6	100.0
25	Pre-dam	19.6	62.0	93.3	99.2	99.4	99.7	100.0	——	——
	Post-dam	2.4	27.3	79.4	90.6	93.0	94.3	96.0	98.2	100.0
26	Pre-dam	6.4	54.8	92.2	98.4	100.0	——	——	——	——
	Post-dam	1.8	26.6	84.0	94.0	97.0	98.0	98.6	98.8	100.0
27	Pre-dam	12.8	52.3	90.3	98.8	99.5	99.8	100.0	——	——
	Post-dam	4.0	32.0	79.6	90.6	94.4	96.8	98.6	99.4	100.0
28	Pre-dam	16.1	54.4	89.9	97.9	99.4	99.7	100.0	——	——
	Post-dam	3.0	28.8	81.6	92.2	96.4	98.2	99.0	99.6	100.0
29	Pre-dam	17.8	59.0	93.5	99.3	100.0	——	——	——	——
	Post-dam	11.6	41.8	89.8	97.6	98.8	99.8	100.0	——	——
30	Pre-dam	18.8	59.0	91.0	97.5	99.3	99.8	100.0	——	——
	Post-dam	4.0	36.0	84.8	93.0	95.8	97.0	98.4	99.8	100.0
31	Pre-dam	18.3	60.5	92.5	99.5	99.5	99.8	100.0	——	——
	Post-dam	4.4	35.6	81.4	91.2	93.4	93.6	96.8	98.6	100.0
32	Pre-dam	12.0	61.4	94.4	99.2	100.0	——	——	——	——
	Post-dam	3.0	34.0	87.6	96.2	99.2	99.8	100.0	——	——
33	Pre-dam	18.2	65.2	94.2	98.2	99.5	99.7	100.0	——	——
	Post-dam	6.4	41.2	86.0	95.3	98.4	99.6	99.6	100.0	——
34	Pre-dam	22.8	68.2	96.0	98.8	99.7	99.8	99.8	100.0	——
	Post-dam	5.6	45.2	88.0	94.8	96.2	97.0	97.4	99.0	100.0
35	Pre-dam	20.3	67.2	95.7	98.8	99.3	99.8	100.0	——	——
	Post-dam	9.5	54.5	91.8	97.7	98.8	99.5	100.0	——	——
36	Pre-dam	10.2	58.1	89.4	94.4	95.3	96.9	97.8	99.0	100.0
	Post-dam	4.0	45.0	88.2	97.1	97.6	98.8	99.4	99.9	100.0
37	Pre-dam	19.0	62.9	94.6	98.4	99.7	99.9	100.0	——	——
	Post-dam	11.0	60.0	92.8	98.8	99.6	99.8	100.0	——	——
38	Pre-dam	24.7	66.0	96.5	99.3	99.8	100.0	——	——	——
	Post-dam	8.8	55.6	94.4	99.4	100.0	——	——	——	——

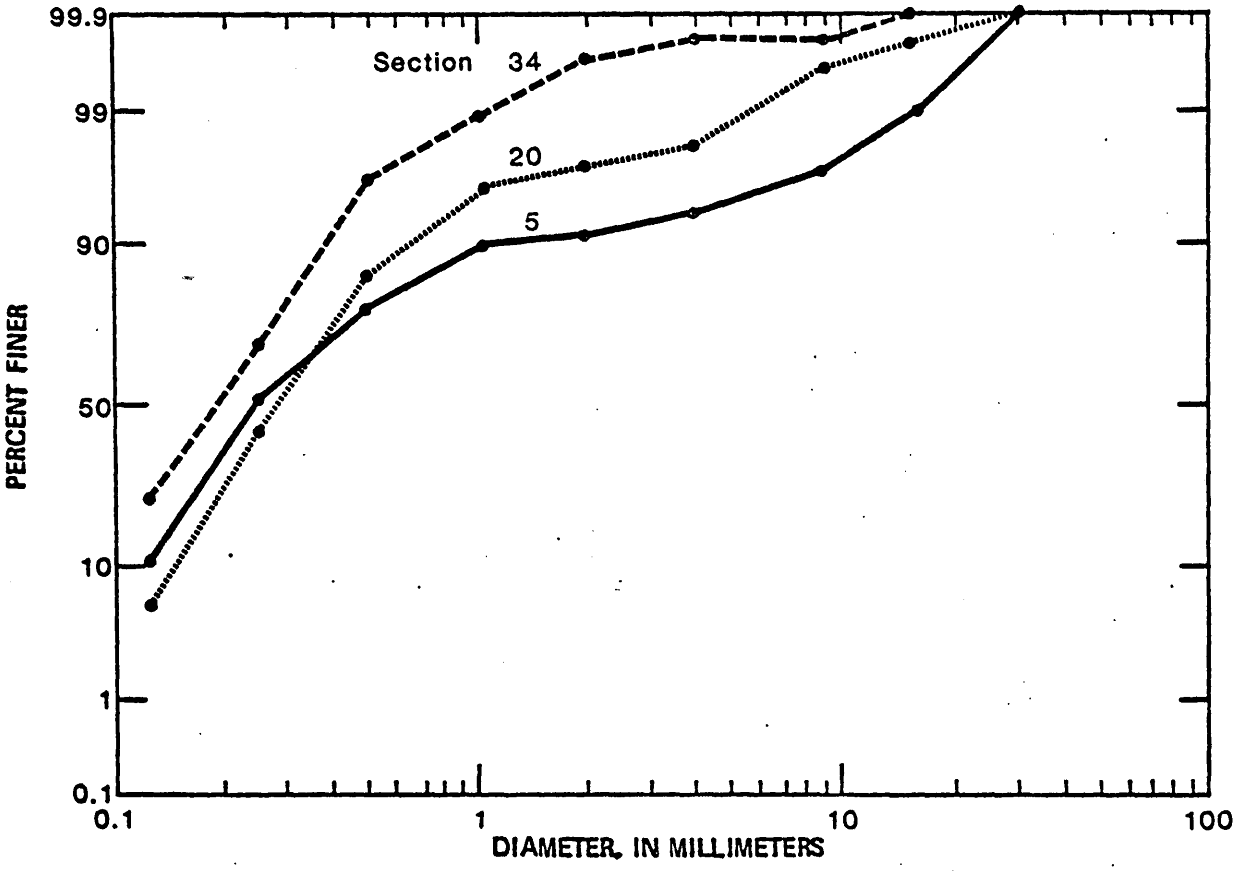

Figure 10.— Pre-dam average bed-size distributions (cross sections 5, 20, and 34).

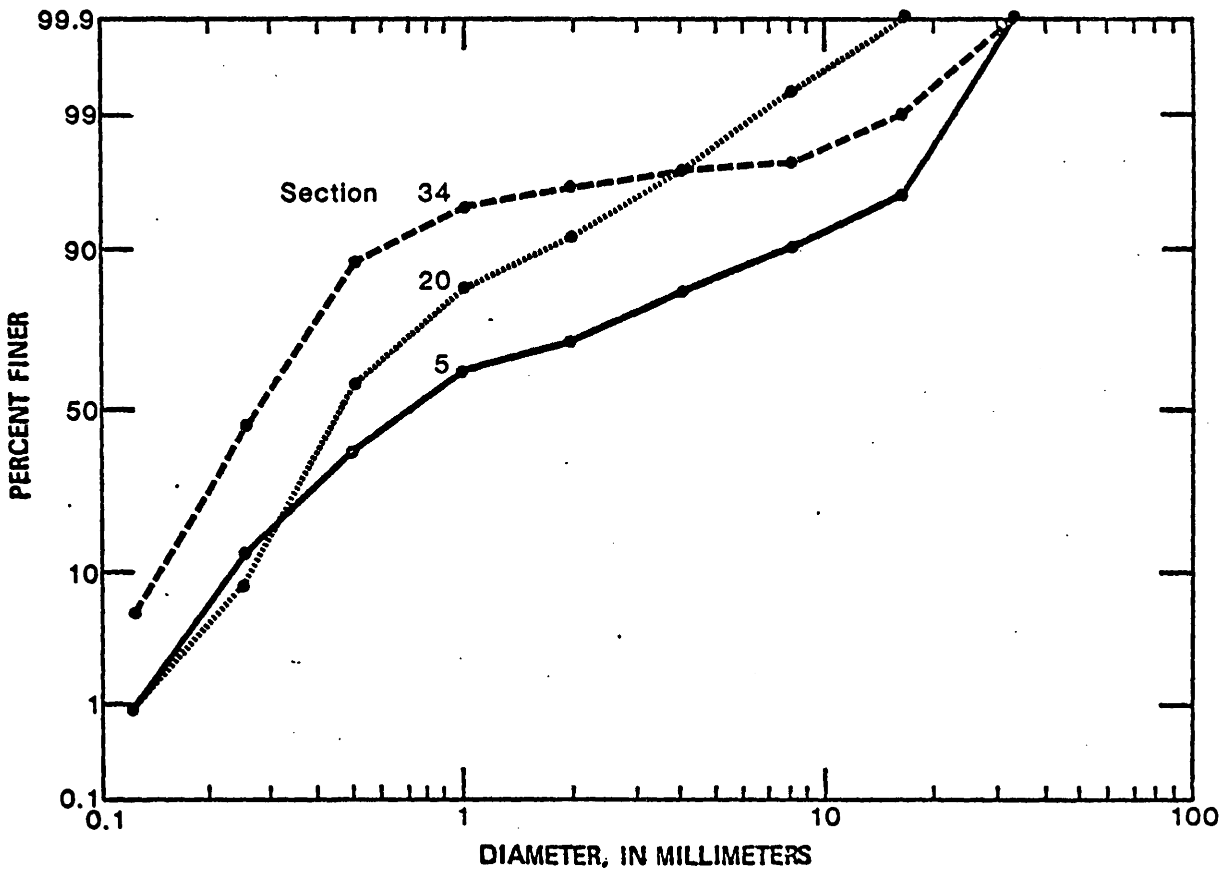

Figure 11.-- Post-dam average bed-size distributions (cross sections 5, 20, and 34).

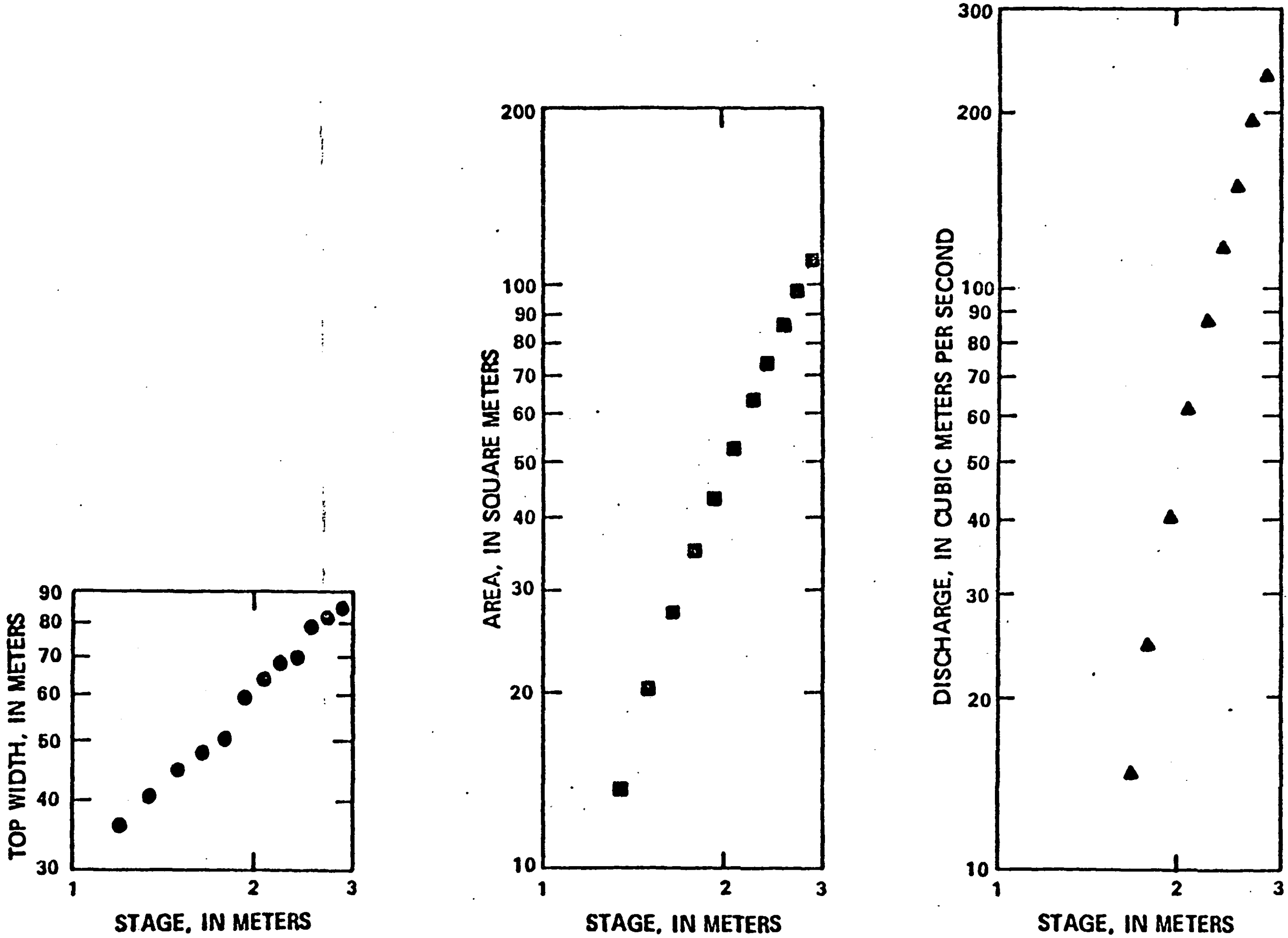

Figure 12 .-- Hydraulic relationships at cross section 2, June 1973.

There are flow losses along the reach due to irrigation, and additions due to tributaries and storms. Hydrographs of water discharge varying with time at Cochiti, San Felipe, and Albuquerque are shown in figure 13. Variations in suspended-sediment concentration, water temperature, and discharge at Albuquerque are shown in figure 14.

During the period of data collection, maximum flow was measured in the summer of 1973. During June, 1973, the maximum average velocity measured was 2.1 m/s at cross section 13, and the minimum was 1.1 m/s at cross section 34.

APPLICATION

Impoundment of water at Cochiti Dam began on November 12, 1973. Some data were collected on or about November 19 on the upper part of the reach only. Comparison of the mean bed elevations at those sections measured both on or about November 19, and on or about June 11, 1973, revealed a minimal difference; the record of June 11-26, 1973, was fairly complete also. Hence, the June 1973 cross-section descriptors, Z_i, A_i, T_i, were used in both pre-dam calibration and in post-dam prediction runs.

Because it was possible to accurately reproduce the water-surface profile from June 11-26, 1973, and the discharge ranged from 99 to 170 m^3/s indicating relatively large sediemnt-transport rates, this time period was considered adequate for calibrating the active-layer thickness parameter, N.

For both pre-dam and post-dam simulations, the Albuquerque cross section was made the downstream boundary point, because little bed change was osberved at that cross section or farther downstream. A stage-discharge rating curve valid for the simulated time period provided the necessary boundary condition.

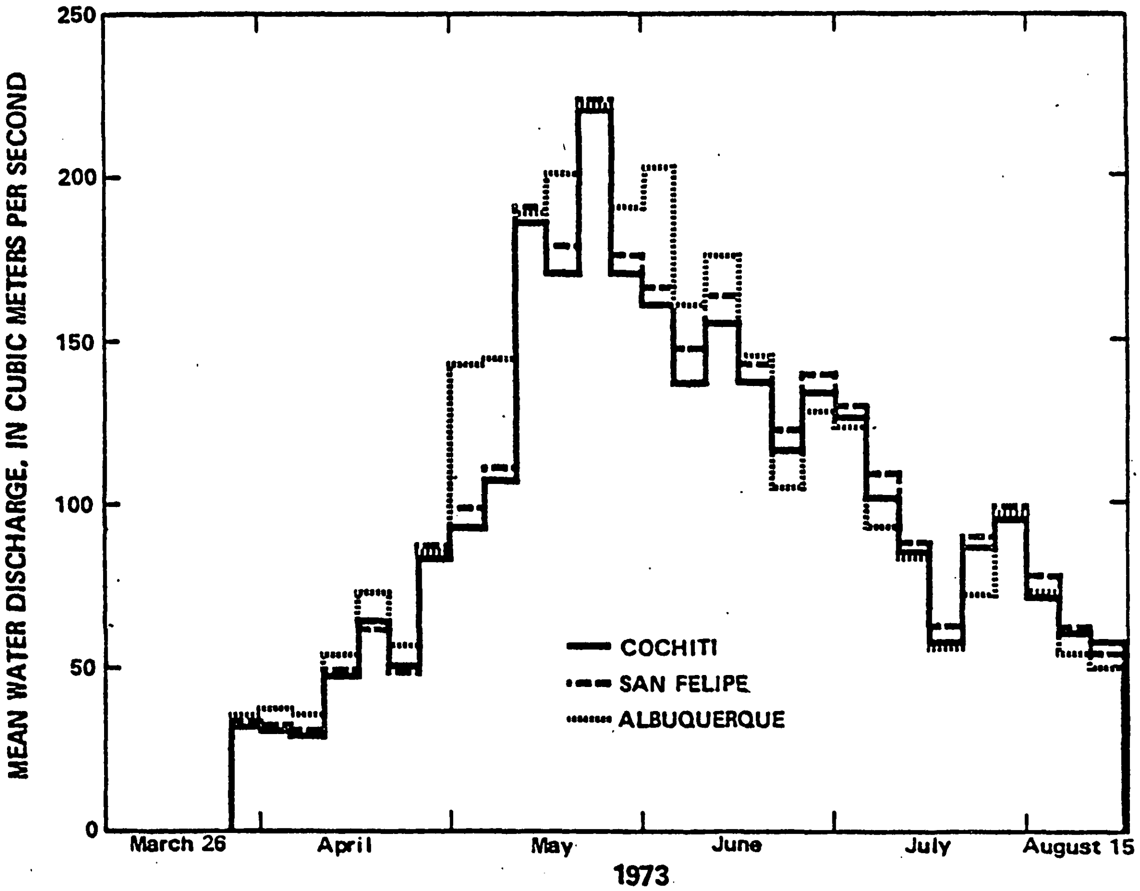

Figure 13.— Discharge variation downstream from Cochiti Dam.

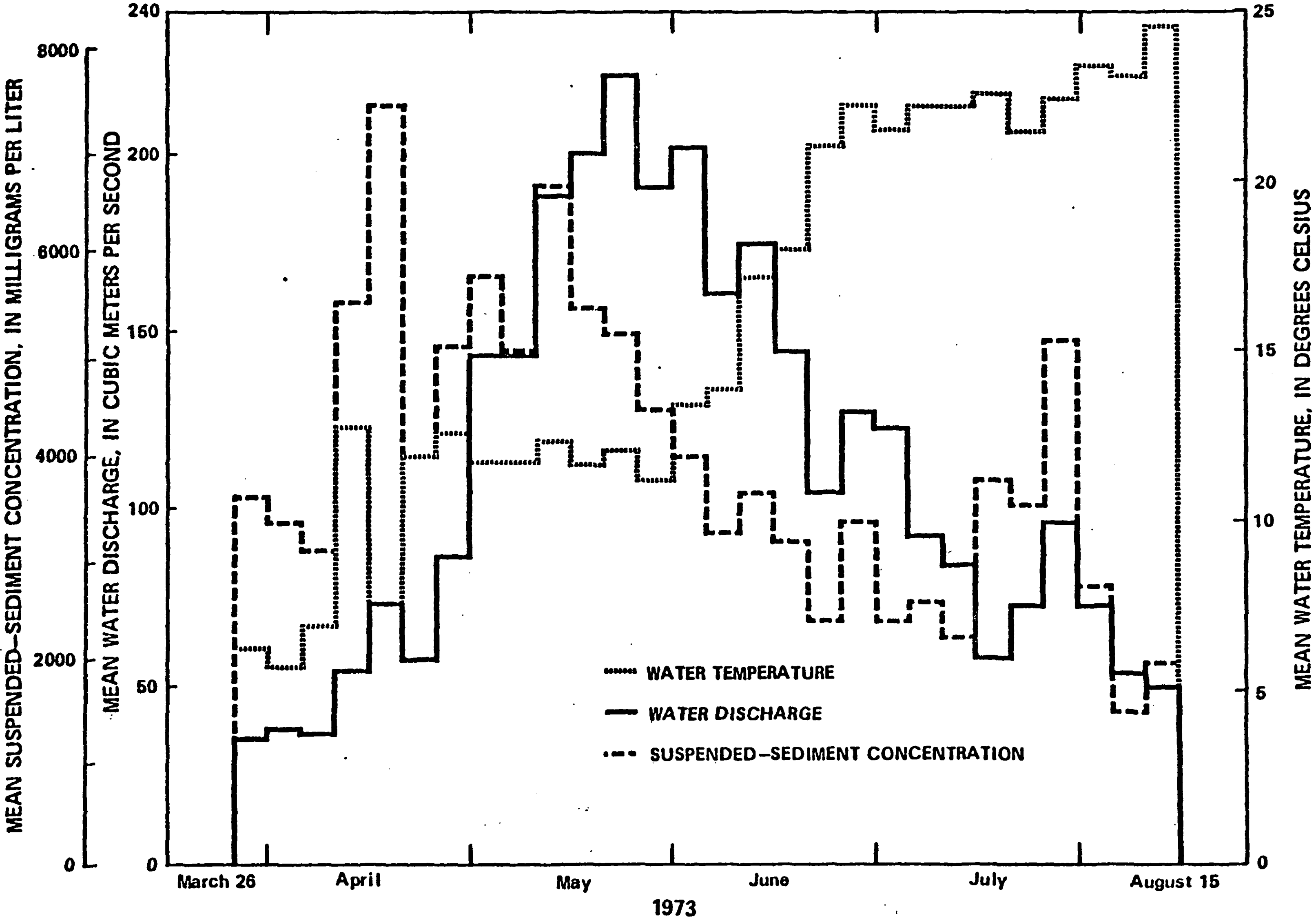

Figure 14.-- Suspended-sediment concentration, water temperature, and discharge variations at Albuquerque.

The upstream boundary point for the pre-dam simulation was cross section 2. There, a stage-discharge rating curve provided the upstream stage boundary condition, and the bed material per size class per time step was used in the model. In the post-dam simulation the upstream boundary was 305 m downstream from the dam. Given the discharge, a new rating curve determined the stage at that point, and no sediment was input to the reach.

A time step of at least 1 day is desirable, and the input daily (also, monthly, yearly) average discharge and water temperature at Cochiti were obtained from reports by the U.S. Geological Survey (1973, 1974, 1975, 1976). Water discharges at San Felipe, cross section 17, and at Jemez River confluence, cross section 25, also were input; the total reach was subdivided into three smaller subreaches (see section on solution method).

There were not sufficient data in the report by Dewey, Roybal, and Funderberg (1979) to determine the discharge-dependent sediment transport per size class at cross section 2 (the boundary cross section for the pre-dam simulation); that is, a bed-material discharge rating curve. Those data from the report that could be used with the bulk of the points and data from Nordin and Beverage (1965, tables 2, 8, 13, and 14) comprised a data set on which a discharge-transport relation per size class was developed (fig. 15a and 15 b and tables 3, 4, 5, and 6).

Initial bed elevations were determined from data in Dewey, Roybal, and Funderberg (1979) for each cross section. The active width at each cross section was selected as that width in which there is vertical movement of the bed, based on the cross-section depictions in Dewey, Roybal, and Funderberg (1979).

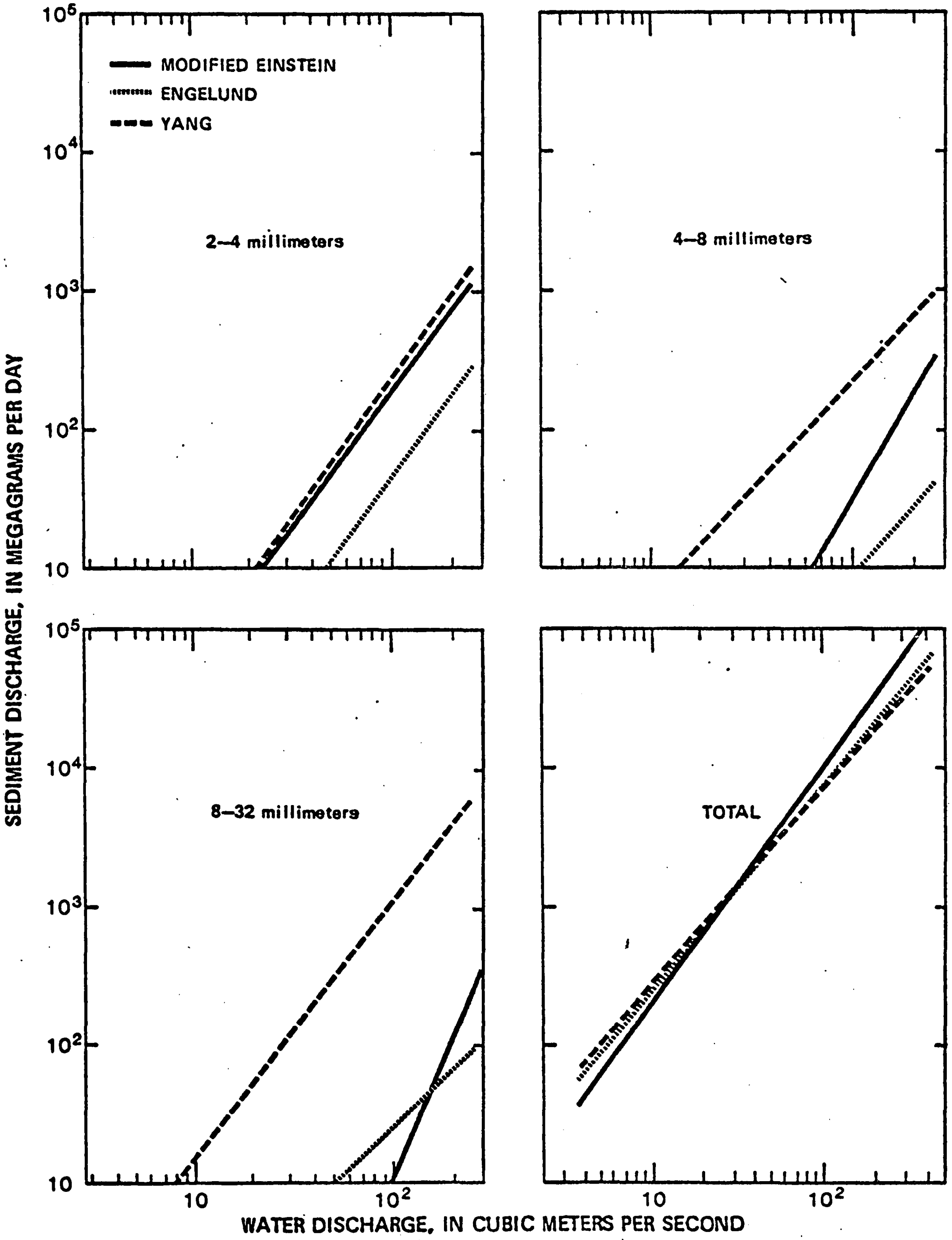

Figure 15b.— Sediment-load comparisons by size class at Cochiti Dam (Continued).

Table 3.—*Hydraulic data base for modified Einstein computation in figure 14 at Cochiti*

Date	Q (ft^3/s)	W (ft)	D (ft)	V (ft/s)	Temp °C	S
6-11-73	5,130	268	3.52	5.44	10.0	0.00078
5-12-70	2,640	196	2.71	4.97	16.5	.00128
5-03-71	1,100	135	2.36	3.45	18.0	.00119
3-20-72	1,700	128	2.99	4.44	11.5	.00080
11-10-72	1,230	133	2.16	4.28	7.0	.00089
5-29-56	943	233	1.31	3.09	18.9	.00129
4-03-56	964	300	1.44	2.23	8.3	.00129
6-22-61	674	280	1.09	2.21	24.4	.00128
5-18-61	2,620	281	2.39	3.90	15.0	.00137
5-02-61	3,680	288	2.82	4.53	13.9	.00137
4-26-61	2,090	282	2.18	3.40	11.1	.00134
6-24-58	1,000	263	1.71	2.22	23.9	.00118
6-17-58	2,040	285	2.24	3.20	21.1	.00118
6-12-58	5,060	298	4.03	4.21	17.2	.00113
6-09-58	4,990	297	3.64	4.62	16.7	.00123
6-03-58	8,680	295	4.85	6.07	17.0	.00127
5-26-58	9,810	335	4.39	6.67	16.0	.00127
5-20-58	8,920	316	4.34	6.50	14.0	.00120
5-12-58	8,900	328	4.09	6.63	14.0	.00120
5-07-58	7,960	308	3.93	6.58	12.8	.00129
6-26-57	4,800	291	3.13	5.27	19.4	.00129
6-12-57	5,520	297	3.31	5.62	16.7	.00129
5-29-57	3,350	287	2.51	4.65	17.0	.00129
5-16-57	3,470	283	2.55	4.81	12.2	.00129
12-29-54	464	124	1.65	2.27	2.2	.00129
12-15-54	327	115	1.43	1.99	3.3	.00129
11-17-54	347	115	1.49	2.03	9.4	.00129
10-19-54	294	100	1.60	1.84	14.4	.00129
10-05-54	144	88	1.18	1.39	22.2	.00129
9-23-54	68	77	.91	.97	21.7	.00129
9-08-54	500	178	1.50	1.87	21.1	.00129
8-24-54	252	175	.96	1.50	21.1	.00129
8-10-54	264	172	1.02	1.50	22.8	.00129
7-12-54	784	295	1.24	2.14	25.0	.00129
6-01-54	881	300	1.34	2.19	19.4	.00129
5-20-54	1,590	284	1.89	2.96	19.4	.00129
5-04-54	1,170	300	1.73	2.25	17.0	.00129
5-20-54	709	300	1.22	1.94	14.4	.00129
4-07-54	541	288	.98	1.92	14.4	.00129
3-23-54	309	177	1.01	1.73	10.6	.00129
3-10-54	416	208	1.17	1.71	12.2	.00129
6-14-54	667	204	1.73	1.39	18.3	.00129

Table 4.—Measured suspended size class distribution (in percent); total average concentration (in parts per million), at Cochiti

Date	Size class distribution (percent)						Total Concentration (C') (pp/m)
	.002–0.0625 mm	0.0625–0.125 mm	0.125–0.25 mm	0.25–0.5 mm	0.5–1.0 mm	1.0–2.0 mm	
6-11-73	18	28	43	9	2	0	1210
5-12-70	32	31	32	5	0	0	1920
5-03-71	32	8	10	35	15	0	1080
3-20-72	16	18	18	32	16	0	1990
11-10-72	22	35	27	16	0	0	2270
5-29-56	31	40	27	2	0	0	969
4-03-56	25	8	7	28	27	5	5000
6-22-61	80	5	11	4	0	0	153
5-18-61	11	5	20	37	23	4	2750
5-02-61	56	12	23	8	1	0	2379
4-06-61	41	12	36	11	0	0	1210
6-24-58	43	18	35	4	0	0	247
6-17-58	4	1	24	45	25	1	5240
6-12-58	1	3	21	25	38	12	8840
6-09-58	7	4	17	21	46	5	7670
6-03-58	17	14	29	22	18	0	3110
5-26-58	32	27	27	7	5	2	3110
5-20-58	36	26	28	9	1	0	3110
5-12-58	41	28	23	5	3	0	4350
5-07-58	45	19	24	7	3	2	6090
6-26-57	14	8	29	29	16	4	3940
6-12-57	20	5	11	22	32	10	5410
5-29-57	19	13	31	24	13	0	2770
5-16-57	26	23	36	11	4	0	2550
12-29-54	32	21	26	21	0	0	561
12-15-54	28	15	39	18	0	0	362
11-17-54	40	32	21	7	0	0	637
10-19-54	41	13	29	17	0	0	182
10-05-54	78	17	5	0	0	0	186
9-23-54	69	8	19	4	0	0	118
9-08-54	90	6	4	0	0	0	3130
8-24-54	99	0	1	0	0	0	2920
8-10-54	53	9	15	19	4	0	750
7-12-54	88	7	5	0	0	0	1270
6-01-54	55	31	13	1	0	0	425
5-20-54	60	28	10	2	0	0	2000
5-04-54	78	14	7	1	0	0	1780
4-07-54	89	2	3	6	0	0	290
3-23-54	81	2	7	9	1	0	57
3-10-54	46	2	23	29	0	0	83
6-14-54	40	33	24	3	0	0	298

Table 5.--*Representative average bed-size distribution on Conchiti for the pre-dam modified Einstein computation*

[Average bed-size distribution in percent]

0.002-0.0625 mm	0.0625-0.125 mm	0.125-0.25 mm	0.25-0.5 mm	0.5-1 mm	1-2 mm	2-4 mm	4-8 mm	8-32 mm
1	3	18	42	17	5	3	2	9

Table 6.--*Bed material rating curves*

[Q_s megagrams per day, Q in cubic meters per second]

Relation	Location	a	b	Standard error (Log units)
$Q_{s_1} = aQ^b$	X-sec. 2	0.631	2.01	0.35
$Q_{s_2} = aQ^b$	X-sec. 2	0.770	1.97	0.44
$Q_{s_3} = aQ^b$	X-sec. 2	0.425	1.91	0.42
$Q_{s_4} = aQ^b$	X-sec. 2	1.28×10^{-2}	2.30	0.44
$Q_{s_5} = aQ^b$	X-sec. 2	2.07×10^{-2}	1.93	0.30
$Q_{s_6} = aQ^b$	X-sec. 2	3.24×10^{-3}	2.44	0.39
$Q_{s_7} = aQ^b$	X-sec. 2	1.72×10^{-6}	3.36	0.40
$Q_s = aQ^b$	X-sec. 2	1.92	1.99	0.35
$Q_s = aQ^b$	X-sec. 36 (1973)	15.8	1.56	0.13
$Q_s = aQ^b$	X-sec. 36 (1974-75)	1.66	1.71	0.21

The size classes considered were: 0.125-0.25 mm, 0.25-0.5 mm, 0.5-1.0 mm, 1.0-2.0 mm, 2.0-4.0 mm, 4.0-8.0 mm, and 8.0-32.0 mm. The representative diameter of each class is the mean of the size class limits, except in the coarsest class, where the representative diameter was chosen as 12 mm. These limits were chosen because particles finer than 0.125 mm (washload) are postulated to be transported through the reach. Such transport is not described by the bed-material transport function, (eq. 8); and these limits are the ones used in the modified Einstein computation of total load (Colby and Hembree, 1955), which produced the observed load that the transport function predictions were compared with at cross section 2.

Average pre-dam and post-dam size distributions were obtained from the data report, and size fractions were determined for the above-named size classes (fig. 2). Average pre-dam size fractions were used as initial size fractions in both simulations, assuming that average post-dam distribution will be arrived at by the end of the post-dam simulation.

CALIBRATION

The parameters to be calibrated are Chezy C in the flow equation, and mixing-layer thickness parameter N in the armoring simulation. In addition, two possible parameters of calibration in Engelund's equations are investigated. Yang's equation is in its final form and has already been calibrated, in the sense that it agrees quite well with certain data.

Engelund's Parameters

The Engelund parameters are bedload thickness, a, and fall velocity-shear velocity-ratio criterion for suspension, $\frac{\omega}{V*}$. In the proposed version of Engelund's formulation, a is taken as 2d; and $\frac{\omega_m}{V*}$ must be less than 0.8 for suspension; although in this study, $\frac{\omega_m}{V*}$ was taken to be less than 1 for suspension. The proposed version is plotted in figures 15a and 15b, with Yang's predictions, to test their agreement with the observations per size class at section 2. Although agreement is good (standard error is less than standard deviation, and trend lines are close) in the first size class, 0.125-0.25 mm, and in the total load comparison, the other figures show the simulated loads noticeably lower than the observed loads. This is due primarily to the lack of suspended load in the coarser size classes in Engelund's formulation. A coarse suspended load is computed in the modified Einstein computation.

Einstein (1950) points out that: if $\frac{\omega_m}{V*} > 2$, the suspended load is insignificant compared with the bedload; and, the load in that size class is essentially bedload. The velocity ratio limit of 2 for suspension gives better results, in that suspended load is predicted in size classes 2 as 0.25-0.5 mm, and in size class 3, as 0.5-1.0 mm; this is supported by measured suspended-size analysis on the Rio Grande (table 4).

Recomputing with the velocity ratio criterion as 2, the total suspended load obtained is found to be considerably less than that obtained when the velocity ratio criterion is 1. This is due to normalization, which will tend to enlarge the original bedloads, q_{b_m}, and decrease the original suspended loads, q_{s_m}'. This occurs because the bedload calculated using the mean diameter of the total material is larger than the sum total of the bedloads computed by size class; in the case of suspended load, the suspended load computed using the effective fall velocity is less than or equal to the sum total of the suspended loads computed by size class, especially if the velocity ratio limit is large. If normalization is to be obtained, the velocity ratio must be low rather than high; therefore, the value of 1 was kept.

The other alternative is to discard normalization altogether, and compute loads per size class, the sum of those loads being the total load. By adjusting the bedload thickness layer, a, good agreement with the modified Einstein computations was obtained in the size classes for which the concentration at the bed was significant. In the coarser size classes, there was no improvement in agreement because of the very small concentrations at the bed; in fact, normalization gives better agreement because computed bedloads are increased. If a was made to increase with size class, however, predicted trend lines in the first three size classes tended to approach observed trend lines; for instance, in the 0.25-0.5 mm class, a was taken as 7d; whereas, in the 0.125-0.25 mm class, a was found to be 3d. This tendency does not seem to be substantiated in nature; one would expect coarser particles to travel closer to the bed.

Also in Engelund's approach, the predicted concentration at the bed is not dependent on bedload layer thickness, but is based solely on dimensionless shear stress. This is in contrast to Einstein's computation (1950) of concentration at the bed, wherein concentration would decrease if the bedload layer were increased, due to increased water flow through the bedload zone. Hence, a is not a reasonable calibration parameter.

Chezy C

Starting from the downstream section, 36, and working up the reach with the backwater equation, it was possible to reproduce the actual June 1973 water surface profile. The computed profile was within 0.03 m of the observed stage and the computed velocity was within 0.03 m/s (meter per second) of the observed velocity at each section. The values of Chezy C so determined were the initial values in the pre-dam investigation.

However, upon iteration of Chezy C at a section with equation 6, supercritical flow and an unrealistic profile resulted. To prevent this, the water-surface slope in equation 6 should be replaced by the energy gradient between sections. Indeed, when the June 1973 profile was accurately reproduced, the backwater equation was employed in the following manner:

$$C_1 = \frac{V_1}{\sqrt{(2E-S_{f_2})D_1}}\ , \qquad (41)$$

where

$$E(\text{the energy gradient between sections}) = \frac{-(TH_2-TH_1)}{\Delta x_1}\ ,$$

$$S_{f_2} = \frac{V_2^2}{C_2^2\ D_2}\ ,$$

and 1 denotes the upstream section and 2, the downstream section. Equation 41 is plotted in figure 19 for sections 22 and 23. The graph of equation 41 is a hyperbola, with a horizontal asymptote of $C_1 = \frac{V_1}{\sqrt{2ED_1}}$ and a vertical asymptote of $C_2 = \frac{V_2}{\sqrt{2ED_2}}$. For instance, on the reach between section 22 and section 23, if 66 is taken as the Chezy C at section 23 and a certain energy gradient is imposed, then 31 is the corresponding Chezy C at section 22. The value $\frac{V_2}{\sqrt{ED_2}}$ as C_2, gives $\frac{V_1}{\sqrt{ED_1}}$ as C_1, and turns out to be the symmetrical ordered pair, (47, 38) in figure 16.

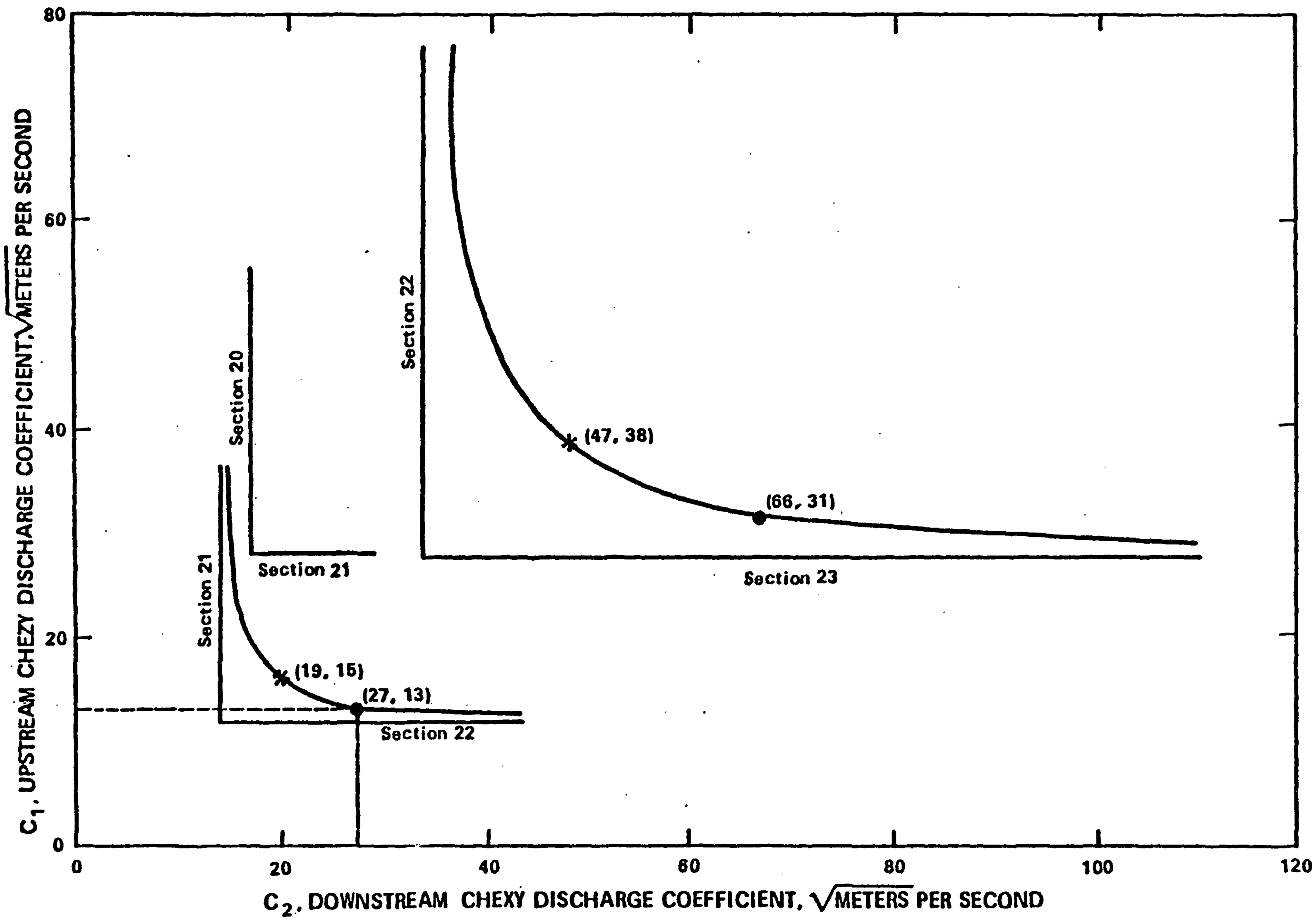

Figure 16.-- Coupling of Chezy C based on the backwater equation.

For the pre-dam case, it was possible to find one Chezy C at each section that satisfied both the downstream- and upstream-energy head constraints; in the post-dam case, this was not possible, because of the change in the depth-area and depth-top width relations that cannot be simulated. The cross section only rises and falls; it is geometrically preserved. Also, the June 1973 profile was obtained under high flows with overbank flow occurring at some sections, thus giving a loose constraint, in that convergence will occur no matter what Chezy C is in force at the overflow section.

As an example of the post-dam instability in Chezy C at a section, refer to figure 19. Under the energy gradient from section 22 to section 23, C_1 must be greater than 27 (the horizontal asymptote); but, if C at section 22 is taken as 27 or more, then under the energy constraint from sections 22 to 21, C at section 21 must be less than 13 and greater than 11, which does not intersect the defined region (C_2 >17) for the upstream reach (section 21 - section 20).

It was decided in the post-dam case to couple values of Chezy C at a section, one for the downstream subreach and one for the upstream subreach. For example, in figure 16, section 22 would have 38 (from section 23) and 19 (from section 21). It was also found that if the coupled values detemined from the data of May 1974 (the first complete post-dam record encountered) were compared to those coupled values determined from the November 1975 data, there was little difference. Nordin and Beverage (1965) pointed out that for sand-bed sections on the study reach, there were distinct groupings of Chezy C below 60 m^3/s and above 99 m^3/s; the apparent agreement seems to support this premise, since both data records were taken at low flow (less than 60 m^3/s).

Therefore, assuming the post-dam transient will exhibit the same flow regime, dependent Chezy C, it was decided not to change Chezy C at a section in either the post-dam or pre-dam case, unless a new flow regime comes into effect.

The area-depth and top width-depth relations are stored as arrays in the computer, and intermediate values are linearly interpolated between the 0.1525 meter increments. The starting value for the Newton iteration is set to the smallest depth tabulated at each section, and convergence is achieved in 15 iterations or less, with a tolerance of 0.0003 meter between iterated depths. Analytically, the discretized backwater equation or function, $F(Y_i)$ (eq. 10) is large positive and decreases to within a small tolerance around zero.

Utilization of arrays is especially conducive to simulation of overbank flow at a section. In most cases of overbank flow, a maximum energy head is in effect; that is, velocity and stage do not increase beyond a certain point, and overflow does not contribute to sediment transport in the channel. Hence, iteration for the depth is cut off at the maximum value tabulated, representing the maximum edge of channel.

The backwater routine must be convergent over a wide range of flows in this simulation, that is, from 4 m^3/s to 170 m^3/s. For certain extreme flows, a Chezy C at a section is too high, inferring no resistance and a relatively large velocity. The iteration will try to converge to a depth less than that tabulated in the array. Analytically, equation 10 becomes negative and the derivative stays negative, thus plummeting the iterated depth below the least tabulated value. For this to occur at high flows, Chezy C must be on the order of 330; this problem is not encountered in simulation. For low flows of 10 m^3/s or less, a Chezy C of 33 could be too large. To counteract this problem, the interation is simply terminated at the smallest depth tabulated if continued iteration causes C to decrease beyond the feasible region for a section. There is no serious side effect of this procedure, because the load flux gradient for such low flows is so low that it will result in zero bed change.

Parameter N

Parameter N (originally developed as an integer multiple of the largest representative diameter of the size classes) is the controlling parameter in the sediment routing process because it limits the amount of material available for scour. In addition, the value of N, with the sequential nature of the routing process, controls aggradation.

In the routing process, the bed-material load difference over a Δx is computed per size class, based on the initial size fractions (ϕ_m) of the time step. After the load difference is translated into ΔZ_m by equation 40, then ΔZ_m is added or subtracted from the active layer at a section, depending on the sign of the load flux difference, starting with $m = 1$, until all size classes are routed. Since compsition of the active layer has changed as a result of the single routing, the compositions (which are the thicknesses available for transport) must be updated. Routing of one sediment size affects all subsequent routings of coarser sizes; that is, if there are 5 size classes, then each size fraction will change 5 times between t and $t + \Delta t$.

The following observations result from the non-simultaneous simulation process described above:

1. The active layer thickness is not a limit on the total net bed scour at a section (ΔZ_i).

2. The final fraction for any size class can be zero only through aggradation in another size class.

3. Because of (2) above, net aggradation can be made to vary by adjustment in the active layer thickness; however, net aggradation, which is the sum of the bed changes per size class, must have at least one negative term (degradation in a size class).

4. As a result of both degradation and aggradation being regulated by N, and the sediment routing procedure being upstream dependent, N is a load calibration factor at a section.

5. Due to 4, for the same hydraulic conditions and initial size distribution at a section, different loads can be produced, depending on N. The larger N, the larger load at a section, up up to the load predicted by the transport function; after that, there is no change in the load, and correspondingly, no regulation.

6. N determines the change in size fraction; that is, the larger N, the less change in ϕ; and the smaller N, the more change in ϕ.

Bennett and Nordin (1977, p. 560) mention that "the parameter N is related to Δt; the larger Δt, the smaller N must be to yield the same predictions". Deigaard (1978) however, employing a different size-composition accounting scheme, sets the active-layer thickness equal to the dune or bed-form height regardless of time step size. In any case, the best value of N must be determined by comparison of predicted loads with observed loads in the pre-dam run, at some control section where measured total load data exist.

Albuquerque was the obvious candidate for the control section because many measurements existed; it was also an element of the transient reach, in the sense that the loads simulated there would be affected by N. The data were instantaneous measurements of total load, including wash load, but a good estimate of the bed material load (>0.125 mm) could be obtained because the measured suspended sediment size distribution was presented, and the reference size in the modified Einstein computation was 0.125-0.25 mm.

There were enough measurements at Albuquerque to determine a discharge-total bed-material discharge rating curve. The measurements for the pre-dam rating curve were taken from the data report (Dewey and others, 1979), while those for the post-dam rating curve were taken from the Water Resources Data for New Mexico (1974, 1975, 1976). Therefore, at Albuquerque, an average bed-material load is ascribed to a given average discharge. This is more desirable than comparing simulated average loads to instantaneous measurements. The rating curve derived was consistent in magnitude with those discharge-total bed-material relations discussed by Nordin and Beverage (1965).

When N = 14, the active layer is 168 mm and there was no availability limit at Albuquerque. As can be seen in figure 17, Yang's equation compares well with the observed, and Engelund's does not. This is misleading, however, since Yang's equation is correlated with discharge (eq. 17) and the "observed" points are actually based on discharge from the sediment rating. Engelund's equation with normalization does not compare well with the modified Einstein computation of the Rio Grande because the trial-and-error determined Rouse numbers (z) for the modified Einstein computation are much smaller than those calculated by equation 25 in the Engelund formulation. In an effort to boost

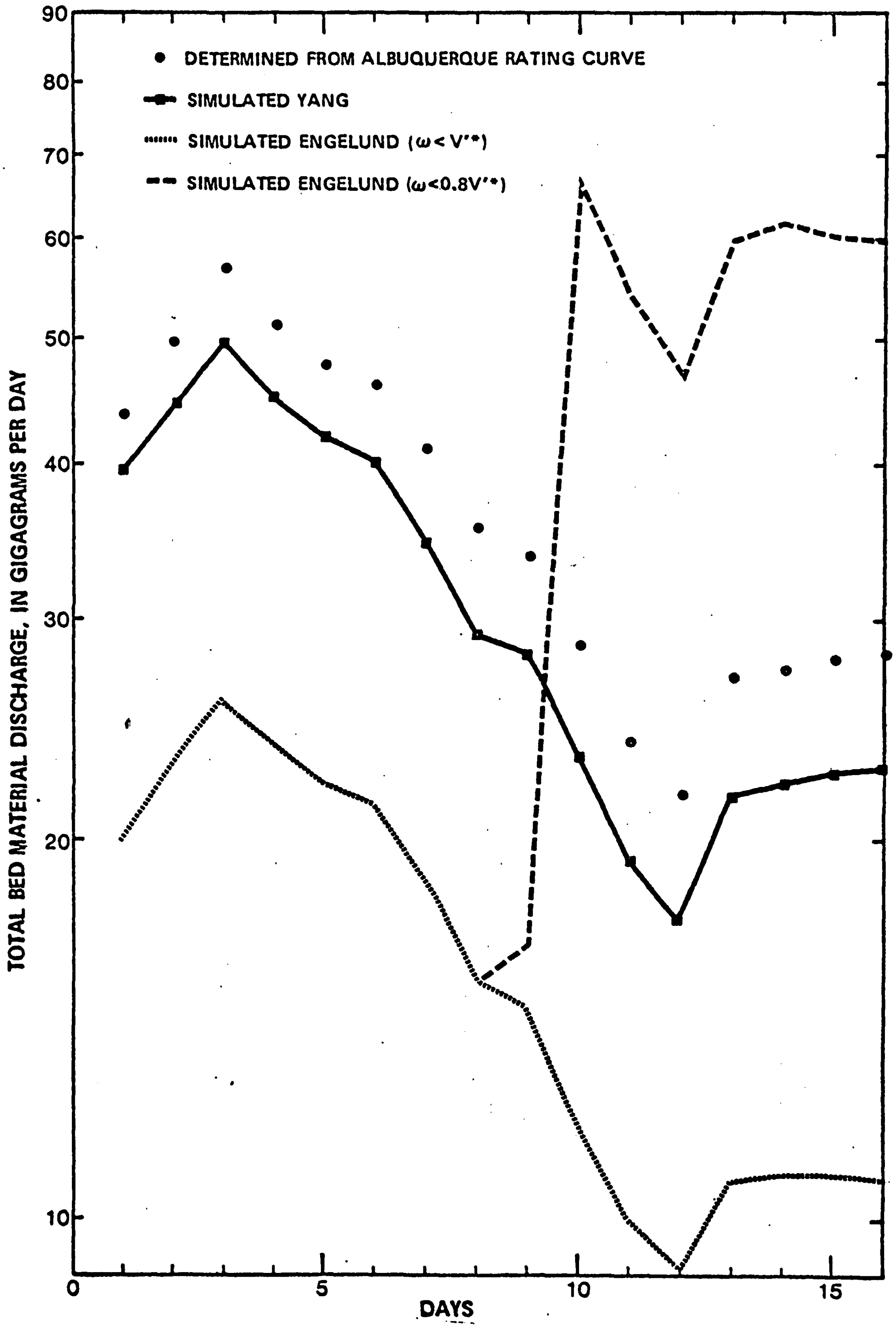

Figure 17.— Total load comparisons at Albuquerque, with N=14.

superficially the total load agreement (the actual load by size-class agreement would still be poor) of Engelund's formulation, the fall velocity-shear velocity ratio criterion for suspension was lowered to 0.8. This resulted on day 10 in a disproportionate climb to a new load level, because the effective suspended diameter was 0.1875 mm, and all the suspended load was in the 0.125-0.25 mm class. This increase is not supported by measured suspended size analysis on the Rio Grande for high flows. Since a measure of the model's performance will be net-load outflow compared to observed net-load outflow (modified Einstein is the best), it is preferable to run the post-dam simulation only with Yang's equation.

This author feels that N varies directly with Δt rather than inversely as postulated by Bennett and Nordin (1977). Values of N tried in the pre-dam run were: 1.2, 12, 36, 72, 144, and 168 mm, with a time step of one day; only in the latter three cases was any agreement reached between the simulated and the observed loads. If a river has a certain dune height or thickness of movable sediment and a time period for sorting that bed form, then the amount of material available for scour must be less than the dune height if Δt is less than the time period. Conversely, if Δt is greater than the time period, then the amount available must be greater than the dune height. In Bennett and Nordin's simulation on the East Fork (1977), the active-layer thickness was 40 mm for a time step of one-half hour. Assuming the same sorting rate for the Rio Grande and an inverse relationship, an active layer thickness of 0.83 mm is obtained for a time step of one day. This unrealistically limits the loads.

RESULTS AND DISCUSSION

The results of the simulation are shown in figures 18, 19, and 20. The simulated bed changes after 204 days of post-dam flow are compared with the observed changes in figure 18. The major observed changes are +0.52 meters at section 26 (38.3 km), just below the Jemez River confluence, and -0.47 meters at section 4 (6.8 km). The corresponding values for the model are +0.35 meters at section 13 (19.3 km), and -0.92 meters at section 2 (3.4 km). The largest differences between the model and the observed are at sections 2, 4, and 7 (10.5 km). Section 2 is the first plotted point; section 3 is the second; and so on.

The rest of the differences are less than 0.5 meters, and a fairly good trend is present. The observed net bed change of the reach, computed by distributing the changes in figure 18 over the Δx segments and active widths is +5.1 mm ±133%. The simulated figure is -40.3 mm ±30%. The estimated net outflow of bed material is 4.40×10^5 Mg ±18%. If the simulated net bed change is converted to load, the net bed material outflow is 5.81×10^5 Mg; if the estimated net outflow is distributed over the reach, the net bed change is -30.5 mm. It is evident that not much transition occurred by the end of the 204-day time span ending in May 1974. However, if the bed changes over the period from dam opening to November 1975 are examined, there is a definite degradation trend.

Results of the 2-year simulation from November 1973 to November 1975 are pictured in figure 19. There was a mild runoff event in the spring, 1975. A maximum average flow of 165 m^3/s was observed at San Felipe, as opposed to 244 m^3/s in the runoff event of spring, 1973. This is considered to be the reason for the degradation trend, because from November 1973 to May 1974, no flow was greater than 58 m^3/s.

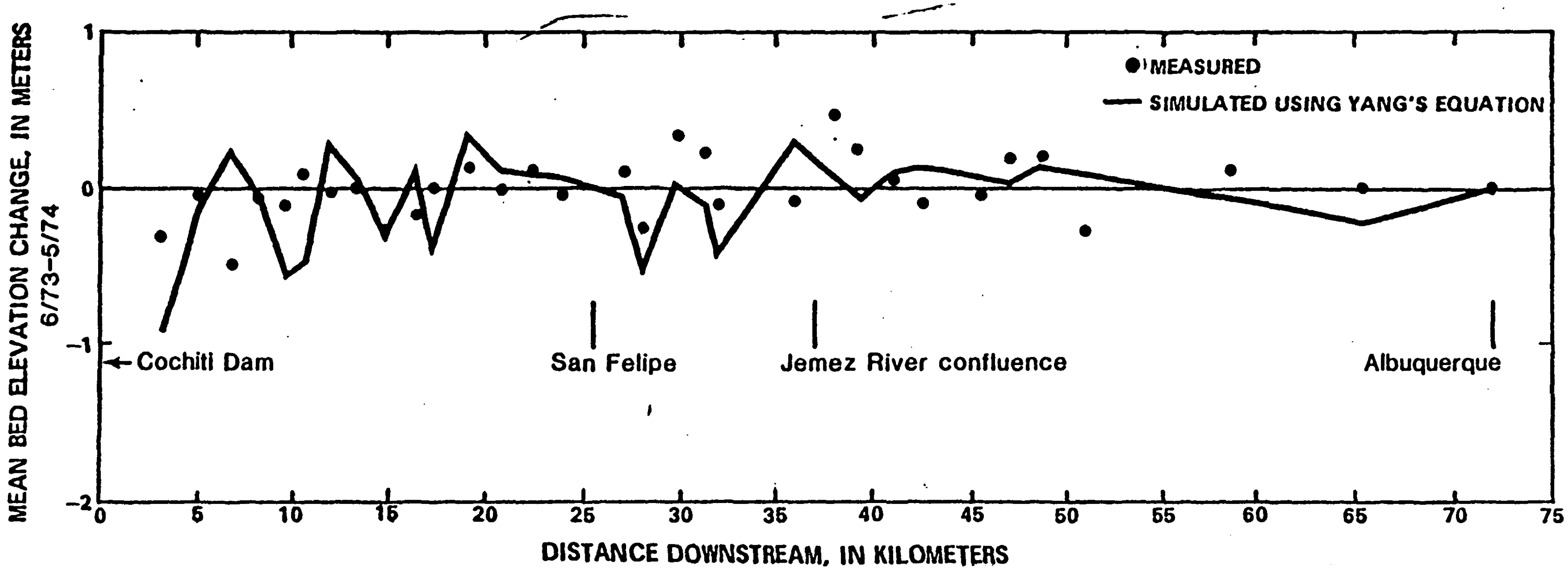

Figure 18.-- Measured versus simulated bed changes after 204 days.

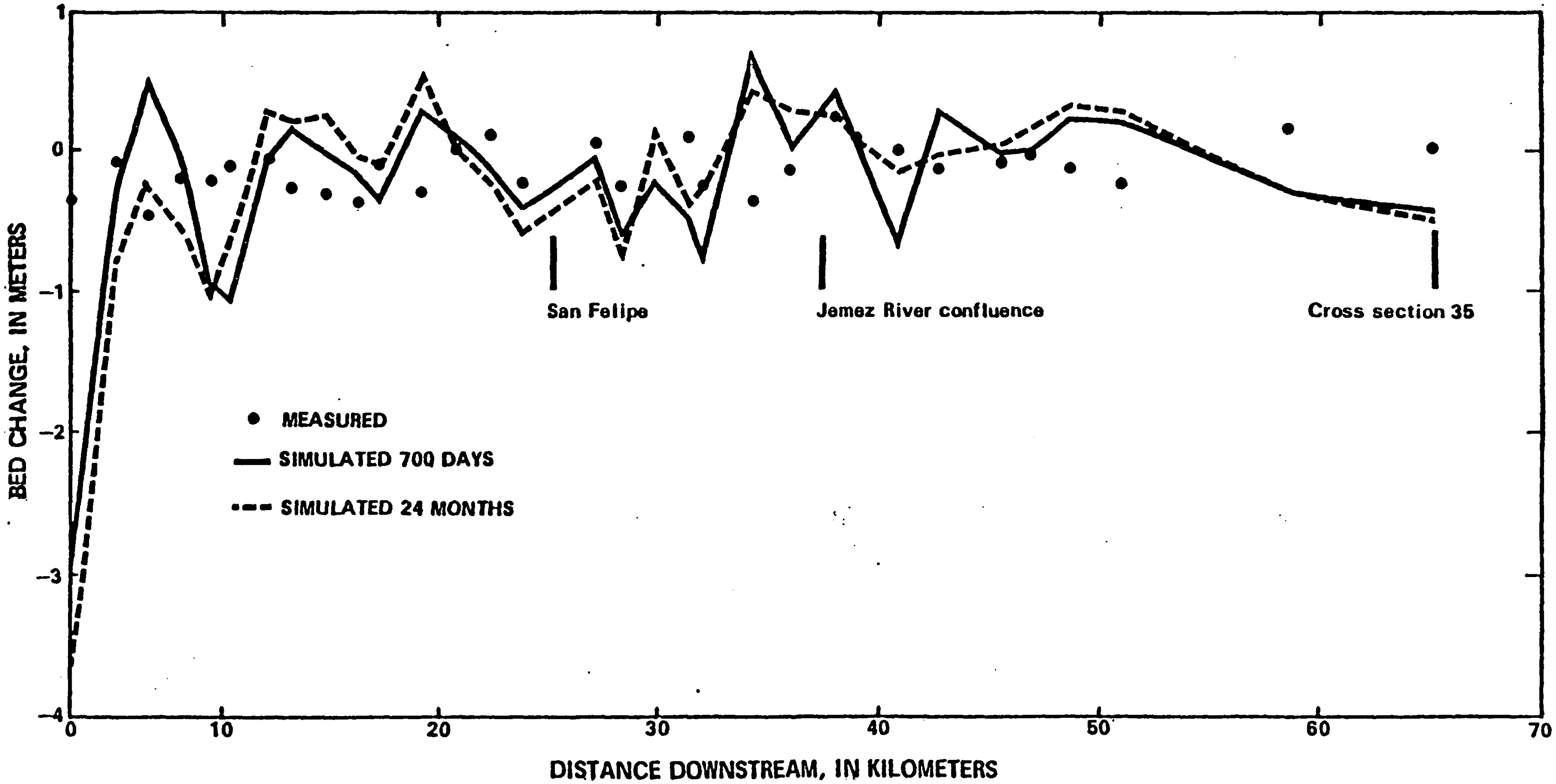

Figure 19.-- Measured versus simulated bed changes after the 1975 runoff event.

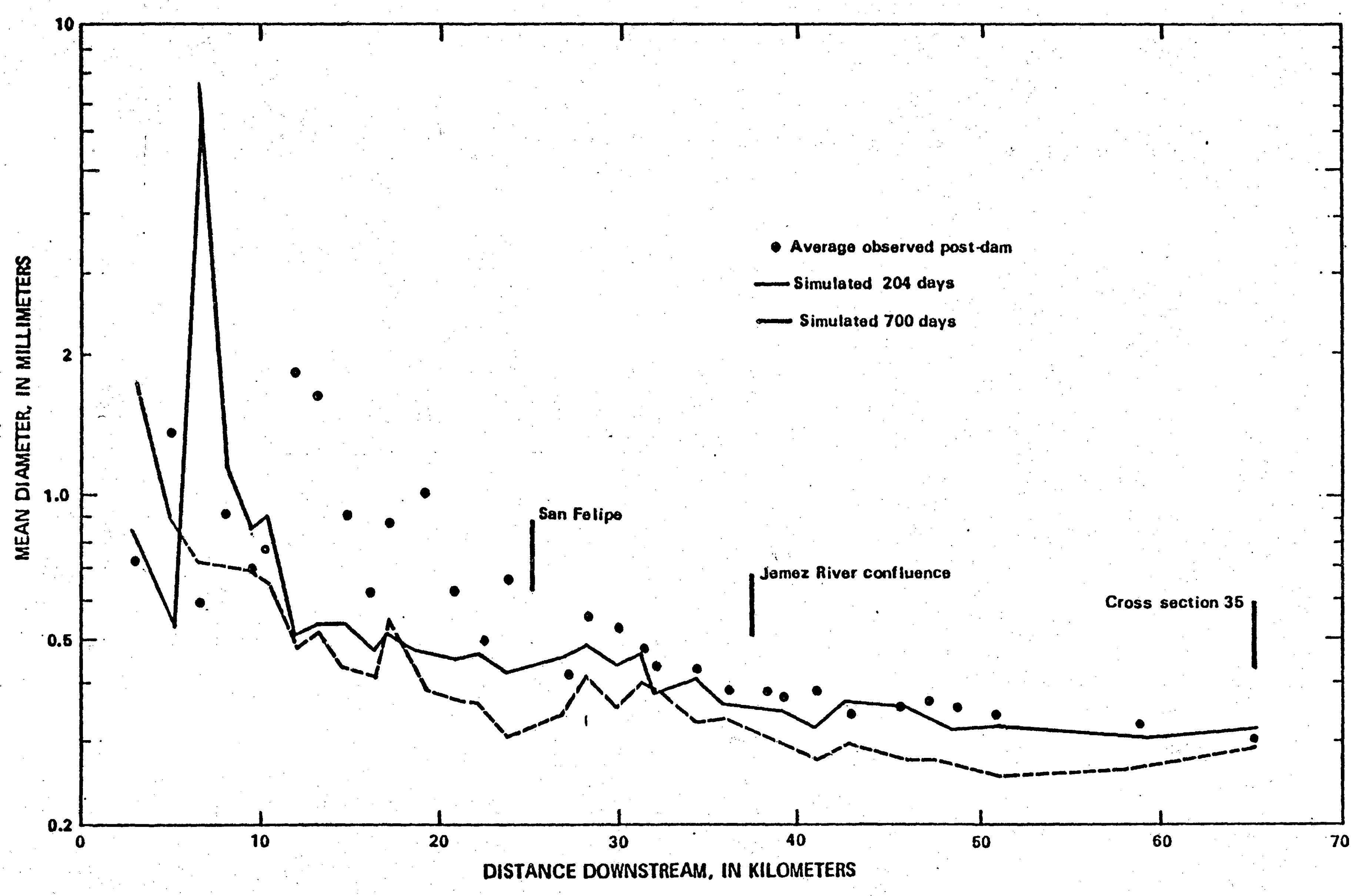

Figure 20.-- Comparison of average post-dam observed and simulated longitudinal size distributions.

The net observed bed change over the whole reach for November 1975 is -85.5 mm ±26%. The observed change over the reach from section 2 to San Felipe is -214 mm ±16%, and from section 2 to Jemez River confluence is -171 mm ±17%. The corresponding simulated values are -360 mm ±40% for the upper reach (sections 2-16); -240 mm ±40% for the upper and middle reaches (sections 2-24); and -166 mm ±40% for the entire reach. The simulated net-reach change is approximately double the observed. The preceding simulated values were for a time step of one day; the total time period of simulation was 700 days.

A simulation was also done with a time step of one month. As can be seen from figure 19, trends with the 700-day simulation are quite good: the net reach change is -170 mm ±40% with a time step of one month.

In the 204-day simulation, agreement between estimated net bed-material outflow and the load computed from net-reach change was poor; this was not the case in the long-run simulation. For the 700-day run, Yang's outflow is 2.28 x 10^6 Mg ±26%; estimated observed outflow is 2.69 x 10^6 Mg ±50%; and outflow computed from net-reach change is 2.39 x 10^6 Mg ±40%. For the 24-month run, Yang's outflow is 2.29 x 10^6 Mg ±26%; estimated observed outflow is 2.36 x 10^6 Mg ±50%; and outflow computed from net-reach change is 2.46 x 10^6 Mg ±40% However, if the observed net-reach change is converted to load, the figure is 1.22 x 10^6 Mg ±40%. This is perhaps an indication that the bed material is actually coarser than what is being represented as bed material (0.125 mm).

The major observed changes on the reach are the -0.45 meter ±1% at section 4, and the +0.25 meter ±2% at section 26. Corresponding figures for the simulation are -2.89 meters ±40% at section 2, and +0.69 meter ±40% at section 23. The simulated changing at section 2 is disturbing to the modeler. The observed change at sections 2, 3, and 4 is essentially non-existent from May 1974 to November 1975. The only possible explanation is that the bed in these sections is actually much coarser than is represented by the data. In fact, referring to figure 20, there is only good reproduction of the observed average post-dam size distribution downstream from section 23.

The bed change at section 2 simulated by the month time-step run (-3.59 m ±40%) is greater than the change simulated by the day time-step run. This is unusual, because more flow variation for a one-day time step than for a month time step should result in higher flows and, therefore, higher transport. In the 24-month simulation, the active layer thickness was increased 30 times over the 700-day simulation. This thickness obviously did not limit the loads enough; in fact, resulting ending month distributions for most sections showed predominantly fine material and did not agree with the points in figure 20. It can be deduced that, although the active layer should be thicker for a time step of a month, the proportion is not linear. This thickness would be calculated by calibrating for a time step of a month at a section known to have a limited sediment supply section; such a section may be hard to find. Also, for a time step of one month, some of the bed changes simulated were on the order of 0.3 meter. A change of that magnitude could be expected to affect the water surface in the time step. This is a violation of one of the basic assumptions under which the model was derived (see background assumptions).

There are two disturbing consequences of the simulation in figure 20. At section 4, the bed material is quite coarse in comparison with the other sections; even more odd, the distribution at section 2 has become finer from May 1974 to November 1975. From dam opening to May 1974, only fine material is transported, but during the runoff of spring 1975, coarser materials will be transported. Yang's equation predicts unusually high transport rates for the coarser material (figs. 15a and 15b.). Also, the hydraulic energy gradient between section 2 and section 3 is very even; while from sections 3 to 4, there is a significant drop. Thus, an unusual amount of coarser material transported out of section 2, flushed through section 3, and deposited in section 4. These anomalies at sections 2 and 4 are mainly the fault of the tendency in Yang's transport equation to pridict higher transport rates for the coarser sizes.

For the 204-day simulation, the flow was consistently low, and Chezy C was not changed at all over the period of simulation. For the 700-day and 24-month simulations, the high-flow values for Chezy C were determined from the May 1975 hydraulic data from the data report. Instantaneous flows ranged from 85 m^3/s to 130 m^3/s. Instantaneous flows in the hydraulic data of May 1974 ranged from 11 to 26 m^3/s, and the Chezy Cs derived from this run were found to agree with those derived from the run of November 1975, flows of which ranged from 37 to 51 m^3/s. There is some error in the coupled values for Chezy C, in that they were not derived for the same flow at each section. However, there will probably be more error in simulation in the modeling of the hydraulic features for those flows in the transient range: 58 to 99 m^3/s. In the simulation, the high-flow Chezy C preempted the low-flow Chezy C at 58 m^3/s or greater. There were no data available to determine some kind of transient-flow Chezy C at a section. The absence of calibrated values for Chezy Cs could account for the greater amplitude of oscillation in the predicted values than in the observed (fig. 19). Also, the greater the variation of input average flows, the greater the distortion of respective water-surface profiles; consequently, the greater the inaccuracies in the hydraulic properties that determine the transport rates. However, this author feels that the procedure of coupling Chezy C is an improvement over the use of one value at a section, or the use of one value for the reach, because a more accurate water-surface profile is obtained.

Finally, bed-composition accounting may be inadequate. The accounting system always provides for replenishment of material; that is, bed material is assumed to extend infinitely downward in the same composition as that posed initially. This may not be an accurate characterization at each section of the reach, such as sections 2 and 4. It seems for sections downstream of section 19, the infinite downward assumption proved reasonable; however, for the upstream sections, a heavy coarse layer under the active layer should probably have been posed.

In addition, routing of one size affecting routing of another does not seem correct in the bed-composition routine. Some work must be done on simultaneous routing of all sizes; it is believed that Bennett (1978) has already done some research toward this end.

CONCLUSIONS

The coupling of Chezy C in the backwater equation improves reproduction of water-surface profile, especially in the absence of initial conditions and other input control parameters.

Yang's equation describes multi-size transport on the Rio Grande well, while Engelund's formulation does not, due mainly to irreconcilable differences with the modified Einstein computation. However, Yang's equation tends to predict too much load in the coarser sizes on the Rio Grande, resulting in inexplicable phenomena occurring in simulated bed-size distributions at some sections.

The active-layer thickness varies directly with time-step size; on the Rio Grande it limits the loads little, if at all, with Yang's equation employed as the transport function. This may be a reason for the more radical changes predicted by the model.

Though the active-layer thickness varies directly with time-step size, this variation is less than linear. For this reason, as well as the fact that too much bed-elevation change may occur in a time step, it is inaccurate to use simulation on the Rio Grande with time steps larger than one day.

Since the estimated observed outflow of bed material is consistently larger than the outflow computed from the net-observed reach change, it may be deduced that the actual bed material is much coarser than what is represented as bed material, that is, sediment which is coarser than 0.125 mm. Perhaps, 0.25 mm is a better cutoff for the wash load.

There is a definite degradation trend in effect on the study reach, but this trend is in direct proportion to the amount of flow in the reach. The model tends to exaggerate the observed in a ratio of 2:1 on a net-reach change basis.

REFERENCES CITED

Bennett, J. P., 1978, One-dimensional surface-water transport models: U.S. Geological Survey National Training Center, Denver, Colo., video tape series no. 2500, tapes 10-14.

Bennett, J. P., and Nordin, C. F., 1977, Simulation of sediment transport and armouring: Hydrological Sciences Bulletin, v. 22, no. 4, p. 555-569.

Chen, Y. H., 1973, Mathematical modeling of water and sediment routing in natural channels: University Microfilms, 1975, 253 p.

Colby, B. R., and Hembree, C. H., 1955, Computations of total sediment discharge, Niobrara River near Cody, Nebr.: U.S. Geological Survey Water-Supply Paper 1476, 123 p.

Deigaard, Rolfe, 1978, Longitudinal grain sorting in alluvial streams: The Danish Center for Applied Mathematics and Mechanics, no. 152, p. 16-35.

de Vries, M., 1977, Morphological computations: Delft University of Technology Lecture Notes, 67 p.

Dewey, J. D., Roybal, F. E., and Funderburg, D. E., 1979, Hydrologic data on channel adjustments 1970 to 1975, on the Rio Grande downstream from Cochiti Dam, New Mexico, before and after closure: U.S. Geological Survey Water-Resources Investigations 79-70, May 1979, 531 p.

Einstein, H. A., 1950, The bedload function for sediment transportation in open channel flows: U.S. Department of Agriculture Technical Bulletin 1026, 71 p.

Engelund, Frank, and Fredsøe, Jørgen, 1976, A sediment transport model for straight alluvial channels: Nordic Hydrology, v. 7, p. 293-306.

Komura, Soburo, and Simons, D. B., 1967, River-bed degradation below dams: Proceedings of the American Society of Civil Engineers, v. 93, no. HY4, p. 1-14.

Krishnappan, B. G., and Snider, N., 1977, Mathematical modeling of sediment-laden flows in natural streams: Inland Waters Directorate, Scientific Series no. 81, 48 p.

Nordin, C. F., and Beverage, J. P., 1965, Sediment transport in the Rio Grande, New Mexico: U.S. Geological Survey Professional Paper 462-F, 35 p.

Ponce, V. M., Garcia, J. L., and Simons, D. B., 1979a, Modeling alluvial channel bed transients: Proceedings of the American Society of Civil Engineers, v. 105, no. HY3, p. 245-256.

Ponce, V. M., Indlekofer, Horst, and Simons, D. B., 1979b, The convergence of implicit bed transient models: Proceedings of the American Society of Civil Engineers, v. 105, no. HY4, p. 351-363.

Strelkoff, Theodor, 1969, The one-dimensional equations of open channel flow: Proceedings of the American Society of Civil Engineers, v. 95, no. HY3, p. 861-876.

Water Resources Data for New Mexico, 1973, Surface water and water quality records: U.S. Geological Survey, Water Resources Division, Abuquerque, N. Mex., pt. 1, 248 p.; pt. 2, 271 p.

______, 1974, Surface water and water quality records: U.S. Geological Survey, Water Resources Division, Albuquerque, N. Mex., pt. 1, 238 p.; pt. 2, 291 p.

______, 1975, Water year 1975: U.S. Geological Survey, Water Resources Division, Albuquerque, N. Mex., 603 p.

______, 1976, Water year 1976: U.S. Geological Survey, Water Resources Division, Albuquerque, N. Mex., 655 p.

Yang, C. T., 1973, Incipient motion and sediment transport: Proceedings of the American Society of Civil Engineers, v. 99, no. HY10, p. 1679-1704.

APPENDIX

COMPUTER PROGRAM AND PRINTOUT

The computer simulation program and some sample output are presented in this section. The index to the computer variables is given first, followed by the program, then the sample printout. The program is not completely general, and all variables are in inch-pound units unless otherwise specified in the index. In a printout, the first row lists: the net bed change, CHANGE; the net stage change, CNET; the bed elevation, ZN(I); the stage, ELEVN(I); and the total bed material load, QBT(I); from left to right, leading from the cross-section number on the extreme left. Cross sections 17 and 25 are not represented because of lack of data. QBT(I) is in tons per time step. The second row with the same section number presents from left to right: the average velocity, V(I); the mean depth, D(I); the area of water, AREA(H,I); the Chezy C, C(I); and the bed change in the time steps, BE(I). The three numbers above the table are the flows on the reach from downstream to upstream, reading left to right. In the program the step backwater computation is on page 80; Subroutine Yang is on page 86; Subroutine Engelund is on page 84; and the bed composition accounting routine is on page 83. Some pre-dam output and all post-dam output are given.

Index to Computer Variables

* - Input variable	M - Size class index
E - Subroutine Engelund only	J - Depth increment
Y - Subroutine Yang only	K - Subreach increment
I - Cross-section index	

A	The relative bedload layer thickness, E
A(I,J)	The area array for each section, *
AO(M)	A coefficient in the bed material discharge rating curve for size class M at section 2, *
A1	A coefficient in the stage rating curve at the upstream boundary section, *
AREA(H,I)	The area of water function at depth H and section I
B(I,J)	The top width array for each section, *
BO(M)	The exponent in the bed material rating curve for size class M at section 2, *
B1	The exponent in the stage rating curve at the upstream boundary section, *
BE(I)	The net bed level change at section I in the time step
BLAMDA	The linear concentration at the bed, E
C(I)	Chezy C at a section
C1(I)	The low flow Chezy C for the upstream iteration, *
C2(I)	The low flow Chezy C for the downstream iteration, *
C3(I)	The high flow Chezy C for the upstream iteration, *
C4(I)	The high flow Chezy C for the downstream iteration, *
CB	The volumetric concentration at the bed, E, C_b'
CFS(?)	The discharge array for the downstream rating curve boundary condition, *
CHANGE	The net difference in bed elevation
CNET	The net difference in water surface elevation
CR	The shear velocity Reynolds number, Y
CTLOG	The logarithm to the base 10 of the concentration in parts per million, Y
D(M)	The representative size class diameter, * (mm)

D50	The mean diameter of the total bed distribution, E (mm)
DADY	Derivative of area with respect to depth
DDDY	Derivative of hydraulic depth with respect to depth
DFXDH	Derivative of the discretized backwater equation with respect to depth
DBE(M)	The change in bed elevation per size class M
DISC(M)	The size class limits, starting with the lowest limit, * (mm)
DX(I)	The downstream Δx for each section I
ELEV(I)	The water surface elevation at each section in time step 1
ELEVN(I)	The water surface elevation at each section
FX	The discretized backwater equation
H(I)	The depth at section I
HD	The iterated hydraulic depth
HDP(I)	The hydraulic depth at section I
HN	The iterated depth variable
INCR(I)	The number of depth increments at each section I, *
ISTART(K)	The starting sections of the various subreaches, from downstream to upstream, *
N	The parameter controlling the active layer thickness, *
NBTWN	The print out time step increment, *
NDAY	The total number of time steps of simulation, *
NPRINT	The first print out time step, *
NR	The number of subreaches in the total reach, *
NSZ	The total number of size classes, *
NX	The downstream section for each subreach
NXT	The total number of cross sections in the reach, *

P(I,M)	The original size fraction for size class M at section I, *
PFACT	P factor in Einstein's calculation, E
PHIB(M)	The bedload intensity, E , Φ_b
PHIS(M)	The suspended load intensity, E, Φ_s
PN(I,M)	The size fraction in the active layer for size class M and section I
PROB	The probability of particle movement, E
Q1(K)	The controlling discharge over each subreach, *
QBN(M,I)	The bed material load per size class M at section I
QBT(I)	The total bed material load at section I
QBX(1)	The total bedload per foot of width, E
QBX(M)	The bedload per size class M per foot of width, E
QSX(1)	The total suspended load per foot of width, E
QSX(M)	The suspended load per size class M per foot of width, E
SE	The water surface slope
SF(H,I, HD)	The friction slope function
SI, SI_2	Integrals involved in the suspended load computation, E, I, I_2
SK	The grain roughness factor, E, k_s
TAL	The active layer thickness
TEMP	The temperature of the water in degrees C, *
TH(H,I)	The energy head at section I for depth H
THETAP	The nondimensional shear stress, E, θ'
TKA(M,I)	The thickness of the active layer occupied by size class M at section I
TKI(M,I)	The thickness of the inactive layer occupied by size class M at section I

TOP(H,I)	The top width function for a depth H at section I
TOTAL	The total load passing the downstream most section
TTI	The thickness of inactive deposition
U(M)	The fall velocity for size class M
UC	The critical fall velocity, below which suspension takes place, E, ω_c
UE	The effective fall velocity, E, ω_e
V(I)	The mean velocity at section I
VCRW	The critical velocity divided by fall velocity, Y, $V_{cr/\omega}$
VISC	The kinematic viscosity, Y, ν
VP	The shear velocity, E & Y, V* & V*'
W(I)	The active width of transport at section I, *
WSE(I,J)	The depth array at section I, *
Z	The Rouse number, E, $^{\omega}/.4V*'$
Z(I)	The original bed elevation at section I, *
ZN(I)	The bed elevation at section I

```
      PROGRAM BACK(INPUT,OUTPUT,DATAD,FACK,POSTDM,D1175T,TAPE3=DATAD,
+     TAPE7=FACK,TAPE4=POSTDM,TAPE5=D1175T,TAPE6=OUTPUT)
       DIMENSION A0(10),B0(10),JIGI(7),C1(50),C2(50)
       DIMENSION H(50),DX(50),RM(50),C3(50),C4(50)
      DIMENSION QBT(50),BE(50),QSN(10,50),PN(10,50),U(10)
      COMMON/ZAP/C(50),B(50,20),A(50,20)/YOW/Y(50),CAV,G,WSE(50,20),
+      INCR(50),ZM(50)
      COMMON/SED1/ISTART(10),Q1(10),P(10,50),D(10),W(50),DISC(20)
       COMMON/SED/TAL,TKA(10,50),TKI(10,50),P4(10,50)
       DIMENSION ELEV(50),ELEVM(50),Z(50),HDP(50),CFS(50)
      DATA JIGI(1)/12/,JIGI(2)/14/,JIGI(3)/18/,JIGI(4)/19/,JIGI(5)/26/
      DATA JIGI(6)/30/,JIGI(7)/34/
 35 FORMAT(10E10.4)
 33 FORMAT(9F8.4)
 26 FORMAT(7F10.3)
 800 FORMAT('RIGHT ON')
 717 FORMAT('INPUT L,Q,H(L+1),HDP(L+1),C(L+1)',/)
 404 FORMAT('INPUT HEAD,CHEZY C',/)
 1 FORMAT(16I5)
 9 FORMAT(7F10.2)
 10 FORMAT(10F6.2)
 12 FORMAT(F8.2,F7.2,7F6.2)
 14 FORMAT(8F8.0)
 705 FORMAT('INPUT GUESS',/)
 20 FORMAT(I5,1X,F7.3,1X,F7.3,1X,F8.2,1X,F8.2,1X,F10.2)
 25 FORMAT(I5)
 702 FORMAT('X-SEC DELTA Z DELTA H     Z          H            QBT    ')
 700 FORMAT(F8.2,I5,F6.2)
 711 FORMAT(I5,F8.0)
 712 FORMAT(3F5.0,F4.1)
C INPUT NUMBER OF X-SECS.,= OF SIZES,= OF DAYS, PARAMETER N,
C  FIRST PRINT OUT STEP, = OF SUBREACHES,INTERVAL BETWEEN PRINTOUT
       READ(3,1) NXT,NSZ,NDAY,N,NPRINT,NR,NBTWN
      NDAY=700
      NPRINT=175
      NBTWN=175
     WRITE(6,800)
       G=32.0
       READ(3,1) (ISTART(I),I=1,NR)
      ISTART(NR)=2
      WRITE(6,800)
        DO 3 I=2,NXT
C  RIVER MILE,AREA-STAGE AND TOP WIDTH-STAGE RELATIONS,
C DOWNSTREAM RATING CURVE,SIZE CLASS LIMITS, UPSTREAM LOAD PER SIZE
C RATING CURVES, UPSTREAM STAGE-DISCHARGE RATING CURVE,CHEZY CS
      READ(3,700) WSE(I,1),INCR(I),RM(I)
      LIM=INCR(I)
      READ(3,9)  (A(I,J),J=1,LIM)
      READ(3,9)  (B(I,J),J=1,LIM)
 3 CONTINUE
       READ(3,14)  (CFS(I),I=1,36)
      READ(3,33)  (DISC(M),M=1,NSZ)
C SIZE CLASS DIAMETERS(D50S) INPUT
      READ(3,35)  (A0(M),M=1,NSZ)
      READ(3,33)  (B0(M),M=1,NSZ)
      READ(3,33)  (D(M),M=1,NSZ)
      READ(3,33)   A1,B1
```

```
     READ(3,10)  (C(I),I=2,NXT)
    READ(4,10)  (C2(I),I=2,NXT)
    READ(4,10)  (C1(I),I=2,NXT)
     READ(5,10)  (C4(I),I=2,NXT)
     READ(5,10)  (C3(I),I=2,NXT)
     DO 11 I=1,NXT
C  BED ELEVATION, ACTIVE WIDTH, AND ORIGINAL BED MATERIAL COMPOSITION
C  CHANGE OF STAGE TO DEPTH IN AREA AND TOP-WIDTH RELATIONS
11 READ(3,12) Z(I),W(I),(P(J,I),J=1,NSZ)
     DO 400 I=2,NXT
     LIM=INCR(I)
     WSE(I,1)=WSE(I,1)-Z(I)
     DO 401 J=2,LIM
401  WSE(I,J)=WSE(I,1)+(J-1)*0.5
400 CONTINUE
C ACTIVE LAYER THICKNESS (TAL) COMPUTED AND ORIGINAL COMPOSITION
C OF ACTIVE LAYER(PN(M,I)),THICKNESS OF SIZE CLASS M IN ACTIVE
C LAYER(TKA(M,I)) AND IN INACTIVE LAYER(TKI(M,I)
       TAL=14.*D(NSZ)/304.8
    WRITE(6,33)   TAL
    NX1=NXT-1
    TOTAL3=0.0
   TOTAL4=0.0
    TOTAL=0.0
     DO 24 I=1,NXT
     ZN(I)=Z(I)
     TP=0.0
     CAV=CAV+C(I)
     DO 15 M=1,NSZ
15 TP=P(M,I)+TP
     DO 41 M=1,NSZ
     PN(M,I)=P(M,I)/TP
     P4(M,I)=P(M,I)/100.
     TKA(M,I)=TAL*PN(M,I)
     P(M,I)=PN(M,I)
41 TKI(M,I)=0.0
24 CONTINUE
C CALCULATION OF DELTA XS(DX(I))
    RM(1)=0.19
     DO 4 I=1,NX1
4 DX(I)=ABS(RM(I+1)-RM(I))*5280.
    DO 13 J2=1,NDAY
C READ IN WATER DISCHARGE AT VARIOUS CONTROL POINTS ALONG REACH
    READ(4,712)  (Q1(I),I=1,NR),TEMP
C COMPUTATION OF UPSTREAM TOTAL BED LOAD DISCHARGE
    A1=1.218
    B1=.172
    ELEVN(ISTART(NR)-1)=A1*Q1(NR)**B1+5224.29
     DO 36 M=1,NSZ
    QBN(M,1)=0.0
36 CONTINUE
    QBT(1)=0.0
    IF(J2.EQ.NPRINT)WRITE(6,26)   (Q1(I),I=1,NR)
650 NX=NXT
     DO 91 I1=1,NR
     Q=Q1(I1)
     IF(I1.GE.2)GO TO 300
```

```
C   ALBUQUERQUE RATING TABLE
 706 K=1
  5  IF(Q.GE.CFS(K).AND.Q.LE.CFS(K+1))GO TO 301
   K=K+1
   GO TO 5
 301 G1=0.1*K+3.9
    GAGE=G1+0.1*(Q-CFS(K))/(CFS(K+1)-CFS(K))
   Z(NX)=4946.2
   ELEVN(NX)=GAGE+ZN(NX)
  H(NX)=ELEVN(NX)-ZN(NX)
    HDP(NX)=AREA(H(NX),NX)/TOP(H(NX),NX)
    V(NX)=Q/AREA(H(NX),NX)
   C(NX)=C1(NX)
    IF(Q.GE.2000.)C(NX)=C3(NX)
C DOWNSTREAM DEPTH(H(NX)) AND VELOCITY(V(NX)) KNOWN
 300  CONTINUE
    I4=1
   IST=ISTART(I1)
   NX11=NX-1
   DO 6 I=IST,NX11
   L=NX-I4
   C(L)=C2(L)
    IF(Q.GE.2000.)C(L)=C4(L)
C NEWTON ITERATION FOR REMAINING DEPTHS AND VELOCITIES
 716 HN=WSE(L,1)
    K=1
 101 HD=AREA(HN,L)/TOP(HN,L)
    V(L)=Q/AREA(HN,L)
   FX=TH(H(L+1),L+1)-TH(HN,L)+DX(L)*(SF(H(L+1),L+1,HDP(L+1))
+   +SF(HN,L,HD))/2.
   CALL FACTOR(DADY,DDDY,HN,L)
   R=DADY*Q**2/(G*AREA(HN,L)**3)-1.
   T=DX(L)*SF(HN,L,HD)*(2.*DADY/AREA(HN,L)+DDDY/HD)/2.
   DFXDH=R-T
   HN1=HN-FX/DFXDH
   IF(HN1.LT.WSE(L,1))HN1=HN
    DIFF=ABS(HN1-HN)
    IF(DIFF.LT.0.001)GO TO 7
   IF(HN1.GE.WSE(L,INCR(L)))HN1=WSE(L,INCR(L))
   IF(HN1.EQ.WSE(L,INCR(L)))GO TO 7
    HN=HN1
     K=K+1
    GO TO 101
  7 I4=I4+1
C DEPTH AT X-SEC, L (H(L)) AND VELOCITY AT L(V(L)) KNOWN
  H(L)=HN1
  ELEVN(L)=H(L)+ZN(L)
    HDP(L)=AREA(HN1,L)/TOP(HN1,L)
    V(L)=Q/AREA(HN1,L)
   C(L)=C1(L)
    IF(Q.GE.2000.)C(L)=C3(L)
  6 CONTINUE
 91 NX=ISTART(I1)
C ALL VELOCITIES AT ALL X-SECS ARE KNOWN, CALL BED LOAD CALCULATION
   CALL BEDLD(QBT,PN,NXT,NSZ,DX,HDP,BE,QBN,U,ELEVN,TEMP)
    DO 19 I=2,NXT
   IF(J2.EQ.1)ELEV(I)=ELEVN(I)
```

```
C TOTAL BED CHANGE IS ADDED TO OLD BED ELEVATION
      ZN(I)=ZN(I)+BE(I)
   19 CONTINUE
      TOTAL=TOTAL+QBT(NXT)
      TOTAL3=.0162*Q1(1)**1.71+TOTAL3
      TOTAL4=0.0675*Q1(1)**1.56+TOTAL4
  600 IF(J2.NE.NPRINT)GO TO 28
        WRITE(6,702)
        DO 2 I=1,NXT
        CHANGE=ZN(I)-Z(I)
        CNET=ELEVN(I)-ELEV(I)
C OUTPUT OF NEW BED LEVATION(ZN(I)),TOTAL LOAD AT EACH
C X-SEC.(QBT(I)) ,ACTIVE LAYER COMPOSITION(PN(M,I)),NET CHANGE
C IN BED ELEVATION (CHANGE)
      WRITE(6,20) I,HDP(I),Y(I),AREA(H(I),I),C(I),BE(I)
    2 WRITE(6,20) I,CHANGE,CNET,ZN(I),ELEVN(I),QBT(I)
        NPRINT=NPRINT+NBTWN
C       OUTPUT OF PROFILE INFO AND FINAL SIZE DISTRIBUTION
  703 DO 704 I=2,NXT
  704 WRITE(7,26) RM(I),ZN(I),ELEVN(I)
         IF(J2.NE.NDAY)GO TO 28
        DO 707 I=2,NXT
  707 WRITE(7,26) (PN(M,I),M=1,NSZ)
        DO 708 I=2,NXT
  708 WRITE(7,26) (P(M,I),M=1,NSZ)
      WRITE(6,35) TOTAL,TOTAL3,TOTAL4
   28 WRITE(6,25) J2
   13 CONTINUE
      STOP
      END
      SUBROUTINE FACTOR(DADY,DDDY,HN,L)
      COMMON/ZAP/EE(50),B(50,20),A(50,20)
        COMMON/YOW/E(52),WSE(50,20),INCR(50)
        J=1
       IF(HN.GE.WSE(L,INCR(L)))GO TO 603
  601 IF(HN.GE.WSE(L,J).AND.HN.LT.WSE(L,J+1))GO TO 602
        J=J+1
        GO TO 601
  602 DDDY=(A(L,J+1)-A(L,J))/0.5/TOP(HN,L)
      DADY=(A(L,J+1)-A(L,J))/0.5
        RETURN
  603 DDDY=1.
        DADY=TOP(HN,L)
      RETURN
      END
C     AREA CALCULATION
      FUNCTION AREA(HX,M1)
        COMMON/ZAP/EE(50),B(50,20),A(50,20)
        COMMON/YOW/E(52),WSE(50,20),INCR(50)
        J=1
      IF(HX.GE.WSE(M1,INCR(M1)))GO TO 402
  404 IF(HX.GE.WSE(M1,J).AND.HX.LT.WSE(M1,J+1))GO TO 403
         J=J+1
         GO TO 404
  403 AREA=A(M1,J)+(HX-WSE(M1,J))*(A(M1,J+1)-A(M1,J))/0.5
         RETURN
  402 AREA=A(M1,INCR(M1))
         RETURN
      END
```

```
C TOP WIDTH CALCULATION
   FUNCTION TOP(HY,M2)
  COMMON/ZAP/EE(50),B(50,20)/YOW/E(52),WSE(50,20),INCR(50)
   J=1
   IF(HY.GE.WSE(M2,INCR(M2)))GO TO 502
501 IF(HY.GE.WSE(M2,J).AND.HY.LT.WSE(M2,J+1))GO TO 500
    J=J+1
    GO TO 501
500 TOP=B(M2,J)+(HY-WSE(M2,J))*(B(M2,J+1)-B(M2,J))/0.5
    RETURN
502 TOP=B(M2,INCR(M2))
    RETURN
   END
C ENERGY GRADE LINE FUNCTION(TH)
  FUNCTION TH(HZ,M3)
  COMMON/YOW/V(50),CAV,G,EE(50,20),II(50),ZN(50)
   TH=V(M3)*V(M3)/2./G+HZ+ZN(M3)
  RETURN
  END
C FRICTION SLOPE CALCULATION WITH CHEZY C
   FUNCTION SF(HF,M4,HDX)
   COMMON/ZAP/C(50)/YOW/V(50),CAV
  SF=V(M4)*V(M4)/C(M4)/C(M4)/HDX
  RETURN
  END
   SUBROUTINE BEDLD(QBT,PN,NXT,NSZ,DX,HDP,BE,QBN,U,ELEVN,TEMP)
  COMMON/SED1/ISTART(10),Q1(10),P(10,50),D(10),W(50),DISC(20)
   COMMON/SED/TAL,TKA(10,50),TKI(10,50),P4(10,50)
   COMMON/ZAP/C(50)/YOW/V(50),CAV,G
   DIMENSION QBN(10,50),DX(50),BE(50),QBT(50),PN(10,50)
  DIMENSION DBE(10),P1(10,50),HDP(50),U(10),QBTN(10)
  DIMENSION ELEVN(50)
22 FORMAT(8F10.3)
23 FORMAT(F8.6)
   DX(NXT)=DX(NXT-1)
  ELEVN(NXT+1)=2.*ELEVN(NXT)-ELEVN(NXT-1)
   W(NXT+1)=W(NXT)
  CALL VISFAL(TEMP,U,VISC)
   DO 17 I=2,NXT
C  SUMMING FOR INACTIVE LAYER THICKNESS AND CALCULATION OF
C WATER SURFACE SLOPE
  BE(I)=0.0
  QBT(I)=0.0
   TTI=0.0
   DO 77 M=1,NSZ
77 TTI=TTI+TKI(M,I)
  SE1=(ELEVN(I-1)-ELEVN(I))/DX(I-1)
  SE2=(ELEVN(I)-ELEVN(I+1))/DX(I)
  SE=(SE1+SE2)/2.
  CALL YANG(QBN,I,HDP(I),V(I),SE,NSZ,VISC,U,PN)
  GO TO 81
709 CONTINUE
  CALL DMEAN(PN,I,DISC,D50)
  CALL ENGLND(D50,NSZ,I,V(I),HDP(I),W(I),SE,U,PN,QBN,D)
  DO 36 M=1,NSZ
36 QBN(M,I)=QBN(M,I)*12.0896
  GO TO 81
```

```
 81  QBT(I)=0.0
C CALCULATION OF BED CHANGE PER SIZE CLASS(DBE(M)) AND
C  ARMORING SIMULATED
     DO 18 M=1,NSZ
    NUM=QBN(M,I-1)-QBN(M,I)
     DIV=0.075*(DX(I)+DX(I-1))*(2.*W(I)+W(I-1)+W(I+1))
     DBE(M)=NUM/DIV
     IF(DBE(M).GE.0.0)GO TO 55
     IF(-DBE(M).LE.TKA(M,I))GO TO 60
     DBE(M)=-TKA(M,I)
     DVOL=DBE(M)*0.075*(DX(I)+DX(I-1))*(2.*W(I)+W(I-1)+W(I+1))
    QBN(M,I)=QBN(M,I-1)-DVOL
     IF(QBN(M,I).LT.0.0)QBN(M,I)=0.0
C BED COMPOSITION ACCOUNTING BEGINS
 60  IF(TTI.GT.0.0)GO TO 70
     DO 80 K=1,NSZ
     TKA(K,I)=-DBE(M)*P(K,I)+TKA(K,I)
    IF(K.EQ.M)TKA(M,I)=TKA(M,I)+DBE(M)
 80  PN(K,I)=TKA(K,I)/TAL
     GO TO 50
 70  IF(-DBE(M).GT.TTI)GO TO 65
     DO 85 K=1,NSZ
     P1(K,I)=TKI(K,I)/TTI
     TKA(K,I)=-DBE(M)*P1(K,I)+TKA(K,I)
     IF(K.EQ.M)TKA(K,I)=TKA(K,I)+DBE(M)
     TKI(K,I)=TKI(K,I)+DBE(M)*P1(K,I)
 85  PN(K,I)=TKA(K,I)/TAL
     TTI=TTI+DBE(M)
     GO TO 50
 65  DO 75 K=1,NSZ
     P1(K,I)=TKI(K,I)/TTI
     TKA(K,I)=(-DBE(M)-TTI)*P(K,I)+TTI*P1(K,I)+TKA(K,I)
     IF(K.EQ.M)TKA(K,I)=TKA(K,I)+DBE(M)
     TKI(K,I)=0.0
 75  PN(K,I)=TKA(K,I)/TAL
     TTI=0.0
     GO TO 50
 55  TTI=TTI+DBE(M)
     IF(DBE(M).GE.TAL)GO TO 66
     DO 95 K=1,NSZ
     TKA(K,I)=TKA(K,I)-DBE(M)*PN(K,I)
     IF(K.EQ.M)TKA(K,I)=TKA(K,I)+DBE(M)
     TKI(K,I)=TKI(K,I)+DBE(M)*PN(K,I)
 95  PN(K,I)=TKA(K,I)/TAL
     GO TO 50
 66  DO 67 K=1,NSZ
     TKI(K,I)=TKA(K,I)+TKI(K,I)
     IF(K.EQ.M)TKI(K,I)=TKI(K,I)+DBE(M)-TAL
     TKA(K,I)=0.0
     IF(K.EQ.M)TKA(K,I)=TAL
 67  PN(K,I)=TKA(K,I)/TAL
C BE(I) IS TOTAL BED CHANGE AND QBT(I) IS TOTAL BED LOAD AT X-SEC.
 50  BE(I)=DBE(M)+BE(I)
     QBT(I)=QBT(I)+QBN(M,I)
 18  CONTINUE
     QBT(I)=QBT(I)/12.0896
 17  CONTINUE
     RETURN
     END
```

```
      SUBROUTINE ENGLND(D50,NSZ,I,V,H,W,SE,U,PNN,QBN,D)
      DIMENSION D(10),QBN(10,50),PNN(10,50),U(10),QBX(10),QSX(10)
       SK=2.5*D50/304.8
       VP=V/(.99+5.75*ALOG10(H*304.8/D50))
   63 VP1=V/(6.25+2.5*ALOG(VP*VP/SK/SE/32.2))
       DIFF=ABS(VP1-VP)
       IF(DIFF.LE.0.00001)GO TO 62
       VP=VP1
       GO TO 63
   62 VP=VP1
   29 DUMMY=D50/1000.
      THETAC=0.05
       PFACT=ALOG(30.*H*304.8/2.5/D50)
       PQ=1.
      UC=0.8*VP
        M50=NSZ+1
      QST=0.0
      QBT=0.0
      SUM1=0.0
      SUM=0.0
     DO 59 M=1,NSZ
      IF(U(M).GE.UC)GO TO 59
      SUM=U(M)*PNN(M,I)+SUM
      SUM1=PNN(M,I)+SUM1
   59 CONTINUE
      UE=SUM/SUM1
      UX=UE
      DO 52 M=1,M50
      THETAP=(VP*0.3048)**2/9.8/1.65/DUMMY
      PROB=(1.+(0.267/(THETAP-THETAC))**4)**0.25
      PROB=1./PROB
      PHIB=5.*PROB*(SQRT(THETAP)-0.7*SQRT(THETAC))
      QBX(M)=PHIB*SQRT(1.65*9.8*DUMMY**3)*PQ
      IF(QBX(M).LT.0.0)QBX(M)=0.0
      IF(UX.GE.UC)GO TO 54
      Z=UX/0.4/VP
      GEE=THETAP-THETAC-0.267*PROB
      IF(GEE.LT.0.0)GO TO 54
      BLAMDA=SQRT(GEE/0.027/2.65/THETAP)
      CB=PQ*0.65/(1.+1./BLAMDA)**3
      A=2.*DUMMY/H/0.3048
      CALL ROUSE(A,Z,SI1,SI2)
      PHIS=11.6*SQRT(THETAP)*CB*2.*(PFACT*SI1+SI2)
      IF(M.EQ.1)PHIT=PHIB+PHIS
      QSX(M)=PHIS*SQRT(1.65*9.8*DUMMY**3)
      GO TO 53
   54  QSX(M)=0.0
   53  DUMMY=D(M)/1000.
        UX=U(M)
      PQ=PNN(M,I)
       IF(M.EQ.1)GO TO 52
      QBT=QBT+QBX(M)
      QST=QST+QSX(M)
   52 CONTINUE
       DO 55 M=2,M50
     IF(QBT.EQ.0.0)GO TO 58
     QBX(M)=QBX(M)*QBX(1)/QBT
   58 IF(QST.EQ.0.0)GO TO 55
     QSX(M)=QSX(M)*QSX(1)/QST
```

```
55 QBN(M-1,I)=(QBX(M)+QSX(M))*W*76926.
   QBN(M50,I)=(QBX(1)+QSX(1))*W*76926.
   QBX(M50+1)=QBX(1)
   QSX(M50+1)=QSX(1)
   DO 61 M=1,M50
    QSX(M+1)=QSX(M+1)*W*76926.
    QBX(M+1)=QBX(M+1)*W*76926.
61 CONTINUE
   RETURN
    END
   SUBROUTINE ROUSE(A,Z,SI1,SI2)
    T=0.1
    J=1
    C=1.
    B=T
   DH=(C-B)/30.
   N=29
    SJ1=0.0
    SJ2=0.0
2   SUM2=(1./B-1.)**Z-(1./C-1.)**Z
    SUM3=(1./B-1.)**Z*ALOG(B)-(1./C-1.)**Z*ALOG(C)
    DO 1 I=1,N,2
    SUM2=SUM2+4.*(1./(B+I*DH)-1.)**Z+2.*(1./(B+(I+1)*DH)-1.)**Z
1   SUM3=SUM3+4.*(1./(B+I*DH)-1.)**Z*ALOG(B+I*DH)+2.*(1./(B+(I+1)*DH)
+  -1.)**Z*ALOG(B+(I+1)*DH)
    SJ1=SJ1+SUM2*DH/3.
    SJ2=SJ2+SUM3*DH/3.
    IF(J.EQ.0)GO TO 4
    T1=T*0.1
    IF(A.LT.T1)GO TO 3
    C=T
    B=A
   DH=(C-B)/20.
   N=19
    J=0
   GO TO 2
3  C=T
   B=T1
   DH=(C-B)/20.
   N=19
   T=T1
   GO TO 2
4  SI1=SJ1*0.216*A**(Z-1.)/(1.-A)**Z
   SI2=SJ2*0.216*A**(Z-1.)/(1.-A)**Z
   RETURN
   END
   SUBROUTINE DMEAN(PN,I,DISC,D50)
   DIMENSION PN(10,50),DISC(20)
   UND=0.0
   J=1
78 OLD=PN(J,I)+UND
    IF(OLD.GE.0.5)GO TO 79
    J=J+1
   UND=OLD
   GO TO 78
79 D50=DISC(J+1)-(OLD-0.5)*(DISC(J+1)-DISC(J))/(OLD-UND)
    RETURN
    END
```

```
      SUBROUTINE YANG(QBN,I,HD,V,SE,MSZ,VISC,U,PM)
      DIMENSION U(10),PM(10,50),QBN(10,50)
      COMMON/SED1/ISTART(10),Q1(10),P(10,50),D(10)
      COMMON/ZAP/C(50)
   23 FORMAT(I5)
   22 FORMAT(8F8.6).
      IF(SE.LE.0.0)WRITE(6,23) I
      VP=SQRT(32.2*HD*SE)
      IF(I.GE.ISTART(1))Q=Q1(1)
      IF(I.LT.ISTART(1).AND.I.GE.ISTART(2))Q=Q1(2)
      IF(I.LT.ISTART(2))Q=Q1(3)
      DO 3 M=1,MSZ
      DK=D(M)/304.8
      CR=VP*DK/VISC
      IF(CR.GT.70.)GO TO 1
      VCRW=2.5/(ALOG10(CR)-0.06)+0.66
      GO TO 2
    1 VCRW=2.05
    2 DIFF=V*SE/U(M)-VCRW*SE
      IF(DIFF.LT.0.0)GO TO 4
      CTLOG=5.435-0.286*ALOG10(U(M)*DK/VISC)-0.457*ALOG10(VP/U(M))+(1.799-
     0.409*ALOG10(U(M)*DK/VISC)-0.314*ALOG10(VP/U(M)))*ALOG10(
     V*SE/U(M)-VCRW*SE)
      PX=PM(M,I)
      QBN(M,I)=0.0027*Q*PX*10.**CTLOG
      GO TO 3
    4 QBN(M,I)=0.0
    3 QBN(M,I)=QBN(M,I)*12.0896
      RETURN
      END
      SUBROUTINE VISFAL(TEMP,U,VISC)
      DIMENSION U(10),UU(4,5),VSC(5)
      DATA VSC(1)/1.931E-5/,VSC(2)/1.410E-5/,VSC(3)/1.091E-5/,VSC(4)/.808E-5/
     ,VSC(5)/.710E-5/
      DATA UU(1,1)/.053/,UU(1,2)/.062/,UU(1,3)/.074/,UU(1,4)/.082/,UU(1,5)
     /.088/,UU(2,1)/.144/,UU(2,2)/.164/,UU(2,3)/.184/,UU(2,4)/.197/
     ,UU(2,5)/.217/,UU(3,1)/.335/,UU(3,2)/.361/,UU(3,3)/.387/,UU(3,4)
     /.413/,UU(3,5)/.427/
      TEMP=TEMP/10.+1.
      K=1
   88 IF(TEMP.GE.K.AND.TEMP.LT.K+1)GO TO 89
      K=K+1
      GO TO 88
   89 DO 90 M=1,3
   90 U(M)=UU(M,K)+(TEMP-K)*(UU(M,K+1)-UU(M,K))
      VISC=VSC(K)+(TEMP-K)*(VSC(K+1)-VSC(K))
      U(4)=.771
      U(5)=.869
      U(6)=1.21
      U(7)=1.64
      RETURN
      END
READY.
```

YANG, PRE-DAM, DAY 16

4273. 4573, 4420

X-SEC	DELIM Z	DELTA H	Z	H	QST
1	0.000	0.000	0.00	0.00	0.00
1	0.000	0.000	5213.40	0.00	0.00
2	3.465	5.085	869.27	170.00	0.00
2	0.000	-.217	5213.40	5219.27	29024.81
3	3.314	4.942	894.28	50.00	.03
3	.720	.239	5204.60	5209.97	26121.74
4	2.436	4.506	980.82	120.00	.04
4	.664	.798	5195.50	5201.65	23315.26
5	2.159	4.064	1087.62	57.50	.01
5	.593	-.027	5188.50	5194.84	22068.79
6	2.530	4.098	1078.50	65.00	.00
6	-.502	-.623	5179.31	5185.60	21992.24
7	2.192	4.517	978.47	90.00	.01
7	.001	-.237	5177.16	5181.95	21223.75
8	2.552	4.070	1085.90	60.00	.03
8	.600	.363	5167.77	5173.44	18011.23
9	2.282	3.706	1192.62	100.00	.02
9	.816	.540	5162.51	5169.04	15588.80
10	2.309	4.110	1075.53	60.00	-.02
10	-.338	-.704	5150.19	5162.04	18469.74
11	3.521	4.160	1062.48	100.00	-.03
11	-.590	-.962	5146.76	5156.04	20601.23
12	2.341	4.933	896.00	65.00	-.05
12	-1.096	-1.184	5143.89	5151.25	25170.73
13	3.881	5.500	803.63	225.00	.02
13	.200	.719	5132.50	5142.88	23126.78
14	3.398	5.334	828.63	70.00	.01
14	.897	.460	5131.44	5137.99	21746.89
15	2.943	4.869	907.75	100.00	.00
15	.476	-.953	5126.95	5131.43	21564.12
16	5.100	5.143	659.39	60.00	-.02
16	-.965	-1.451	5117.55	5126.05	23705.43
17	3.373	5.141	899.58	80.00	-.00
17	-.022	-.385	5106.65	5111.28	23903.77
18	2.586	5.426	842.87	105.00	-.01
18	.017	-.619	5103.10	5107.06	24519.77
19	4.014	5.664	807.37	73.00	-.00
19	-.499	-1.114	5092.71	5100.33	24785.50
20	3.632	4.679	977.42	93.00	-.01
20	-1.012	-1.637	5089.89	5095.27	25172.82
21	3.370	5.232	874.00	55.00	.06
21	-.329	-.387	5086.35	5091.61	20846.23
22	2.752	5.397	947.33	100.00	.01
22	.803	.491	5080.20	5087.99	19831.42
23	1.722	4.159	1025.02	73.00	.01
23	.034	-.382	5074.25	5079.62	16387.93
24	4.098	3.793	1123.80	110.00	.02
24	.218	.195	5066.67	5072.20	15245.20
25	2.143	3.970	1073.71	58.00	-.02
25	.371	-.323	5061.99	5068.48	17337.47
26	2.381	4.778	892.22	190.00	-.00
26	-.894	-.892	5056.54	5060.61	17794.63
27	1.935	4.065	1048.77	65.00	.02
27	.761	.233	5051.49	5056.19	13683.24
28	1.753	4.689	909.19	225.70	-.01
28	-.236	-1.171	5040.47	5045.33	15944.69
29	2.572	4.611	924.60	81.30	-.00
29	-.386	-.715	5036.41	5041.78	16206.30
30	3.019	4.944	862.33	86.65	-.02
30	-.190	-.609	5030.05	5035.59	18539.97
31	1.885	4.395	855.24	154.25	.00
31	.191	-.983	5025.65	5029.12	18101.83
32	2.233	3.892	1095.26	66.23	.00
32	-.061	-.348	4995.84	5002.65	15615.00
33	1.613	4.841	880.57	160.38	-.02
33	-.049	-1.209	4974.65	4979.67	23790.65
34	2.718	4.823	983.90	66.59	-.00
34	-.003	-.332	4946.20	4952.67	25274.28
16					

ENGELUND, PRE-DAM, $\omega/V^* < 1$, DAY 16
4273, 4573, 4420

X-SEC	DELTA Z	DELTA H	Z	H	QBT
1	0.000	0.000	0.00	0.00	0.00
1	0.000	0.000	5213.40	0.00	0.00
2	3.465	5.085	969.27	170.00	0.00
2	0.000	-.217	5213.40	5219.27	29024.81
3	3.054	5.513	801.78	50.00	.17
3	3.592	2.624	5207.47	5212.35	13892.85
4	2.536	3.994	1106.62	120.00	.08
4	.859	1.226	5195.70	5202.08	7222.34
5	2.108	4.288	1030.75	57.50	-.00
5	.601	-.129	5188.52	5194.74	7480.43
6	2.569	3.896	1134.47	65.00	-.04
6	-1.075	-1.028	5178.73	5185.20	10808.30
7	2.245	4.152	1064.42	90.00	-.00
7	-.079	-.125	5177.08	5192.07	11090.55
8	2.496	4.435	996.72	60.00	-.00
8	.266	-.157	5167.44	5172.92	11129.30
9	2.414	3.184	1388.00	100.00	-.02
9	-.269	-.252	5161.42	5163.25	13088.40
10	2.309	4.112	1074.83	60.00	.02
10	.290	-.119	5150.32	5162.62	11141.43
11	3.319	5.850	755.59	100.00	-.06
11	.051	-1.610	5147.40	5155.39	15817.77
12	2.341	4.771	926.52	65.00	-.07
12	-1.952	-1.931	5143,04	5150.51	22996.01
13	4.073	5.962	741.35	225.00	.03
13	.146	.310	5132.45	5142.47	19197.13
14	3.502	5.086	869.11	70.00	.03
14	.949	.659	5131.49	5138.19	15853.74
15	2.900	4.952	892.61	100.00	.06
15	1.163	-.381	5127.63	5132.00	10259.93
16	5.087	5.009	882.39	60.00	-.00
16	-.399	-.772	5118.12	5126.73	10400.23
17	3.206	5.410	845.25	30.00	.00
17	.032	-.501	5106.70	5111.16	10187.82
18	2.726	4.480	1020.69	105.00	.01
18	-.152	-.244	5102.93	5107.43	9259.42
19	3.932	5.783	790.81	73.00	-.01
19	.495	-.197	5093.70	5101.25	9935.74
20	3.496	5.203	878.89	93.00	-.01
20	-.562	-1.480	5089.34	5095.43	10357.13
21	3.370	5.232	874.00	55.00	.00
21	-.353	-.358	5086.33	5091.64	9996.41
22	2.654	5.612	814.97	100.00	-.05
22	-.538	-.931	5078.86	5086.57	18729.02
23	1.707	3.401	1253.30	73.00	-.11
23	-.230	-.260	5073.99	5079.74	42044.66
24	2.835	5.928	719.19	110.00	.04
24	1.102	-.506	5067.55	5071.49	36993.22
25	2.135	3.431	1242.52	58.00	.08
25	-.656	-1.165	5060.96	5067.64	28457.70
26	2.331	4.778	892.22	190.00	.11
26	.042	-.065	5057.47	5061.43	12242.78
27	1.933	4.081	1044.53	65.00	.01
27	.520	-.006	5051.25	5055.95	9906.51
28	1.394	3.456	1233.63	225.70	-.05
28	-.776	-.729	5039.93	5045.77	20787.82
29	2.475	4.620	834.46	81.30	.05
29	1.052	.558	5037.85	5043.06	15122.21
30	2.896	5.277	607.91	86.65	.03
30	.327	-.340	5030.57	5035.86	11557.57
31	1.899	4.822	684.16	154.25	-.01
31	-.187	-1.180	5025.37	5028.82	15199.34
32	2.231	3.897	1094.05	66.23	-.01
32	.035	-.236	4995.93	5002.76	23376.81
33	1.611	4.851	978.32	160.38	.02
33	.021	-1.181	4974.72	4979.69	12563.83
34	2.719	4.823	663.90	66.59	.00
34	.002	-.382	4946.20	4952.67	11783.64

'6

ENGELUND, PRE-DAM, ω/V* < .8, DAY 16
4273,4573, 4420

X-SEC	DELTA Z	DELTA H	Z	H	QBT
1	0.000	0.000	0.00	0.00	0.00
1	0.000	*******	5213.40	5229.45	0.00
2	3.436	5.300	334.01	170.00	-.09
2	-1.280	-1.561	5212.12	5217.94	9611.16
3	3.411	4.753	929.92	50.00	-.03
3	-.712	-.992	5203.17	5208.74	12654.72
4	2.437	4.506	991.02	120.00	.07
4	.153	.250	5194.99	5201.10	6873.81
5	2.172	4.003	1104.04	57.50	.01
5	.196	-.371	5188.12	5194.49	6038.88
6	2.500	4.263	1036.93	65.00	-.04
6	-.979	-1.153	5178.83	5185.07	9295.51
7	2.226	4.364	1012.74	90.00	-.01
7	-.651	-.800	5176.51	5181.39	10102.49
8	2.528	4.227	1045.66	60.00	.01
8	-.123	-.436	5167.05	5172.64	9201.98
9	2.328	3.516	1257.13	100.00	-.00
9	-.217	-.384	5161.47	5168.12	9640.39
10	2.341	3.825	1155.44	60.00	-.00
10	-.418	-.645	5150.11	5162.10	9753.63
11	3.301	4.950	892.86	100.00	.02
11	.363	-.713	5147.71	5156.29	8249.71
12	2.341	5.019	830.67	65.00	-.11
12	-1.149	-1.214	5143.84	5151.22	19254.02
13	4.226	6.129	721.17	225.00	.04
13	.214	.246	5132.51	5142.41	15105.95
14	3.343	5.471	807.86	70.00	-.04
14	.180	-.291	5130.72	5137.24	18634.68
15	3.460	4.156	1063.53	100.00	.02
15	-.171	-1.078	5126.30	5131.30	16518.21
16	5.043	4.656	949.29	60.00	-.01
16	-.286	-.281	5118.23	5127.22	17176.66
17	2.990	5.804	787.91	80.00	-.02
17	.243	-.481	5106.91	5111.18	19886.54
18	2.942	3.883	1177.58	105.00	-.06
18	-.749	-.318	5102.33	5107.36	24210.42
19	3.995	5.691	803.49	73.00	.21
19	1.242	.399	5094.45	5101.84	10445.09
20	3.530	5.116	893.87	93.00	-.14
20	.117	-.620	5090.02	5096.29	16527.86
21	3.370	5.232	874.00	55.00	-.38
21	.148	.528	5086.83	5092.53	45132.00
22	2.760	6.110	748.46	100.00	.10
22	-.546	-1.325	5078.85	5086.18	26374.20
23	1.702	3.118	1367.18	73.00	-.01
23	-.443	-.432	5073.78	5079.57	28748.85
24	2.753	6.106	698.15	110.00	.03
24	1.391	-.294	5067.84	5071.71	24378.64
25	2.133	3.338	1277.22	58.00	.00
25	-.546	-.923	5061.07	5067.88	24225.63
26	2.122	5.718	745.59	190.00	.01
26	.166	-.223	5057.60	5061.28	23417.93
27	1.953	3.937	1082.78	65.00	-.02
27	-.672	-1.102	5050.06	5054.85	27463.20
28	1.994	3.456	1233.63	225.70	-.00
28	-.672	-1.078	5040.04	5045.42	28407.71
29	2.356	4.084	1043.72	81.30	-.00
29	.465	.469	5037.27	5042.97	28823.78
30	2.669	5.750	741.38	86.65	.02
30	1.042	.136	5031.28	5036.33	26201.46
31	1.932	4.365	972.14	154.25	-.07
31	-.984	-1.641	5024.58	5028.36	54877.06
32	2.223	3.912	1089.73	66.23	.06
32	.586	.232	4996.49	5003.23	20295.72
33	1.605	4.896	870.65	160.39	-.07
33	.072	-1.049	4974.77	4979.83	54161.23
34	2.719	4.823	983.90	66.59	-.03
34	-.025	-.382	4946.17	4952.67	65962.40

YANG, POST-DAM, DAY 51

1830.000 1830.000 1700.000

X-SEC	DELTA Z	DELTA H	Z	H	OBT
1	0.000	0.000	0.00	0.00	0.00
1	0.000	*******	5213.40	5228.67	0.00
2	2.527	3.164	537.38	0.00	-.03
2	-1.263	1.131	5212.14	5216.59	2934.61
3	2.338	3.021	562.70	51.00	-.00
3	-.264	1.648	5203.62	5207.71	3242.57
4	2.234	2.220	765.67	45.00	.01
4	.582	3.292	5195.42	5200.99	2463.12
5	2.069	1.721	987.89	26.00	-.00
5	.035	2.116	5138.00	5194.12	2564.80
6	1.756	2.479	685.80	64.00	-.02
6	-.850	-1.171	5178.96	5184.32	4510.81
7	1.673	3.215	528.71	50.00	-.01
7	-1.171	.607	5175.99	5179.67	5439.42
8	2.792	2.959	574.47	48.00	.01
8	.837	2.979	5168.01	5171.97	4765.29
9	2.331	2.477	686.24	58.00	.01
9	.700	3.658	5162.39	5167.83	3757.96
10	2.273	2.295	740.94	37.00	-.00
10	-.127	4.894	5150.40	5161.45	3847.36
11	4.366	2.717	625.62	39.00	-.01
11	-.211	2.277	5147.14	5154.29	4745.11
12	2.235	3.270	519.85	59.00	-.00
12	-.500	2.594	5144.49	5150.55	4921.22
13	4.180	2.832	600.24	46.00	.01
13	.516	4.723	5132.82	5141.89	-4276.80
14	2.602	2.985	569.47	47.00	.00
14	.057	2.889	5130.60	5135.99	4021.48
15	2.056	2.854	589.46	69.00	.01
15	.182	1.762	5126.65	5129.98	3488.71
16	3.992	2.524	673.61	46.00	.00
16	-.088	3.757	5118.43	5125.80	3280.94
17	3.245	2.139	855.59	28.00	-.01
17	.111	1.117	5106.78	5111.29	4123.16
18	2.095	3.058	598.44	55.00	-.01
18	-1.032	.524	5102.05	5105.16	4975.62
19	2.669	3.424	534.50	68.00	.00
19	.592	2.186	5093.80	5100.07	4672.79
20	3.130	2.329	785.91	43.00	-.01
20	-.305	.090	5089.60	5095.31	5271.01
21	2.562	2.857	640.60	35.00	-.01
21	-.869	1.192	5085.81	5090.19	5701.72
22	4.048	3.428	533.71	36.00	.01
22	.488	3.058	5079.89	5086.21	4236.19
23	1.709	2.214	826.58	42.00	.00
23	.094	1.393	5074.31	5079.33	3672.14
24	2.810	2.567	712.79	48.00	-.00
24	-.179	1.294	5066.27	5070.23	4199.30
25	1.863	2.757	663.75	64.00	.01
25	.165	1.755	5061.79	5067.31	3569.05
26	2.246	2.250	813.28	60.00	.00
26	.234	.949	5057.66	5061.53	3220.66
27	1.779	2.450	747.08	45.00	-.00
27	-.186	1.176	5050.54	5054.66	3700.31
28	2.206	2.987	612.61	71.00	.00
28	.057	1.395	5040.77	5044.87	3582.31
29	2.082	2.530	723.31	64.00	.00
29	.097	1.560	5036.90	5041.70	3322.06
30	2.590	2.541	720.09	46.00	-.00
30	-.025	1.071	5030.21	5035.21	3584.66
31	1.956	1.748	1046.67	49.00	.00
31	.102	1.966	5025.56	5029.42	1798.31
32	1.740	2.314	790.96	46.00	-.00
32	-.067	.977	4995.83	5001.99	3521.31
33	1.577	2.193	834.52	64.00	-.00
33	-.134	2.335	4974.57	4979.49	-3607.40
34	2.174	3.055	599.04	51.00	-.01
34	-.007	.670	4946.19	4951.75	6681.59
51					

YANG, POST-DAM, ~~DAY~~ 102

	709.000	709.000	712.000		
X-SEC	DELTA Z	DELTA H	Z	H	QBT
1	0.000	0.000	0.00	0.00	0.00
1	0.000	*******	5213.40	5228.06	0.00
2	1.766	2.560	278.09	0.00	-.01
2	-2.038	-1.119	5211.36	5214.34	763.56
3	1.680	2.410	295.41	51.00	-.00
3	-.303	.200	5203.55	5206.26	790.64
4	1.617	2.056	346.25	45.00	.00
4	.715	1.802	5195.55	5199.49	785.41
5	1.310	1.615	440.93	26.00	.00
5	.077	.243	5188.00	5192.24	728.70
6	1.365	1.902	374.38	64.00	-.00
6	-1.293	-2.569	5178.52	5182.93	967.92
7	1.193	2.876	247.58	50.00	-.01
7	-1.549	-.873	5175.61	5178.19	1597.47
8	1.893	2.185	325.93	48.00	.00
8	1.041	1.845	5168.21	5170.84	1132.54
9	1.472	2.729	260.94	52.00	-.01
9	.709	1.647	5162.40	5165.82	1818.14
10	3.600	2.749	258.98	37.00	-.00
10	-.251	1.506	5150.28	5158.06	1875.68
11	3.302	1.950	365.18	39.00	.01
11	-.034	.231	5147.32	5152.25	1089.73
12	1.673	3.075	231.57	58.00	-.01
12	-.883	.559	5144.11	5148.51	1767.17
13	3.422	2.404	296.11	46.00	.00
13	.814	1.993	5133.11	5139.16	1354.42
14	2.248	2.382	298.33	47.00	.00
14	.285	1.466	5130.82	5134.56	1046.91
15	1.171	2.487	286.33	69.00	-.00
15	.199	.628	5126.67	5128.85	1144.56
16	2.425	1.838	387.41	46.00	.00
16	.028	2.124	5118.55	5124.16	907.79
17	1.700	1.595	444.47	28.00	.00
17	-.021	-.569	5106.65	5109.60	868.38
18	1.283	2.083	340.37	55.00	-.00
18	-1.278	-.661	5101.80	5103.98	986.67
19	1.320	2.851	248.68	68.00	-.01
19	.391	.586	5093.60	5098.47	1331.82
20	2.568	1.641	432.11	43.00	.00
20	-.335	-1.703	5039.57	5093.52	1144.16
21	1.308	2.343	302.57	35.00	-.00
21	-1.210	-.564	5085.47	5088.45	1502.12
22	3.042	2.383	297.50	86.00	.00
22	.782	1.098	5080.18	5084.25	847.48
23	1.478	2.075	341.64	42.00	-.00
23	.100	.081	5074.32	5078.02	1116.19
24	1.539	1.898	373.48	48.00	.00
24	-.192	-.065	5066.26	5068.87	974.99
25	1.448	2.492	284.47	64.00	-.00
25	.191	.294	5061.81	5065.85	1078.17
26	1.629	1.570	451.52	60.00	.00
26	.386	-.037	5057.82	5060.54	675.67
27	1.197	2.222	319.11	45.00	-.00
27	-.330	-.251	5050.40	5053.23	1211.05
28	2.039	2.244	315.95	71.00	.00
28	.141	.174	5040.85	5043.65	890.21
29	1.331	2.388	296.89	64.00	-.00
29	.091	.143	5036.89	5040.28	1061.04
30	2.092	1.522	465.87	46.00	.00
30	.065	.108	5030.30	5034.24	602.54
31	1.298	2.004	353.80	49.00	-.00
31	.148	.213	5025.61	5027.67	892.31
32	1.909	1.697	417.77	46.00	.00
32	-.106	-.112	4995.79	5000.90	830.06
33	1.563	3.155	224.73	64.00	-.00
33	-.340	-.271	4974.36	4976.89	2305.68
34	2.042	1.629	435.26	51.00	.00
34	.003	.026	4946.20	4951.10	362.37
102					

YANG, POST-DAM, DAY 153

X-SEC	DELTA Z	DELTA H	Z	H	QBT
	774.000	938.000	846.000		
1	0.000	0.000	0.00	0.00	0.00
1	0.000	********	5213.40	5228.17	0.00
2	1.994	2.596	325.90	0.00	-.01
2	-2.587	-1.371	5210.81	5214.09	911.22
3	1.896	2.532	334.11	51.00	-.00
3	-.336	.382	5203.54	5206.44	988.15
4	1.714	2.087	405.43	45.00	.00
4	.783	2.162	5195.62	5199.85	910.54
5	1.930	1.695	499.19	26.00	.00
5	.094	.498	5183.01	5192.50	879.34
6	1.415	2.067	409.34	64.00	-.00
6	-1.637	-2.788	5178.17	5192.71	1266.78
7	1.272	2.766	305.83	50.00	-.00
7	-1.684	-.730	5175.48	5179.33	1516.16
8	1.981	2.392	353.71	48.00	.00
8	1.090	2.058	5168.26	5171.05	1401.95
9	1.639	2.846	297.23	58.00	-.00
9	.469	1.607	5162.16	5165.78	1997.55
10	4.071	2.727	310.25	37.00	.00
10	-.321	2.089	5150.21	5158.64	1872.81
11	3.277	2.334	362.50	39.00	.00
11	.271	.517	5147.62	5152.53	1528.64
12	1.813	3.041	278.22	58.00	-.00
12	-1.076	.696	5143.91	5148.65	1949.93
13	3.584	2.482	340.84	46.00	.00
13	1.026	2.746	5133.33	5139.91	1604.02
14	2.262	2.523	335.32	47.00	.00
14	.368	1.840	5130.91	5134.93	1400.68
15	1.288	2.532	334.14	69.00	.00
15	.241	.858	5126.71	5129.08	1396.79
16	2.697	1.966	430.29	46.00	.00
16	.119	2.488	5118.64	5124.53	1188.04
17	2.044	1.749	536.17	28.00	-.00
17	-.121	-.322	5106.55	5109.85	1385.84
18	1.487	2.368	396.18	55.00	-.00
18	-1.486	-.662	5101.59	5103.98	1611.08
19	1.609	2.968	316.04	68.00	-.00
19	.240	.766	5093.45	5098.65	1857.99
20	2.806	1.948	481.63	43.00	.00
20	-.431	-1.510	5089.47	5093.71	1523.63
21	1.568	2.371	395.56	35.00	-.00
21	-1.290	-.237	5085.39	5088.77	1962.94
22	3.375	2.842	330.06	36.00	.00
22	.951	1.600	5080.35	5084.75	1470.60
23	1.517	2.092	369.98	42.00	.00
23	.167	.259	5074.39	5078.19	1247.04
24	1.601	1.979	391.03	48.00	.00
24	-.183	.016	5066.27	5068.95	1085.98
25	1.531	2.468	313.56	54.00	-.00
25	.188	.440	5061.81	5066.00	1108.67
26	1.598	1.763	438.96	60.00	.00
26	.474	.006	5057.90	5060.58	873.53
27	1.261	2.213	349.70	45.00	-.00
27	-.423	-.237	5050.31	5053.25	1270.33
28	2.047	2.409	321.34	71.00	.00
29	.194	.256	5040.90	5043.74	1044.57
29	1.411	2.383	324.82	64.00	-.00
29	.083	.251	5036.88	5040.40	1111.29
30	2.089	1.667	464.34	46.00	.00
30	.191	.228	5030.43	5034.36	752.26
31	1.350	1.986	389.65	49.00	-.00
31	.144	.331	5025.60	5027.78	925.49
32	1.847	1.761	439.41	46.00	-.00
32	-.112	-.050	4995.79	5000.97	938.53
33	1.678	3.203	241.63	64.00	-.00
33	-.532	-.348	4974.17	4976.81	2332.08
34	2.044	1.731	447.25	51.00	.00
34	.003	.076	4946.20	4951.15	1025.99

YANG, POST-DAM, DAY 204

579.000 579.000 715.000

X-SEC	DELTA Z	DELTA H	Z	H	QBT
1	0.000	0.000	0.00	0.00	0.00
1	0.000	*******	5213.40	5229.06	0.00
2	1.973	2.233	301.29	0.00	-.01
2	-3.010	-1.946	5210.39	5213.52	642.25
3	1.696	2.408	299.17	51.00	-.00
3	-.393	.126	5203.49	5206.18	739.32
4	1.641	1.994	360.04	45.00	.00
4	.841	1.999	5195.68	5199.69	697.33
5	1.790	1.661	432.18	26.00	.00
5	.112	.242	5183.03	5192.24	562.43
6	1.357	1.943	369.49	64.00	-.00
6	-1.895	-3.188	5177.31	5182.31	926.11
7	1.220	2.668	267.07	30.00	-.00
7	-1.760	-.993	5175.40	5178.07	1152.59
8	1.840	2.316	310.01	48.00	.00
8	1.099	1.815	5168.27	5170.81	1070.00
9	1.470	2.756	260.53	58.00	-.00
9	.287	1.220	5161.98	5165.39	1404.53
10	3.745	2.528	234.01	37.00	.00
10	-.305	1.778	5150.23	5158.33	1296.28
11	2.873	2.256	318.29	39.00	.00
11	.414	.258	5147.76	5152.27	1096.35
12	1.651	2.909	246.91	58.00	-.00
12	-1.220	.340	5143.77	5148.29	1414.42
13	3.408	2.434	295.02	46.00	.00
13	1.158	2.325	5133.46	5139.49	1186.47
14	2.243	2.448	293.30	47.00	.00
14	.438	1.574	5130.98	5134.67	1007.39
15	1.190	2.445	293.64	69.00	-.00
15	.265	.722	5126.74	5128.94	1036.53
16	2.371	1.895	375.90	46.00	.00
16	.185	2.228	5118.71	5124.27	922.37
17	1.481	1.499	386.23	28.00	.00
17	-.181	-.949	5106.49	5109.22	620.73
18	1.101	1.998	291.24	55.00	-.00
18	-1.650	-1.214	5101.43	5103.42	706.32
19	1.295	2.765	209.37	68.00	-.00
19	.092	.060	5093.30	5097.94	1003.65
20	2.197	1.570	368.77	43.00	.01
20	-.431	-2.174	5089.47	5093.05	741.61
21	1.210	2.173	266.43	35.00	-.00
21	-1.352	-.372	5085.33	5088.14	1003.28
22	2.604	2.275	254.56	86.00	.00
22	1.076	.955	5080.48	5084.11	582.04
23	1.352	1.954	296.30	42.00	-.00
23	.212	-.007	5074.43	5077.93	754.25
24	1.346	1.847	313.56	48.00	.00
24	-.146	-.267	5066.30	5068.67	681.98
25	1.346	2.308	250.84	64.00	-.00
25	.195	.121	5061.82	5065.68	699.04
26	1.364	1.596	362.87	60.00	.00
26	.530	-.226	5057.96	5060.35	513.21
27	1.110	2.113	274.04	45.00	-.00
27	-.495	-.599	5050.23	5052.29	835.43
28	1.826	2.150	269.34	71.00	.00
28	.233	-.048	5040.94	5043.43	613.84
29	1.207	2.253	257.01	64.00	-.00
29	.077	-.052	5036.88	5040.09	697.41
30	1.961	1.441	401.69	46.00	.00
30	.312	.053	5030.55	5034.19	417.60
31	1.160	1.939	298.66	49.00	-.00
31	.130	-.017	5025.59	5027.44	623.02
32	2.136	1.727	335.34	46.00	-.00
32	-.116	-.502	4995.78	5000.51	654.23
33	1.349	2.992	193.49	64.00	-.00
33	-.682	-.928	4974.02	4976.33	1472.40
34	2.034	1.413	409.71	51.00	.00
34	.002	-.081	4946.20	4950.99	517.97

4928E+06

204

YANG, POST-DAM, MONTH 12

	459.000	476.000	451.000		
X-SEC	DELTA Z	DELTA H	Z	H	QBT
1	0.000	0.000	0.00	0.00	0.00
1	0.000	*******	5213.40	5227.77	0.00
2	1.540	1.928	233.97	0.00	-.12
2	-4.959	-6.348	5208.44	5211.26	13126.61
3	1.482	1.777	253.74	51.00	.00
3	-.182	-1.426	5203.70	5206.14	12959.39
4	1.119	2.243	201.08	45.00	-.15
4	.425	-1.789	5195.27	5198.55	24867.39
5	1.717	1.126	400.40	26.00	.14
5	.346	-1.644	5188.27	5192.21	13043.54
6	1.311	1.325	340.37	64.00	-.02
6	-2.743	-4.586	5177.07	5181.38	15039.57
7	1.044	2.426	185.91	50.00	-.15
7	-1.737	-2.602	5175.42	5177.83	30293.38
8	1.515	2.048	220.21	48.00	.05
8	1.844	-.090	5169.01	5170.93	24685.35
9	1.367	3.008	149.95	58.00	-.13
9	.383	-2.572	5162.07	5164.80	39333.42
10	3.636	2.115	213.19	37.00	.13
10	.168	-3.754	5150.70	5157.65	24120.25
11	2.013	2.244	200.97	39.00	-.01
11	.602	-3.364	5147.95	5151.34	25062.80
12	1.805	2.736	164.83	58.00	-.05
12	-1.621	-3.501	5143.37	5147.21	29813.99
13	2.504	2.365	190.73	46.00	.09
13	1.982	-2.814	5134.28	5138.85	19149.56
14	1.962	2.142	210.57	47.00	.03
14	.548	-1.689	5131.09	5133.97	15794.19
15	.951	2.293	196.66	69.00	-.04
15	.030	-1.672	5126.50	5128.32	19494.08
16	2.196	1.848	244.08	46.00	.02
16	.263	-1.642	5118.78	5123.29	16440.96
17	1.324	1.382	344.43	28.00	.01
17	-.573	-3.141	5106.10	5108.67	15641.35
18	.970	2.053	231.83	55.00	-.10
18	-2.344	-3.099	5100.74	5102.57	22518.26
19	1.325	2.437	195.33	68.00	.03
19	-.218	-1.855	5092.99	5097.51	20271.58
20	1.797	1.632	291.63	43.00	-.10
20	-.159	-3.077	5089.74	5092.97	24645.14
21	1.199	2.082	228.67	35.00	-.03
21	-1.479	-2.669	5085.20	5087.84	26862.99
22	2.341	2.286	208.22	86.00	.06
22	1.413	-1.460	5080.81	5083.90	15562.52
23	1.224	1.801	254.79	42.00	-.01
23	.285	-1.309	5074.50	5077.83	17772.77
24	1.156	1.795	257.11	48.00	.00
24	-.006	-1.545	5066.44	5068.57	17255.72
25	1.255	2.084	220.29	64.00	.02
25	.379	-1.260	5062.00	5065.66	14974.73
26	1.067	1.669	274.95	60.00	.01
26	.660	-1.198	5058.09	5060.13	13518.23
27	1.034	1.950	235.33	45.00	-.03
27	-.744	-2.130	5049.99	5052.50	19644.25
28	1.534	2.155	212.99	71.00	.02
28	.382	-1.436	5041.09	5043.16	15231.54
29	1.120	2.124	216.10	64.00	-.01
29	-.043	-1.695	5036.76	5039.76	15922.11
30	1.822	1.358	337.91	46.00	.05
30	.602	-.969	5030.84	5034.11	9302.74
31	1.015	1.852	247.90	49.00	-.01
31	.069	-1.813	5025.53	5027.19	15002.82
32	2.173	1.673	274.44	46.00	-.00
32	-.125	-1.859	4995.78	5000.12	16344.04
33	1.226	2.900	158.26	64.00	-.05
33	-.940	-3.470	4973.76	4975.85	40135.17
34	1.947	1.185	387.18	51.00	.07
34	.067	-.777	4946.27	4950.88	9138.24
12					

YANG, POST-DAM, MONTH 24

1482.000 1474.000 1403.000

X-SEC	DELTA Z	DELTA H	Z	H	QBT
1	0.000	0.000	0.00	0.00	0.00
1	0.000	********	5213.40	5228.53	0.00
2	4.232	1.161	1208.18	0.00	-.16
2	-11.766	-8.710	5201.63	5208.90	17472.35
3	2.334	2.778	505.05	51.00	-.40
3	-2.620	-2.099	5201.26	5205.47	53685.67
4	2.038	2.109	665.20	45.00	-.06
4	-.739	-.933	5194.10	5199.40	58120.68
5	2.279	1.937	724.39	26.00	-.42
5	-1.866	-2.068	5186.05	5191.78	93873.47
6	1.878	1.860	754.48	64.00	.23
6	-3.240	-4.110	5176.57	5181.85	74917.03
7	1.664	2.717	516.31	50.00	-.27
7	-2.308	-1.679	5174.85	5178.75	102420.50
8	2.540	3.014	465.43	48.00	-.02
8	.913	.493	5168.08	5171.51	104141.45
9	2.172	1.330	1054.65	58.00	.77
9	.753	.681	5162.44	5168.05	18790.31
10	2.208	2.342	599.00	37.00	-.61
10	.868	1.205	5151.40	5162.61	90319.17
11	4.013	3.156	444.48	39.00	-.97
11	-.147	-.866	5147.20	5153.84	169139.74
12	2.190	2.925	479.68	58.00	.68
12	-.282	-.812	5144.71	5149.90	100785.15
13	4.402	2.975	471.67	46.00	-.02
13	1.870	.467	5134.17	5142.13	103070.14
14	2.275	2.984	470.10	47.00	-.03
14	.107	-.100	5130.65	5135.56	106290.78
15	1.749	2.773	506.03	69.00	.02
15	-.637	-1.157	5125.83	5128.84	104259.09
16	2.904	2.966	473.09	46.00	-.02
16	-1.909	-2.149	5116.61	5122.79	106453.29
17	3.820	1.365	1079.57	28.00	.55
17	-.674	-1.036	5106.00	5110.77	-41660.45
18	1.594	3.428	430.02	55.00	-1.90
18	-2.507	-.703	5100.57	5104.97	176228.66
19	2.475	2.978	494.97	68.00	1.00
19	.473	-.601	5093.68	5098.76	109536.05
20	3.052	2.494	590.93	43.00	-.58
20	-1.290	-2.012	5088.61	5094.04	134179.33
21	2.570	2.294	642.68	35.00	.58
21	-.935	-.961	5085.74	5089.54	90272.90
22	3.799	3.966	371.62	86.00	-.06
22	1.432	.358	5080.83	5085.72	101510.57
23	1.720	1.652	897.25	42.00	.25
23	.944	.945	5075.16	5080.08	46293.58
24	2.082	2.815	526.38	48.00	-.77
24	.805	1.134	5067.26	5071.25	150995.99
25	1.805	3.279	452.03	64.00	-.07
25	.226	-.165	5061.85	5066.75	158832.53
26	2.381	1.661	892.22	60.00	.78
26	-.470	-1.075	5056.96	5060.25	41052.39
27	1.680	2.488	595.62	45.00	-.17
27	-.094	-.095	5050.64	5054.53	80658.05
28	2.225	2.867	516.97	71.00	.03
28	.113	-.055	5040.82	5044.54	73498.72
29	1.957	2.207	671.47	64.00	.19
29	.577	.393	5037.38	5041.85	51948.52
30	2.320	2.393	619.35	46.00	-.18
30	.990	.938	5031.23	5036.02	74996.16
31	1.846	1.898	780.80	49.00	.05
31	.907	.601	5026.37	5029.60	53456.78
32	1.659	2.211	670.42	46.00	-.05
32	-1.051	-1.226	4994.85	5000.75	82067.65
33	1.822	2.554	580.36	64.00	-.05
33	-1.698	-1.886	4973.00	4977.43	106349.36
34	2.091	2.685	551.94	51.00	-.03
34	-.027	-.080	4946.17	4951.58	118926.50

2532E+07

24

YANG, POST-DAM, DAY 175

827.000 953.000 683.000

X-SEC	DELTA Z	DELTA H	Z	H	QBT
1	0.000	0.000	0.00	0.00	0.00
1	0.000	*******	5213.40	5228.20	0.00
2	2.059	2.598	339.90	0.00	-.01
2	-2.771	-1.469	5210.63	5213.99	940.28
3	1.955	2.561	344.31	51.00	-.00
3	-.358	.420	5203.52	5206.48	1042.72
4	1.737	2.092	422.07	45.00	.00
4	.806	2.256	5195.65	5199.95	943.13
5	1.961	1.714	515.05	26.00	.00
5	.102	.571	5186.02	5192.57	908.58
6	1.421	2.131	414.41	64.00	-.01
6	-1.747	-2.860	5179.06	5182.62	1361.32
7	1.319	2.739	322.36	50.00	-.00
7	-1.726	-.707	5175.43	5178.36	1486.31
8	1.999	2.457	359.35	48.00	.00
8	1.103	2.105	5168.27	5171.10	1478.48
9	1.687	2.867	307.94	58.00	-.00
9	.381	1.577	5162.07	5165.75	1875.93
10	4.247	2.722	324.43	37.00	.00
10	-.315	2.271	5150.21	5158.82	1854.48
11	3.262	2.447	360.86	39.00	.00
11	.346	.579	5147.70	5152.60	1629.14
12	1.876	3.038	290.68	58.00	-.00
12	-1.151	.703	5143.84	5148.66	1896.20
13	3.596	2.488	354.92	46.00	.00
13	1.086	2.957	5133.39	5140.13	1577.66
14	2.255	2.562	344.64	47.00	.00
14	.403	1.941	5130.94	5135.03	1460.23
15	1.320	2.533	348.64	69.00	.00
15	.249	.923	5126.72	5129.14	1398.75
16	2.746	2.016	438.04	46.00	.00
16	.152	2.570	5118.67	5124.61	1247.87
17	2.068	1.757	542.55	28.00	-.00
17	-.155	-.332	5106.51	5109.84	1383.41
18	1.488	2.405	396.27	55.00	-.00
18	-1.559	-.735	5101.52	5103.90	1621.74
19	1.640	2.946	323.45	68.00	-.00
19	.171	.732	5093.38	5098.62	1802.23
20	2.795	1.991	478.76	43.00	-.00
20	-.431	-1.525	5089.47	5093.70	1830.19
21	1.603	2.357	404.25	35.00	-.00
21	-1.322	-.234	5085.36	5088.78	1906.95
22	3.402	2.864	332.77	86.00	.00
22	1.007	1.684	5080.41	5084.84	1446.59
23	1.490	2.063	400.80	42.00	.00
23	.190	.379	5074.41	5078.31	1246.73
24	1.655	2.035	406.48	48.00	.00
24	-.162	.100	5066.29	5069.03	1165.31
25	1.537	2.470	334.88	64.00	.00
25	.188	.550	5061.81	5066.11	1140.90
26	1.610	1.864	443.66	60.00	.00
26	.502	.051	5057.93	5060.63	992.79
27	1.303	2.216	373.27	45.00	-.00
27	-.457	-.188	5050.27	5053.30	1301.35
28	2.059	2.508	329.73	71.00	.00
28	.213	.318	5040.92	5043.80	1134.21
29	1.473	2.380	347.50	64.00	-.00
29	.079	.359	5036.88	5040.50	1135.24
30	2.093	1.773	466.46	46.00	.00
30	.254	.297	5030.49	5034.44	853.02
31	1.390	1.967	420.40	49.00	-.00
31	.126	.420	5025.59	5027.87	927.16
32	1.802	1.809	457.06	46.00	-.00
32	-.101	-.004	4995.80	5001.03	1005.78
33	1.774	3.235	255.66	64.00	-.00
33	-.631	-.347	4974.07	4976.31	2417.79
34	2.046	1.775	465.83	51.00	.00
34	.300	.411	4946.50	4951.53	1082.17

175

YANG, POST-DAM, DAY 350

X-SEC	DELTA Z	DELTA H	Z	H	QBT
	353.000	353.000	256.000		
1	0.000	0.000	0.00	0.00	0.00
1	0.000	*******	5213.40	5227.45	0.00
2	.941	2.108	121.45	0.00	-.00
2	-3.504	-3.663	5209.90	5211.80	153.00
3	1.350	1.134	225.77	51.00	.00
3	-.423	-.311	5203.46	5205.75	65.33
4	1.003	2.396	106.35	45.00	-.00
4	.694	.249	5195.53	5197.94	301.90
5	1.717	.639	400.40	26.00	.00
5	.354	.350	5188.27	5192.35	34.44
6	1.136	1.338	139.30	64.00	-.00
6	-2.263	-4.755	5177.55	5180.74	304.09
7	.803	1.845	138.72	50.00	.00
7	-1.885	-1.802	5175.29	5177.26	203.42
8	1.046	2.079	123.16	48.00	-.00
8	1.064	.457	5168.23	5169.45	327.53
9	1.388	2.103	121.72	58.00	-.00
9	.092	-.080	5161.78	5164.09	348.44
10	2.652	1.710	149.75	37.00	.00
10	-.190	-.273	5150.34	5156.28	254.44
11	1.522	1.852	139.23	39.00	-.00
11	.516	-1.403	5147.37	5150.61	266.73
12	1.555	2.743	93.33	53.00	-.00
12	-1.472	-1.612	5143.52	5146.34	466.88
13	1.912	1.989	128.72	46.00	.00
13	1.397	.239	5133.70	5137.41	268.81
14	1.630	1.670	153.29	47.00	.00
14	.574	.345	5131.11	5133.44	154.89
15	.720	2.134	119.97	69.00	-.00
15	.169	-.199	5126.64	5128.02	300.91
16	1.800	1.772	144.44	46.00	-.00
16	.283	.255	5118.80	5122.30	305.78
17	1.152	1.182	298.65	28.00	.00
17	-.328	-1.423	5106.34	5108.75	245.66
18	.835	2.152	164.05	55.00	-.00
18	-2.072	-2.189	5101.01	5102.45	519.08
19	2.128	3.016	117.03	68.00	-.00
19	-.212	-1.110	5093.00	5096.77	705.67
20	1.612	1.497	235.77	43.00	.01
20	-.112	-2.689	5099.79	5092.53	471.94
21	1.163	2.073	169.85	35.00	-.00
21	-1.536	-1.581	5085.14	5087.43	625.81
22	1.963	2.045	172.59	36.00	.00
22	1.333	.330	5080.73	5093.48	305.12
23	1.161	1.764	200.09	42.00	-.00
23	.168	-.513	5074.39	5077.42	334.63
24	1.034	1.659	212.31	48.00	.00
24	-.124	-.694	5066.33	5068.25	350.04
25	1.086	2.051	172.09	64.00	-.00
25	.220	-.328	5061.84	5065.23	361.12
26	1.042	1.393	253.50	60.00	.00
26	.600	-.600	5058.03	5059.99	251.51
27	.906	1.332	182.70	45.00	-.00
27	-.613	-1.109	5050.12	5052.37	468.04
28	1.433	1.812	194.81	71.00	.00
28	.314	-.502	5041.02	5042.99	294.60
29	.999	2.093	168.68	64.00	-.00
29	.068	-.530	5036.87	5039.61	387.21
30	1.715	1.172	301.24	46.00	.00
30	.491	-.309	5030.73	5033.84	191.49
31	.865	1.733	203.69	49.00	-.00
31	.112	-.409	5025.57	5027.04	333.58
32	1.343	1.549	227.90	46.00	-.00
32	-.130	-1.306	4995.77	4999.73	357.81
33	1.100	2.758	127.97	64.00	-.00
33	-.940	-1.594	4973.76	4975.57	829.24
34	1.383	.951	371.14	51.00	.00
34	.623	.308	4946.33	4951.42	155.50
350					

YANG, POST-DAM, DAY 525

1750.000 1460.000 1090.000

X-SEC	DELTA Z	DELTA H	Z	H	QBT
1	0.000	0.000	0.00	0.00	0.00
1	0.000	*******	5213.40	5229.35	0.00
2	2.334	2.383	457.41	0.00	-.01
2	-4.085	-2.106	5209.31	5213.35	761.27
3	2.162	2.799	390.85	51.00	-.01
3	-.703	.335	5203.18	5206.39	1259.44
4	1.941	1.829	596.01	45.00	.01
4	.733	2.879	5195.57	5200.57	650.12
5	2.085	1.899	574.06	25.00	-.01
5	.334	1.032	5188.25	5193.03	1340.08
6	1.534	2.142	508.89	64.00	-.00
6	-2.691	-3.528	5177.12	5181.97	1463.58
7	1.546	2.658	410.16	50.00	-.00
7	-2.046	-.679	5175.11	5178.38	1514.87
8	2.151	2.816	387.11	48.00	-.01
8	.781	1.943	5167.95	5170.94	2150.67
9	2.120	2.654	410.66	58.00	.00
9	-.008	1.735	5161.68	5165.91	1775.73
10	4.180	2.795	390.01	37.00	-.00
10	-.072	3.302	5150.46	5159.36	2302.45
11	3.517	2.804	358.76	39.00	-.00
11	.231	.723	5147.58	5152.74	2441.95
12	2.038	2.878	378.72	58.00	.00
12	-1.438	.952	5143.55	5148.91	1982.44
13	3.875	2.602	418.91	46.00	.00
13	1.654	4.195	5133.95	5141.36	1946.47
14	2.225	2.755	395.66	47.00	-.00
14	.645	2.540	5131.18	5135.63	2025.61
15	1.525	2.564	425.07	69.00	.00
15	.323	1.288	5126.79	5129.51	1640.25
16	3.109	2.073	525.64	46.00	.00
16	.405	3.369	5118.93	5125.41	1493.40
17	2.663	2.083	700.89	28.00	-.01
17	-.668	-.239	5106.00	5109.93	2809.83
18	1.872	2.749	531.03	55.00	-.00
18	-2.371	-1.066	5100.71	5103.57	2885.52
19	2.346	3.114	468.78	68.00	.00
19	-.286	.988	5092.92	5098.87	2859.64
20	3.062	2.379	613.82	43.00	-.01
20	-.799	-1.138	5089.10	5094.09	3337.76
21	2.433	2.398	608.87	35.00	.01
21	-1.361	.550	5085.32	5089.56	2905.63
22	4.201	3.552	411.09	86.00	-.00
22	1.484	2.964	5080.88	5086.12	3122.62
23	1.704	2.193	801.58	42.00	.00
23	.109	1.355	5074.33	5079.29	2914.94
24	2.716	2.541	688.70	48.00	-.00
24	-.031	1.349	5066.42	5070.28	3395.11
25	1.877	2.545	587.68	64.00	.01
25	.398	2.051	5062.02	5067.61	2311.31
26	1.995	2.636	663.34	60.00	-.01
26	.403	.710	5057.83	5061.29	3659.71
27	1.797	2.226	786.34	45.00	.00
27	-.682	.773	5050.05	5054.26	2846.84
28	2.224	3.218	543.75	71.00	-.00
28	.372	1.459	5041.08	5044.94	3418.77
29	2.169	2.307	758.53	64.00	.01
29	.254	1.810	5037.05	5041.95	2547.85
30	2.373	2.645	661.57	46.00	-.01
30	.526	1.396	5030.77	5035.55	3465.31
31	1.965	1.625	1077.20	49.00	.00
31	.162	2.090	5025.62	5029.54	1514.96
32	1.687	2.378	735.84	46.00	-.00
32	-.222	.669	4995.68	5001.70	3409.05
33	1.568	2.126	823.28	64.00	.00
33	-1.249	1.205	4973.45	4978.36	2783.98
34	2.175	2.919	599.56	51.00	-.01
34	.968	1.606	4947.17	4952.72	5435.74
525					

YANG, POST-DAM, DAY 700

560.000 560.000 460.000

X-SEC	DELTA Z	DELTA H	Z	H	QBT
1	0.000	0.000	0.00	0.00	0.00
1	0.000	*******	5213.40	5227.79	0.00
2	2.283	1.109	414.63	0.00	-.00
2	-9.475	-7.743	5203.93	5207.72	86.35
3	2.332	.977	470.86	51.00	.00
3	-.867	.604	5203.01	5206.66	61.22
4	1.095	2.498	184.16	45.00	-.00
4	1.595	1.759	5196.44	5199.45	346.53
5	1.717	1.149	400.40	26.00	.00
5	.010	.007	5187.93	5192.01	164.39
6	1.262	1.660	277.03	64.00	-.00
6	-3.095	-4.763	5176.71	5180.73	426.51
7	.969	2.692	170.87	50.00	-.00
7	-3.449	-3.179	5173.71	5175.88	600.01
8	1.726	1.655	278.00	48.00	.00
8	-.133	.396	5167.04	5169.39	287.40
9	1.357	2.660	172.95	58.00	-.00
9	.559	.903	5162.25	5165.07	757.83
10	3.032	2.628	175.06	37.00	-.00
10	.003	.334	5150.54	5156.94	785.44
11	2.526	1.642	280.21	39.00	.01
11	-.519	-1.026	5146.83	5150.99	328.77
12	1.776	3.099	148.41	58.00	-.01
12	-1.173	-.532	5143.82	5147.42	896.72
13	2.671	2.243	205.13	46.00	.00
13	.927	.919	5133.23	5138.09	532.23
14	2.067	1.984	231.85	47.00	.00
14	.394	.967	5130.93	5134.06	369.00
15	.896	2.613	176.02	69.00	-.00
15	-.462	-.527	5126.01	5127.69	678.47
16	2.445	1.568	293.29	46.00	.00
16	-1.427	.028	5117.09	5122.07	340.44
17	1.486	1.445	387.61	28.00	-.00
17	-.149	-.909	5106.52	5109.26	399.97
18	.998	2.236	250.42	55.00	-.00
18	-2.066	-1.794	5101.01	5102.84	721.33
19	1.267	2.496	224.36	68.00	-.00
19	-.783	-.725	5092.43	5097.16	768.63
20	1.762	1.974	283.74	43.00	.00
20	-1.566	-3.810	5089.33	5091.41	697.12
21	1.737	1.245	449.86	35.00	.01
21	-2.551	-1.235	5084.13	5087.72	270.82
22	2.021	3.152	177.68	86.00	-.00
22	2.252	1.311	5081.65	5084.46	732.91
23	1.515	1.573	355.95	42.00	.00
23	.079	.119	5074.30	5078.06	394.47
24	1.232	2.006	279.10	48.00	-.00
24	1.315	1.052	5067.76	5069.99	698.63
25	1.189	2.794	200.43	64.00	-.00
25	.363	-.011	5061.99	5065.55	1071.26
26	2.381	.628	892.22	60.00	.01
26	-2.159	-1.244	5055.27	5059.33	62.45
27	1.051	2.301	243.40	45.00	-.00
27	.887	.655	5051.62	5054.14	690.17
28	1.832	2.069	270.67	71.00	.00
28	-.109	-.383	5040.60	5043.10	530.95
29	1.210	2.169	258.22	64.00	.00
29	-.005	-.128	5036.79	5040.01	500.56
30	2.015	1.305	429.28	46.00	.00
30	.719	.592	5030.95	5034.73	274.07
31	1.124	1.961	285.55	49.00	-.00
31	.698	.503	5026.16	5027.95	570.18
32	2.256	1.625	306.65	46.00	-.00
32	-1.000	-1.540	4994.90	4999.50	650.25
33	1.337	2.929	191.23	64.00	-.00
33	-1.464	-1.623	4973.24	4975.53	1292.25
34	2.039	1.349	415.07	51.00	.00
34	.276	.176	4946.48	4951.29	409.23

.2506E+07 .2966E+07 .3866E+07

700